

Staff Working Paper/Document de travail du personnel—2025-32

Last updated: November 7, 2025

A Market-Based Approach to Reverse Stress Testing the Financial System

Javier Ojea-Ferreiro Financial Stability Department JOjeaFerreiro@bankofcanada.ca

Bank of Canada staff working papers provide a forum for staff to publish work-in-progress research independently from the Bank's Governing Council. This work may support or challenge prevailing policy orthodoxy. Therefore, the views expressed in this note are solely those of the authors and may differ from official Bank of Canada views. No responsibility for them should be attributed to the Bank.

DOI: https://doi.org/10.34989/swp-2025-32 | ISSN 1701-9397

© 2025 Bank of Canada

Acknowledgements

I would like to express my gratitude to Eduardo Maqui, Radoslav Raykov, Thibaut Duprey, Ruben Hipp, Kerem Tuzcuoglu, Andrea Ugolini and Andreas Uthemann for their valuable comments and suggestions. I would also like to thank seminar participants at the Bank of Canada (FSE, FLE and BBL), at the 1st CAM-Risk Conference in Pavia, at the XXIX CEMLA Meeting of the Central Bank Researchers Network in Mexico D.F., at the Society for Nonlinear Dynamics and Econometrics Symposium in San Antonio, and at the seminar of the University of Milano-Biccoca. Finally, I am indebted to Sascha Clazie-Thomson for his research assistance. The mistakes are, of course, my own.

Abstract

This article investigates market scenarios that lead to extreme losses in international financial markets. We propose two systemic measures: (1) identifying the foreign event among those with equal probability leading to the worst outcome for the domestic financial system; and (2) classifying tail returns of financial institutions into four groups based on whether losses occur alongside domestic institutions only, foreign institutions only, both, or neither. Using 20 years of weekly equity returns from over 150 institutions across four developed financial systems, results highlight the central role of US and European institutions, with growing importance for Canada and non-bank financial intermediaries.

Topics: Financial institutions, Financial stability

JEL codes: C02, C32, C58, G21

Résumé

Dans cet article, nous étudions les scénarios de marché qui entraînent des pertes extrêmes sur les marchés financiers à l'échelle internationale. Nous proposons deux mesures du risque systémique : 1) l'identification, parmi les scénarios d'égale probabilité, de l'événement susceptible de conduire à l'issue la plus défavorable pour le système financier intérieur; 2) la classification des pertes extrêmes dans quatre groupes, selon qu'elles touchent les institutions financières du pays seulement, les institutions financières étrangères seulement, les deux ou aucune des deux. Issus de l'analyse de 20 ans de rendements boursiers hebdomadaires provenant de plus de 150 institutions réparties dans quatre systèmes financiers développés, les résultats montrent le rôle central que jouent les institutions américaines et européennes, ainsi que l'importance grandissante des institutions canadiennes et des intermédiaires financiers non bancaires.

Sujets: Institutions financières, Stabilité financière

Codes JEL: C02, C32, C58, G21

1 Introduction

Simultaneous extreme losses across multiple financial institutions are a defining feature of systemic risk (ECB 2009; Montagna et al. 2020). Although rare, these joint extreme losses can have long-lasting effects on the economy—from disruptions in the real sector to undermining the transmission of monetary policy (Bianchi 2011; Gadea et al. 2020). The dense structure of financial networks (Diebold and Yılmaz 2014; Demirer et al. 2018) complicates the assessment of systemic risk, as bivariate measures often provide only a partial view of the more complex interconnections at play (Acemoglu et al. 2015, Elliott et al. 2014). Moreover, the growing role of non-bank financial intermediaries (NBFIs) further increases connectedness in the global financial system (see Bank for International Settlements 2025; Financial Stability Board 2024).

Given these challenges, traditional approaches (Adrian and Brunnermeier, 2016; Acharya et al., 2012, 2017; Brownlees and Engle, 2017) may fall short in capturing the multidimensional nature of systemic risk across financial institutions.¹ To address this gap, this paper proposes two market-based measures aimed at capturing a broader picture of the international financial conditions associated with systemic risk. Both follow an approach based on reverse stress testing, starting from tail losses and working backward to identify the underlying market stress scenarios. Specifically, these measures (1) identify the international joint event linked to the worst domestic performance among all international scenarios with the same tail probability, and (2) classify extreme equity losses of finan-

¹In a simple dependence structure where one institution is clearly central, like a star-shaped network, this pairwise analysis may be enough to identify where systemic risk concentrates. However, in more complex and densely connected systems, this approach can underestimate the potential effects of systemic risk, providing a partial view on the systemic institutions.

cial institutions based on whether losses occur domestically, abroad, or jointly, thereby improving our understanding of systemic vulnerability patterns.

The contribution of this study to the literature is threefold. First, it introduces a reverse stress testing perspective into the measurement of systemic risk. Unlike traditional approaches that condition on predefined stress scenarios, the proposed method endogenously identifies the most adverse market conditions, offering a more data-driven view of systemic vulnerability. Second, the framework is applied to a large international sample of equity returns for banks and non-bank financial intermediaries (NBFIs), uncovering asymmetric patterns of tail risk co-movement across sectors and regions. Third, the study develops a high-dimensional dependence model that combines the latent nested bifactor copula of Krupskii and Joe (2015) with score-driven dynamics \dot{a} la Creal et al. (2013), enabling flexible and efficient estimation of evolving cross-border linkages in the tails of the return distribution.

These market-based measures can be seen as extensions of standard systemic risk metrics, adapted to the multidimensional structure of the international financial system. First, the Return-in-Stress (RiS) generalizes the Marginal Expected Shortfall (MES) of Acharya et al. (2012) to capture the individual role of foreign institutions in domestic losses. Rather than conditioning on a single foreign index, the measure identifies the worst domestic outcome across all equally probable foreign tail scenarios. This highlights both the tail dependence among foreign institutions, affecting the likelihood of each scenario, and between foreign and domestic institutions, which are associated with domestic losses. Second, the Expected Shortfall Allocation (ESA) decomposes the tail losses of each institution based on whether they coincide with domestic, foreign, joint, or no systemic tail events. This classification provides a more granular view of the international financial

conditions in which tail risks materialize. While few studies adopt a multivariate view of systemic risk, some exceptions include Segoviano and Goodhart (2010) and Gravelle and Li (2013), where scenarios involve simultaneous distress across institutions. However, these approaches condition on the number of distressed institutions without distinguishing which institutions are involved, missing critical information about the structure of systemic risk. By contrast, Gonzalez-Rivera et al. (2019) and González-Rivera et al. (2024) endogenously identify the combination of risk factors associated with the worst performance for conditional expected GDP growth (or quantile of GDP growth) among all equally probable scenarios, following a reverse stress testing logic. The RiS builds on this idea but defines the stress scenario on a joint tail probability rather than a joint density. This distinction becomes particularly relevant in settings where outcomes below the threshold may exhibit non-linear behaviors or clustering in the tails, which the density-based approach may overlook.² The closest reference to the Expected Shortfall Allocation is Van Oordt and Zhou (2019). They decompose banks' sensitivity to severe shocks in the financial system into two components: one capturing relative tail thickness, and another capturing tail dependence. In contrast, our approach reverses the direction of analysis: rather than starting from a systemic shock and tracing its impact on individual banks, we begin with an institution's own tail loss and assess the extent to which it coincides with tail events across other financial firms. This perspective, grounded in reverse stress testing, reveals how much of a bank's extreme loss occurs under broader systemic distress. The more idiosyncratic the institution's tail loss, the less systemic and vulnerable it appears.

²Conditional quantile measures based on individual quantiles, rather than a set of them, may inherit some of the statistical inconsistencies highlighted by Mainik and Schaanning (2014), such as non-monotonicity.

To implement these measures, the joint distribution of financial institutions' returns is estimated using a high-dimensional non-Gaussian framework. The model parsimoniously captures both domestic and international dependence while allowing for evolving tail risk, building on the nested copula factor structure of Krupskii and Joe (2015) and incorporating time-varying score-driven dynamics à la Creal et al. (2013). By using a latent factor model, we can reduce model risk due to potentially misspecified explicit factors or overly simplistic correlation assumptions, e.g., equicorrelation structure (Lucas et al., 2017; Engle and Kelly, 2012). Latent factor approaches allow the dependence structure to be inferred from the data itself, avoiding the limitations that come with specifying factors ex ante. The proposed model shares similarities with the bifactor structure of Oh and Patton (2017, 2023), but differs in two key aspects. First, it allows dependence between global and group-specific factors through a nested structure, which reduces parameter dimensionality and improves model fit. Second, the group-specific factors are based on geographic regions, consistent with empirical findings (Demirer et al., 2018) and methodologies used by practitioners such as S&P's BICRA framework.³

This general framework is applied to weekly unbalanced equity return data from the US ($N_{\rm USA}=42$), Canada ($N_{\rm CAN}=34$), Western Europe ($N_{\rm WEU}=42$), and Japan($N_{\rm JAP}=34$) from April 2001 to October 2024 (T=1227). Consequently, the database considers several crises and periods of distress in the financial market. The 2008 global financial crisis, the sovereign European debt crisis, the COVID-19 crisis, the UK gilt market crisis, and the collapse of SVB are examples of distress events that were materialized during the sample period. The dataset mainly consists of insurance and banking firms but also includes clearing houses, investment management, mortgage

³See, for instance, the Banking Industry Country Risk Assessment (BICRA) methodology from S&P.

finance, and leasing companies. This broad coverage provides a comprehensive perspective on the interconnections between banks and NBFIs within the international financial system, complementing recent studies on bank–NBFI interconnectedness that focus primarily on domestic markets (e.g., Acharya et al. 2024; Aradillas Fernandez et al. 2024; Ojea-Ferreiro 2025).

This study finds that domestic systemically important banks (DSIBs) play a central role in tail co-movement across international markets, along with the presence of other deposit-taking institutions (DTIs) and some NBFIs in the United States, consistent with the findings of Abad et al. (2022) for Europe. The role of NBFIs in explaining domestic market co-movement is secondary but has increased over time, particularly from insurance companies, followed by investment management and mortgage finance companies. US and European financial institutions generate the largest impact on international financial systems, with Canada's systemic contribution rising from 2017. In contrast, Japanese institutions contribute only marginally to stress propagation in global financial markets, in line with previous evidence from Gravelle and Li (2013).

Our findings have practical implications for financial stability monitoring and policy design. The proposed market-based risk measures can serve as early-warning indicators of potential spillovers across borders by capturing multivariate dependencies often overlooked by standard approaches. In addition, these measures could support the calibration of capital buffers, such as the Countercyclical Capital Buffer (Van Oordt 2023), to better capture the systemic vulnerabilities associated with foreign stress scenarios.

The article is laid out as follows: Section 2 presents the methodology and the tail measures. Section 3 introduces the data and presents a descriptive analysis of our sample. Section 4 presents the results of the estimation and the measures. Finally, section 5

provides the conclusion.

2 Methodology

This section presents the two market-based systemic risk indicators proposed in the paper, followed by the high-dimensional modeling approach used to estimate them.

2.1 Systemic risk measures and tail indicators

Our approach adopts a reverse stress testing perspective: rather than starting from a hypothetical market shock and assessing its impact, we begin with extreme losses in the domestic financial system and work backward to identify the most adverse international scenarios that could give rise to them.

The first measure captures the international tail scenario—among all those with a fixed joint probability α —that results in the worst average performance of a domestic financial index, measured as the market-weighted return of domestic institutions. This procedure avoids underestimating the impact of international shocks on domestic stability by searching over the full set of equally likely joint stress configurations. It also highlights which institutions consistently appear in the most adverse scenarios over time, offering a dynamic view of systemic importance. By focusing on multivariate rather than pairwise dependencies, this approach reduces the risk of underestimating the conditional losses by capturing more complex joint distress scenarios, particularly in systems where mutual dependence—not just bilateral connections—matters.⁴

The second measure follows a reverse stress testing logic by starting from each financial

⁴To illustrate how mutual dependence can exist even when pairwise dependencies are absent, the Appendix presents a simple example that motivates the need for a multidimensional measure of systemic risk. A pairwise independent event refers to any two events that are independent from each other, while mutual independence implies that every event is independent of *any* set or combination of other events.

institution's Expected Shortfall and then decomposing these losses into non-overlapping components depending on whether they coincide with stress occurring domestically, internationally, jointly, or in isolation. This backward-looking approach provides a detailed view of systemic vulnerability, avoiding the strong assumptions typical of traditional decompositions (e.g., Cholesky-based methods). By remaining agnostic about the underlying drivers of stress events, our classification method uncovers patterns of co-movement that conventional monitoring techniques may miss.

Together, these indicators provide new tools for identifying patterns of tail dependence and co-movement that standard stress testing may overlook. The next sections describe each measure in detail.

2.1.1 Return-in-Stress (RiS)

Return-in-Stress (RiS) measures the lowest expected return of a domestic financial system conditional on extreme stress in the international financial system, defined by a joint tail event exceeding a given probability threshold α . It captures the minimum average return in the domestic index under scenarios where the international institutions' returns fall below specified quantiles, ensuring the joint probability of this event is at least α , i.e.,

$$RiS_{t}(\alpha) = \min_{q_{t}} E\left(r_{m,t} | r_{k,t} \leq VaR_{k,t}(q_{k,t}), \dots, r_{l,t} \leq VaR_{l,t}(q_{l,t})\right),$$

$$s.t. \qquad P(r_{k,t} \leq VaR_{k,t}(q_{k,t}), \dots, r_{l,t} \leq VaR_{l,t}(q_{l,t})) \geq \alpha,$$
(1)

where the return of the financial index m is the weighted sum of the FI's returns within the index, i.e., $r_{m,t} = \sum_{i=1}^{N} \omega_{i,t} r_{i,t}$ and $VaR_{i,t}(q_{i,t})$ is the return of the financial institution i associated with quantile $q_{i,t}$. The vector of quantiles q_t is time varying as the change

in the dependence structure over time will imply a change on the stress capture via new values in the vector of quantiles.⁵

This approach helps us assess the vulnerability of domestic markets to international tail events and identifies which foreign institutions contribute most to systemic risk over time. Unlike traditional stress tests that specify scenarios a priori, RiS identifies the worst-case stress scenario endogenously, avoiding overconfidence in system resilience.

Equation (1) represents the domestic index as a sum of weighted conditional expected returns of individual financial institutions. This decomposition provides:

- (i) An estimate of expected losses for the domestic financial system under international stress;
- (ii) The identification of the international tail event that maximizes these losses;
- (iii) Insights into the exposure of each institution to systemic tail risk.

Figure 1 represents graphically how the Return-in-Stress (RiS) is computed. Figure 1a shows, on the left side, a scatter plot with the histogram of two foreign institutions k and j. The purple squared area indicates an scenario with probability 5% defined by the combination of two upper thresholds for both institutions. The upper right corner of the area coincides with the red line. The red line indicates the position of all the possible upper right corner of squared areas with 5% probability for foreign firms j and k. Note that, in the axes limit, the areas indicate univariate scenarios (either in foreign firm k or foreign firm j). Conditional on being on the purple area, the distribution of returns of the

⁵Note that, as a consequence of the constrain $P(r_{k,t} \leq VaR_{k,t}(q_{k,t}), \ldots, r_{l,t} \leq VaR_{l,t}(q_{l,t})) \geq \alpha$, we know that the vector q_t would have a lower bound in α and an upper bound in 1. If any value of the vector reaches the upper bound, it is equivalent to not setting that conditioning variable, i.e., $P(r_k \leq VaR_k(q_k), r_{l,t} \leq VaR_{l,t}(q_{l,t}), r_w \leq VaR_w(1)) = P(r_{k,t} \leq VaR_{k,t}(q_{k,t}), r_{l,t} \leq VaR_{l,t}(q_{l,t}))$. Hence, this measure includes the univariate scenario as the case where the vector q_t is a vector of ones with the exception of the individual conditioning financial firm.

domestic financial index moves from the blue bars to the purple bars. Figure 1b shows the red line, but instead of showing the returns in the axes, we represent the percentiles for the marginal distribution of firms' returns. The color of the line indicates the average return for the domestic financial index, showing that the maximum average losses are found when firm k is below the percentile 70 and firm j is below percentile 5.2.

[INSERT FIGURE 1 HERE]

2.1.2 Expected Shortfall Allocation (ESA)

The tail loss for each financial institution is defined as losses above a threshold, which is usually identified by a quantile, e.g., 5% highest losses. When those tail losses materialized, we can identify other tail losses in the financial system, which allow us to decompose the tail loss of each financial institution in shares of common stress in the financial system. To illustrate this example, Figure 2 shows, in the right side, a scatter plot for the domestic financial sector and the foreign financial sector with histograms in the axes and, in the left side, the histogram for institution i. The realizations of the scatter plot occurring at the same time tail losses for institution i are shown in orange. Zooming in on this subset, we could distinguish those realizations as being in the tail or not, dividing the scatter plot into four areas. This division decomposes the tail returns of institution i into four non-overlapping areas, identifying the share of tail return of institution i happening jointly with tail returns in the domestic sector, foreign, both, or none. The definition of domestic and foreign tail events can vary depending on how stress is measured. One approach is to define stress as a certain number of institutions N (within or outside a given region) experiencing extreme losses. Alternatively, one can use the data to extract latent regional factors and define stress as those factors entering their tail regions. This subsection remains agnostic regarding the approach used to identify regional tail stress, and the Appendix presents the corresponding formulas for each definition.

[INSERT FIGURE 2 HERE]

The Expected Shortfall (ES) of an institution i is defined as the mean return when the return is below a quantile α , i.e.,

$$ES_{i,t} = E(r_{i,t}|r_{i,t} \le VaR_{i,t}(\alpha)).$$

To better understand the association between an institution's tail losses and systemic distress, this paper divides the Expected Shortfall into four components based on whether distress occurs (or not) in the domestic and/or foreign financial systems:

- (i) Idiosyncratic: losses when neither domestic nor foreign systems are in distress,
- (ii) Domestic: losses coinciding with distress in the domestic system only,
- (iii) Foreign: losses coinciding with distress in the foreign system only,
- (iv) Global: losses occurring when both domestic and foreign systems are in distress,

$$ES_{i,t} = \underbrace{E\big[r_{i,t} \mid r_{i,t} \leq VaR_{i,t}(\alpha), r_{d,t} > VaR_{d,t}(\alpha), r_{f,t} > VaR_{f,t}(\alpha)\big]P\big(r_{d,t} > VaR_{d,t}(\alpha), r_{f,t} > VaR_{f,t}(\alpha) \mid r_i \leq VaR_{i}(\alpha)\big)}_{\text{domestic}} \\ + \underbrace{E\big[r_{i,t} \mid r_{i,t} \leq VaR_{i,t}(\alpha), r_{d,t} \leq VaR_{d,t}(\alpha), r_{f,t} > VaR_{f,t}(\alpha)\big]P\big(r_{d,t} \leq VaR_{d,t}(\alpha), r_{f,t} > VaR_{f,t}(\alpha) \mid r_i \leq VaR_{i}(\alpha)\big)}_{\text{foreign}} \\ + \underbrace{E\big[r_{i,t} \mid r_{i,t} \leq VaR_{i,t}(\alpha), r_{d,t} > VaR_{d,t}(\alpha), r_{f,t} \leq VaR_{f,t}(\alpha)\big]P\big(r_{d,t} > VaR_{d,t}(\alpha), r_{f,t} \leq VaR_{f,t}(\alpha) \mid r_i \leq VaR_{i}(\alpha)\big)}_{\text{global}} \\ + \underbrace{E\big[r_{i,t} \mid r_{i,t} \leq VaR_{i,t}(\alpha), r_{d,t} \leq VaR_{d,t}(\alpha), r_{f,t} \leq VaR_{f,t}(\alpha)\big]P\big(r_{d,t} \leq VaR_{d,t}(\alpha), r_{f,t} \leq VaR_{f,t}(\alpha) \mid r_i \leq VaR_{i}(\alpha)\big)}_{\text{global}}$$

(2)

where $r_{d,t}$ and $r_{f,t}$ are the returns of the domestic and foreign financial sectors, respectively.

This decomposition acts like a reverse stress test: starting from an institution's tail losses, it reveals how those losses associate with different systemic stress environments. A larger global share signals a stronger association between institution i's extreme losses and simultaneous systemic distress across international markets. Conversely, smaller non-idiosyncratic shares suggest that tail losses at i tend to occur independently of systemic stress, indicating potential diversification benefits and lower systemic relevance.

2.2 Modeling distribution

To build our systemic risk measures, we need to model the joint return distribution across institutions. We estimate marginal and dependence structures using a copula approach, simplifying the estimation of large panel data. We follow the standard ARMA-GARCH-GJR model used in the literature (Girardi and Ergün 2013; Ojea-Ferreiro and Reboredo 2022; Ojea-Ferreiro et al. 2024) for the marginal distribution. The dependence structure integrates a latent bifactor model to address high dimensionality, with a Skewedt copula to capture skewness and tail dependence, and a score-driven dynamics for time-varying parameters (Creal et al. 2013), which have been shown to outperform alternative approaches (Koopman et al. 2016). The latent factor model not only helps address high dimensionality, but also greatly simplifies the construction of the risk measures. Our approach captures higher moments, heteroskedasticity, autocorrelation, as well as time-varying dependence, asymmetries, and tail risk. This allows us to accurately estimate systemic risk measures sensitive to extreme events.

 $^{^6}$ More details on how the factor structure simplifies the computation can be found in the Venn diagram section of the Appendix.

2.2.1 Marginal behaviour

Following Girardi and Ergün (2013), Ojea-Ferreiro and Reboredo (2022), and Ojea-Ferreiro et al. (2024), the marginal densities of equity returns is characterized by an ARMA(p,q)-GARCH-GJR(h,k) model, i.e.,

$$r_{i,t} = \mu_{i,t} + \epsilon_{i,t},$$

$$\epsilon_{i,t} = \sigma_{i,t} \epsilon_{i},$$

$$\mu_{i,t} = \phi_{0} + \sum_{j=1}^{p} \phi_{j} r_{i,t-j} + \sum_{k=1}^{q} \psi_{k} \epsilon_{i,t-k},$$

$$\sigma_{i,t}^{2} = \omega + \sum_{l=1}^{k} \alpha_{l} \epsilon_{i,t-k}^{2} + \sum_{q=1}^{h} \beta_{q} \sigma_{i,t-q} + \delta \mathbf{1}_{\epsilon_{i,t-1} < 0} \epsilon_{i,t-1}^{2},$$

where ϕ_j and ψ_k are the parameters of the AR and MA components of the marginal model, ω , α_l , β_q , and δ are the components of the GJR-GARCH, which with the parameter δ allows for an leverage effect in the dynamics of the variance, implying a higher increase when there are negative shocks. The standardized innovation ε_i follow a Hansen (1994)'s skewed t distribution, which captures the skewness and excess of kurtosis that we might find in financial returns. The density function is

$$f(\varepsilon_i; \lambda_i, \nu_i) = \begin{cases} bc \left(1 + \frac{1}{\nu_i - 2} \left(\frac{b\varepsilon_i + a}{1 - \lambda_i} \right)^2 \right)^{-\frac{\nu_i + 1}{2}} & \text{for } \varepsilon_i < -\frac{a}{b} \\ bc \left(1 + \frac{1}{\nu_i - 2} \left(\frac{b\varepsilon_i + a}{1 + \lambda_i} \right)^2 \right)^{-\frac{\nu_i + 1}{2}} & \text{for } \varepsilon_i < -\frac{a}{b} \end{cases},$$

where $a=4\lambda_i c(\frac{\nu_i-2}{\nu_i-1})$, $b=\sqrt{1-3\lambda_i^2-a^2}$ and $c=\frac{\Gamma(\frac{\nu_i+1}{2})}{\sqrt{\pi(\nu_i-2)}\Gamma(\frac{\nu_i}{2})}$, the number of degrees of freedom ν_i must be higher than 2 and the parameter of asymmetry λ_i could take a value between -1 and 1. This distribution converges to the Gaussian distribution when $\lambda_i=0$

and $\nu_i \to \infty$ and the symmetric Student-t when the number of degrees of freedom are finite and $\lambda_i = 0$.

2.2.2 Dependence structure

We use a copula approach (Sklar 1959) to model the joint distribution of returns. The joint distribution is obtained linking marginal distributions through a copula function, C, so that $F(x,y) = C(F_x(x), F_y(y))$. The joint density can be written as $f(x,y) = c(F_x(x), F_y(y))f_x(x)f_y(y)$, where c is the copula density. This allows us to express conditional densities easily: for example, $f(y|x) = c(F_x(x), F_y(y))f_y(y)$, which simplifies the analysis of risk measures based on conditional distributions.

The copula approach also allows us to simplify the estimation in a two-step procedure (Joe and Xu 1996), where the marginal features are estimated first and, in a second stage, the dependence structure is estimated based on the pseudo-integral probability transformations of the marginal distributions.⁷

The Skewed Student-t copula. The dependence between financial entities is estimated using a Skewed Student-t copula. The Skewed Student-t distribution has been widely employed to model financial and economic data (Lucas et al. 2014; Lucas et al. 2017; Oh and Patton 2023; Oh and Patton 2018) due to the flexibility to capture different tail behaviours as shown by Figures 3 and 4.

[INSERT FIGURE 3 HERE]

[INSERT FIGURE 4 HERE]

The N-variate Skewed Student-t distribution discussed in Demarta and McNeil (2005)

⁷More details about the estimation process are provided in the appendix.

 $ST(\mu, P, \lambda, \nu)$ has the following density distribution:

$$f_X(x) = c \frac{K_{\frac{\nu+N}{2}}(\sqrt{(\nu+d(x))\lambda'P^{-1}\lambda}) \exp([x-\mu]'P^{-1}\lambda)}{(\sqrt{(\nu+d(x))\lambda'P^{-1}\lambda})^{-\frac{\nu+N}{2}}(1+\frac{d(x)}{\nu})^{\frac{\nu+N}{2}}},$$
 (3)

with $c = \frac{2^{\frac{2-(\nu+N)}{2}}}{\Gamma(\frac{\nu}{2})(\pi\nu)^{\frac{N}{2}}|P|^{1/2}}$, $d(x) = [x-\mu]'P^{-1}[x-\mu]$ and $K_a(b)$ being the modified Bessel function of the second kind. The Skewed-t Student distribution becomes the Student-t distribution when $\lambda = 0$ and converges to the Gaussian distribution when $\lambda = 0$ and $\nu \to \infty$. Note that to have a defined variance, the restriction for the Student-t distribution is $\nu > 2$, while for the Skewed-t distribution $\nu > 4$.

The Skewed Student-t copula is a implicit copula (Smith 2023), meaning that there is not an explicit formula for this dependence but it is defined as the ratio between joint and marginal distributions. In other words, given the definition of the joint distribution as the product of density copula and marginal distributions, we defined the Skewed Student-t copula density as

$$c_{ST}(u,v) = \frac{f_{ST}(F_X^{-1}(u), F_Y^{-1}(v))}{f_X(F_X^{-1}(u))f_Y(F_Y^{-1}(v))},$$

where $f_{ST}(x,y)$ is the Skewed-t bivariate distribution with parameters $\mu=[0,0]',P=\begin{bmatrix}1&\rho\\\rho&1\end{bmatrix}$, $\lambda=[\lambda_1,\lambda_2]'$ and ν , $f_X(x)$ is an univariate Skewed-t distribution with parameters $\mu_1=0,\,P=1,\,\lambda=\lambda_1$, and ν and $f_Y(y)$ is an univariate Skewed-t distribution with parameters $\mu_2=0,\,P=1,\,\lambda=\lambda_2$ and ν .

The estimation of a N-dimensional Skewed Student-t copula could become complicated for large N, as the number of parameters for correlation matrix are $\frac{N(N-1)}{2}$. In order

⁸The appendix presents more details about the Skewed-t copula, the assessment of conditional copulas and cumulative copulas, and some details about the estimation of the Skewed Student-t copula within our framework.

to solve this problem, we take the simplifying assumption that the relationship between financial firms could be explained by a latent nested bi-factor model, which reduces the number of parameters in the correlation matrix to N + G, where G is the number of groups. Following this approach, the joint copula is built as a combination of bivariate copulas as a truncated vine structure (Aas et al. 2009). The next subsection develops this modeling approach.

Nested latent bi-factor structure The nested factor copula is introduced by Krupskii and Joe (2015), where the dependence between variables is explained by a common or global factor and a group-specific factor. The global factor captures the dependence between the group-specific factors. This is a realistic way to replicate the financial network structure. Financial firms within the same country or region would be linked to a latent factor specific for that region, then the latent factors are linked between them via a global factor. The link with the global factor makes that stress periods in some regions would happen at the same time as stress scenarios in other regions. In other words, the global latent factor proxies the current state of the international financial system, which drives other factors, reflecting the situation of domestic financial systems. In

Figure 5 shows an example for n Canadian financial firms and m US financial firms. Canadian firms are related to a Canadian latent factor C, while US firms are connected to a US latent factor U. Both latent factors are not independent as they are connected

 $^{^9}$ For instance, S&P follows a nested approach to assess credit risk in banks starting with a general industry rating (BICRA methodology) and then fine-tuning for the individual financial institutions (SCAP methodology). More information about this approach can be found on the S&P website.

¹⁰I also estimate an alternative bifactor model as a robustness check in the Appendix. I provide its comparison with our model in terms of information criteria (AIC, BIC) and check if the main outcomes from our model hold in this alternative setting, as the bifactor model allows for a higher degree of flexibility, a consequence of the direct link between financial firms from different regions via the global factor without going through their corresponding regional factor, as it happens in the nested factor model.

via a global latent factor G.

[INSERT FIGURE 5 HERE]

This model is a truncated vine copula (Aas et al. 2009) where the two connecting components, the global factor and the group-specific factor, are not directly observed. Since these latent factors are unobservable, the model must consider all possible values these factors could take. Given that the inputs to the copula are uniformly distributed, this involves integrating over the unit interval, from zero to one. The nested structure assumes that the group-specific factors are conditionally independent given a global latent factor, which simplifies computation by reducing the full dependence to a double integral, i.e.,

$$C(U) = \int_0^1 \left(\prod_{g=1}^G \int_0^1 \left(c_V(v_g, v_0) \prod_{i=1}^{N_g} C(u_i | v_g) \right) dv_g \right) dv_0, \tag{4}$$

where there are G groups, U is the matrix of integral distribution functions for matrix X, i.e., $U = F_X^{-1}(X)$, v_0 and v_g are the global and group-specific factors respectively, $C(\ldots|\ldots)$ is the conditional copula, and $c_V(\ldots)$ is the density copula between the group-specific factors and the global factor. It is worth noting that in Eq. (4), the inner parenthesis indicates the conditional probability given the specific-group factor and the global factor, while the outer parenthesis indicates the conditional probability given the global factor. The density copula becomes

$$c(U) = \int_0^1 \left(\prod_{g=1}^G \int_0^1 \left(c_V(v_g, v_0) \prod_{i=1}^{N_g} c(u_i, v_g) \right) dv_g \right) dv_0.$$
 (5)

Note that the structure shown in Figure 5 allows us to follow a sequential estimation procedure, as the global copula sets the dependence across different groups, but the

dependence between variables within the same group is not affected by other groups. First, we estimate the group-specific copula in T_1 . Second, we can estimate the global copula $c_V(\dots)$ in T_2 .¹¹

GAS dynamics. We consider time-varying correlation parameters in the Skewed Student-t copula following a general autoregressive score (GAS) model (Creal et al. 2013). The score-driven model generalizes many financial econometrics models, capturing more data features and outperforming autoregressive models like GARCH (Koopman et al. 2016).

The updating equation in the GAS model is

$$f_{i,t+1} = \omega_i + \alpha_i s_{i,t} + \beta_i f_{i,t}, \tag{6}$$

where ω_i , α_i , and β_i are the parameters of the GAS model, $s_{i,t} = S_{i,t} \nabla_{i,t}$, $S_{i,t}$ is a scaling factor and $\nabla_{i,t}$ is the derivative of the log-likelihood function at time t with respect to the parameter $f_{i,t}$, i.e., $\nabla_{i,t} = \frac{\partial \log(c(u_{i,t},v_t;f_{i,t}))}{\partial f_{i,t}}$. Thus, $f_{i,t+1}$ is determined by an autoregressive updating function that has an innovation term equal to the score of the log-likelihood with respect to $f_{i,t}$. I choose the scaling factor $S_{i,t} = \mathcal{J}_{t|t-1}$, where $\mathcal{J}'_t \mathcal{J}_{t|t-1} = \mathcal{I}^{-1}_{t|t-1}$ and $\mathcal{I}_{t|t-1} = E_{t-1}(\nabla_t'\nabla_t)$. This scaling factor allows us to standardize the value of ∇_t with its standard deviation. Another way to interpret this scaling factor is as a step in a steepest ascent method to update the value of $f_{i,t}$, where the direction is given by the gradient $\nabla_{i,t}$ and the size of the step in that direction is given by the Hessian, which is approximated by the outer product of the gradient. In other words, we use the local curvature of the log-density to improve the step.

The parameter $f_{i,t+1}$ is a transformation from the original correlation parameter of

¹¹The appendix shows more details about the optimization process and the estimation approach.

that the parameter could take, so there is no need to set some restrictions in the values of ω_i , α_i , and β_i . The transformation function $f_{i,t} = h(\rho_{i,t}) = -\log(\frac{1-\rho_{i,t}}{1+\rho_{i,t}})$ makes that the original feasible values in the range (-1,1) for $\rho_{i,t}$ increase to the real line under $h(\rho_{i,t})$. The score of the transformed parameters becomes

$$\frac{\partial \log(c(u_{i,t}, v_t; f_{i,t}))}{\partial f_{i,t}} = \frac{\partial \log(c(u_{i,t}, v_t; f_{i,t}))}{\partial \rho_{i,t}} \frac{\partial \rho_{i,t}}{\partial f_{i,t}},$$

where
$$\frac{\partial \rho_{i,t}}{\partial f_{i,t}} = \left(\frac{\partial h(\rho_{i,t})}{\partial \rho_{i,t}}\right)^{-1} = \frac{1-\rho_{i,t}^2}{2}$$
.

3 Data

Total return equity prices, i.e., stock prices with dividends being reinvested in the same assets, were downloaded from Refinitiv LSEG for financial firms in Canada, the United States, Western Europe (Euro Area, United Kingdom, and Switzerland),¹² and Japan to get a global coverage of the developed financial system. Our sample compresses 152 financial institutions, of which 22% are Canadian, 22% are Japanese, 28% are Western European, and 28% are American.¹³

The data length starts in April 2001, when the first observations for Japanese financial institutions are available, and goes up to the first week of October 2024. The data length includes several crisis and turmoil periods like the global financial crisis (GFC), the European sovereign debt crisis, and the COVID-19 crisis. The analysis is performed in the local currency, preventing any distortion in the distribution introduced by the exchange rates (see Ojea Ferreiro 2020). When needed, the exchange rate is employed *outside* the dependence model to get the same currency for the *RiS* or *ESA* measure of the region, i.e., Western European metrics are provided in euros, which allow us to distinguish the effect of the stock dependency from the effect of the exchange rate, which could add a layer of co-movement between financial firms traded in the same currency.¹⁴ The weekly data, computed on Wednesday, overcomes some biases that could be found in daily frequency, e.g., the bid-ask effect and non-synchronous trading days. Also, high-frequency data

¹²These three regions were merged into the same region due to the higher dependence between the financial institutions from this location.

¹³A balanced distribution of the FIs within each region allows for a better estimation of the global factor. The more unbalanced distribution across regions would tend to give a higher relevance to the region with fewer FIs.

¹⁴For instance, Swiss firms might present a higher dependence in euro returns not due to an actual dependence between firms but because of the use of the same exchange rate.

presents noise that is reduced when using weekly data. Regarding lower frequency data, the monthly frequency produces strong compensation effects for the positive and negative shocks. Using weekly data instead of monthly data leads to more reliable results as a consequence of the larger number of observations.

I get information about the main NAICS six-digit code from EIKON to associate each financial institution to a financial subsector following Office of the Superintendent of Financial Institutions' (OSFI) match between NAICS code and EB/ET return groups, ¹⁵ which allows me to associate each company to banks and NBFIs. In particular, in our sample we have deposit-taking institutions (DTIs), representing 38% of the sample; insurance companies, which account for 20% of the sample; investment management companies, summing up to 13% of our sample; investment dealers, which are 10% of the FIs; leasing and finance companies, 7% of the sample; mortgage finance companies, which are close to 7% of the sample; and clearing houses, which are 5% of the sample.

The selection of financial institutions has been done such that the institutions are representative of most of the market capitalization for each category and region. We have also included some firms which have defaulted or have been merged to prevent an estimation bias from the survival financial firms. Our model is flexible enough to deal with unbalanced data, as a defaulted firm at time t in a set of N firms implies that for time t+1 the latent factor would explain the co-movement between the N-1 survival financial firms at t+1. Our sample includes 13 defaulted or merged firms happening during different economic episodes. The default of Lehman Brothers and Washington Mutual or the Merrill Lynch acquisition by Bank of America, Wachovia acquisition by Wells Fargo, and HBOS acquisition by Lloyds are defaults and mergers happening during

¹⁵More information about this matching can be found in this appendix on the OSFI website.

the GFC. The bailout of Monte de Paschi is an example of defaults and acquisitions happening during the European sovereign debt crisis. Banco Popular in Western Europe, Home Capital in Canada, and Silicon Valley Bank (SVB) in the US are institutions that suffered funding stress events during the period of analysis. Credit Suisse and First Republic Bank occurred during the March 2023 banking crisis. Dexia and MF Global were non-banking institutions that defaulted during the period of analysis.

Table 1 presents the RIC code for the stock, common name, sector classification, and 2-digit ISO code for the country of each institution in the sample.

[INSERT TABLE 1 HERE]

4 Results

The results of the model are presented in three subsections. First, the estimates of the dependence model are displayed, showing the time evolution of the dynamic parameters. Second, we analyze what is driving the latent factor over time and which are the contributions of the different types of financial institutions. Third, we compute the proposed systemic risk measures.

To identify the drivers of the latent factors, we obtain the distribution of the latent factor conditional on the performance of the financial firms and we assess how different market variables could explain the upper tail, the lower tail, and the median conditional value of the latent factor. We also identify the contribution of each type of institution in the overall co-movement from the latent factor, captured via the correlation matrix. That contribution might be not linear, as a result of the flexibility of Skewed-t dependence structure, which implies the use of the principal component analysis to gather the main contributors in the correlation structure. Finally, we consider the uncertainty in the model estimation by aggregating the institutions with highest correlation on a top bucket of co-movement with the latent factor. We rely on a similar estimation as Blasques et al. (2016) to get the in-sample confidence bands for the highest correlation within the regional latent factors and we bucket institutions with similar strength in the connection with the latent factor, as Hurlin et al. (2017) have implemented with systemic risk measures. We examine if the top bucket is aligned with the list of DSIBs in each region, ¹⁷ incorporating

¹⁶Krupskii and Joe (2015) provide the analytical expression of the correlation matrix when the dependence is fully Gaussian.

¹⁷The list of systemic institutions is obtained from the supervisory authorities within each region (OSFI, EBA, BoE, OFR, FINMA) and international authorities (BIS, FSB)

NBFIs into the metric.

Regarding systemic risk measures, we present two measures to better understand the tail co-movement between international financial systems, getting a clearer picture on the role of NBFIs in those tail market linkages. First, we assess the conditional expected return within each financial system that generates the highest losses from all the foreign conditioning scenarios with a 5% probability. This would allow us to identify the role of set of institutions as foreign stress scenarios generating the highest impact on market performance of the domestic financial system. Second, we compute how much of the market tail return for domestic financial institutions is shared with tail scenarios in foreign financial systems. We present this decomposition of the average tail return by type of institution to get a better view on how DTIs and NBFIs co-move in the tail with foreign stress events.

4.1 Model estimates

Table 2 gathers the estimates of the long-run correlation with the regional latent factor, i.e., $h(\bar{\rho}_j) = \frac{\omega_j}{1-\beta_i}$ in Eq.(6) for institution j from region i, together with the 90% confidence interval computed by MonteCarlo simulation in brackets.¹⁸ The DSIBs, which are represented with those codes with an asterisk, present the highest correlation with the latent factor, followed by some large insurance companies in Canada (POW.TO, SLF.TO) and Japan (8750.T), other DTIs in US (PNC, USB), and DTIs and investment management companies in Europe (UBSG.S, BBVA.MC).

[INSERT TABLE 2 HERE]

¹⁸The two-step estimation, also known as IFM estimation, implies that simulation is needed for the confidence intervals to include in the copula estimates the uncertainty about the marginal distribution from which we obtained the pseudo probability integral transformations.

The estimates of the parameters of the copula for the regional latent factors are presented in Table 3, where both skewness parameters are negative, being λ_2 lower than λ_1 for most of the regions, with a low number of degrees of freedom. This generates a dependence pattern similar to a Clayton copula, with strong lower tail dependence (see Figures 3 and 4). Table 3 also presents the estimates of the regional and global GAS parameters, showing a high persistence ($\beta > 0.95$). The long-term correlation of the latent regional factor with the global latent factor distinguish two different groups: Canada, the US, and Europe with a correlation close to 75% and Japan with a correlation around 30%.

[INSERT TABLE 3 HERE]

Figure 6 shows the median and mean correlation of each region, together with the cross-section interquartile range for each region. We see a higher dispersion between financial institutions and the Canadian latent factor than the financial institutions within the United States, Japan, or Europe. The United States latent factor presents a median correlation with the financial firms in that region, with a correlation between 65% to 80%. The European latent factor presents a more stable correlation structure with the firms in the region, with median correlation between 70% to 75%. The Canadian latent sector presents a median correlation between 40% to 70%, which is the largest change in the median correlation within the sample, followed by the median correlation between the Japanese financial institutions and the regional factor, with values that go from 60% to 85%.

[INSERT FIGURE 6 HERE]

The size of the correlation matrix might change over time, as a consequence of a

financial institution that is not quoted anymore or that has started quoting. Figure 7 shows how Merrill Lynch, Mellon Financial, and Wachovia present the highest correlation with the US latent factor before being merged or defaulting around 2008. MF Global and Washington Mutual present the lowest correlation with the US latent factor within the financial firms facing issues in the sample. If a firm within a set of N firms stops being quoted at time t + 1, the s_t and f_t from Eq. (6) would be vectors of length N - 1, with the N - 1 firms still being quoted at time t + 1. This figure shows the flexibility of our econometric model to deal with unbalanced data.

[INSERT FIGURE 7 HERE]

The latent factors are related between them via a correlation with a global latent factor. The US latent factor presents the highest correlation with the global latent factor, close to 90%, which is followed by Western Europe and, in third place, Canada, with an average correlation around 75%. The Japanese latent factor presents a much more volatile pattern, as shown by Figure 8, with an average correlation around 30% but a maximum correlation around 60% during 2018 and minimum below zero at 2003 and 2024. There are two periods in which the Japanese latent factor presents a negative correlation with the global latent factor. The periods are from mid-2002 to mid-2003, when the Bank of Japan was implementing quantitative easing to fight deflation while banks were trying to get rid of nonperforming loans (NPLs) from the bursting of asset price bubbles, ¹⁹ and the end of 2023, when there was still a divergence in monetary policy between Japan and the rest of the regions, as key interest rates in Japan were negative and not increasing up to March 2024.

¹⁹See this bulletin from Bank of Japan (BoJ) and this IMF report.

[INSERT FIGURE 8 HERE]

4.2 Latent factor structure

This subsection analyzes the conditional density distribution of the latent factor on the realization from the financial institutions. It also assesses the role of each type of institution to explain the joint dependence structure, identifying the bucket of financial institutions with the highest correlation with the latent factor. Finally, it explores how characteristics of market information shape the conditional distribution of the regional latent factors.

Figure 9 displays the density distribution of the latent regional factor's quantiles, conditional on the financial firms' quantiles within each region. Note that the unconditional distribution of the latent regional factor's quantiles is distributed as uniform (0,1). The conditional distribution shows a concentration on the upper tail for most of the regions, while the Japanese latent factor shows a U-shaped conditional distribution, indicating a higher probability of the latent factor being at extreme quantiles when incorporating the information about the performance of the financial institutions.

[INSERT FIGURE 9 HERE]

Figure 10 shows, in the left axis, the contribution of each type of financial institution to the first principal component of the regional correlation matrix obtained from the latent factor model, assessed as the sum of coefficient for the institutions within the same type of institutions, while the right axis indicates the share of the correlation matrix that could be explained by this first component. This figure provides two important insights about our model and the sector composition explaining the correlation matrix.

First, the percentage of the correlation matrix from the latent factor model that could be explained by the first component of the principal component analysis (PCA) is between 65% (Japan) and 32% (Canada). This indicates that the PCA fails to capture the rich dependence structure from the latent factor link, although the dependence is created by a single factor. Second, the share of that percentage that is explained by DSIBs and other DTIs decreases in Canada (from 50% to 40%) and Japan (from 35% to 30%), while it is constant over time for the US (25%) and Europe (20%). For NBFIs, the most important shares are related to insurance companies followed by investment management and mortgage finance companies.

[INSERT FIGURE 10 HERE]

The main role of DSIBs is also found in the bucket of institutions with the highest correlation with the regional latent factor. The time-varying estimates of correlation shown by Figure 6 present some estimation uncertainty, so a slightly higher value in the correlation of one financial institution compared to the estimated correlation in another firm might be statistically indistinguishable. We employed the iterative bootstrap-based testing procedure proposed by Hurlin et al. (2017) to identify the top group of institutions that, at each time t, are indistinguishable from each other in terms of correlation with the latent regional factor with a confidence level of 95%, showing the highest connection with this factor. Figure 11 shows in the top chart the number of institutions in the top bucket with stronger correlation with the Canadian latent factor and the type of institution. The number of institutions varies from 1 to 10 depending on the time period, showing the largest group during the global financial crisis (GFC) and the smallest group during the 2018–2020 period. At each time period, at least one DSIB is always present in the top

bucket, with a marginal role of insurance companies. The bottom chart from Figure 11 shows the number of institutions in the right axis and the correlation interval considered in the top bucket in the left axis (red area) together with the observations within that range (red dots). The smaller correlation range is 5% (from 85% to 90% during 2020), and the largest correlation range is 35% (from 55% to 90% at the beginning of the sample).

[INSERT FIGURE 11 HERE]

Figure 12 presents the same type of chart for the US, where the presence of a DSIB is nearly constant over time. Investment dealers are more prominent before the GFC, while insurance companies and other DTIs play a larger role in the post-GFC period. The number of institutions in this top bucket goes from 1 to 11, with a correlation range smaller than the Canadian one. The largest 95% confidence interval for the correlation occurs at the beginning of the sample, ranging from 65% to 90% (a 25 percentage point range). The charts for the European region in Figure 13 present the smallest set of institutions along all the regions, where the biggest set of financial institutions in the top bucket is just nine, with a shorter correlation range with a 95% confidence interval being just 10% (from 80% to 90%). The Japanese financial institutions in the top bucket of correlation with its latent factor in Figure 14 support the central role of DSIBs explaining the latent factor, with a relevant presence of other DTIs during the GFC and at the end of 2023.

[INSERT FIGURE 12 HERE]

[INSERT FIGURE 13 HERE]

[INSERT FIGURE 14 HERE]

We explore which individual characteristics of market information are associated with

the probability of the latent factor being at the tails (below the bottom 10% and above the top 10%) or around the median (between percentile 45 to 55). Following previous research on systemic risk, we consider market features, such as market indices,²⁰ as a high-frequency proxy of the performance of the real activity and bond prices as a proxy of credit activity²¹ yield slope (the difference between 10-year and 1-year sovereign government bonds²²) as a leading indicator of recession. We also use some variables related with exchange rates (effective exchange rates)²³ and commodity prices.²⁴ The dataset is sourced from Refinitiv EIKON, unless stated otherwise.

We explore how the change of the weekly lower/middle/upper 10% of each latent factor i is explained by the following panel regression model:

$$\triangle F_{i,t}(q|U_t) = \alpha_i + \sum_{j=1}^{3} \beta_j r_{i,j,t-1} + \lambda \triangle X_{i,t-1} + \sum_{k=1}^{3} \psi_k r_{k,t-1} + \varepsilon_{i,t}, \tag{7}$$

where $\triangle F_{i,t}(q|U_t)$ could be $F_{i,t}(0.1|U_t) - F_{i,t-1}(0.1|U_{t-1})$ for the bottom 10%, $1 - F_{i,t}(0.9|U_t) - (1 - F_{i,t-1}(0.9|U_{t-1}))$ for the top 10% and $F_{i,t}(0.55|U_t) - F_{i,t}(0.45|U_t) - (F_{i,t-1}(0.55|U_{t-1}) - F_{i,t-1}(0.45|U_{t-1}))$ for the middle 10%, where U_t is the transform integral transformation of the firms within that region at time t, β_j are the coefficients for the returns from market, bond, and exchange rate indices, λ is the coefficient for the change in the yield slope, ψ_k is the coefficient associated to the commodities returns, and α_i denotes the region fixed effects. We also control for unobserved heterogeneity by including year fixed-effect dummies.²⁵ We lagged all control variables to mitigate potential reverse causality concerns

 $^{^{20}}$ TSX60, S&P500,EURO STOXX600, TOPIX

 $^{^{21}\}mathrm{S\&P}$ CAN IG CORP BOND 0-10Y INDEX, Bloomberg Security Corporate Bond USD, IBOXX EURO CORPORATES, S&P JAPAN IG CORP BOND INDEX

²²For Europe, we use the German government bond.

²³Nominal with broad basket obtained from BIS.

²⁴S&P GSCI Commodity, S&P GSCI Non-Energy, S&P GSCI Energy & Metals

²⁵We also applied smoothing time effects by using a cubic spline to capture time trends in a more

and compute robust standard errors using double clustering at the region and time levels (see Petersen 2008).

Table 4 shows the results indicating that the stock return plays a key role explaining the change in the distribution of the latent regional factor, with a higher weight in the upper tail. A return of 1% increases the area within the 10% unconditional probability between a 160 b.p. to 1200 b.p. depending on the tail, shaping the conditional distribution into a more leptokurtic shape with a stronger right tail skewness. The bond index return has an opposite sign and half the magnitude of the stock returns, with an effect around the median and in the upper tail. Finally, the exchange rate is just statistically significant for the left tail, having a negative impact on the left tail if the exchange rate appreciates.

[INSERT TABLE 4 HERE]

4.3 Systemic risk measures

We present in this subsection the results for the Return-in-Stress (RiS) for the market-weighted financial index for each region, analyzing the role of the different foreign financial sectors and types of institutions, and the $Expected\ Shortfall\ Allocation\ (ESA)$, distinguishing between DTIs and NBFIs, in different scenarios for domestic and foreign stress.

4.3.1 Return-in-Stress

The Return-in-Stress~(RiS) shows the minimum average return given a tail stress market scenario with a 5% probability. We build the RiS for the market-weighted return from flexible way with similar results.

each region,²⁶ and we look at the foreign stress scenarios with a 5% probability that would condition those outcomes.

Figure 15 shows the RiS for the four regions under scope. Europe shows the highest vulnerability given the worst foreign scenario with a 5% probability. US and Japan returns show a RiS around -7%, while the Canadian RiS shows the lowest volatility and loss, with a loss lower than 5%, crossing the 10% threshold during the GFC and the COVID-19 crisis.

[INSERT FIGURE 15 HERE]

Figure 16 shows the RiS for each region together with the weighted-market return for the financial institutions within each region. The number of exceedances is similar to a Value-at-Risk with a 95% confidence level (the minimum percentage of exceedances being 3.6% of the sample for Canada and the maximum 5.5% of the sample for Japan).

[INSERT FIGURE 16 HERE]

The foreign market scenarios that condition these average returns vary by region. Figures 17 and 18 show, respectively, the upper threshold of the scenario for individual foreign financial institutions or aggregated by region and type of institution (showing the average threshold by category). The top chart in these figures shows the threshold in terms of quantile, while the bottom chart translates the quantile into returns, capturing the marginal characteristics of the returns. Although the joint probability is always 5%, more institutions could be under stress due to a change in the dependence structure.

²⁶For Europe, the market-weighted return is computed in euros, although the dependence structure is built in the local currency. The exchange rate is set as deterministic at each period of time, without considering how the scenario might affect the FX behavior, as this effect is out of scope for this piece of research.

The return threshold could be more extreme because of the higher probability of large losses, presenting the largest losses in the scenarios in mid-2002, 2008–2009, and 2020, coinciding with the stock market downturn of 2002, the GFC, and the COVID-19 crisis. Most of the stress for Canada comes from US and European DSIBs, with some institutions being practically always present over the sample, like JP Morgan (JPM), BNP Paribas (BNPP.PA), and Société Générale (SOGN.PA), while other institutions present a more discontinuous presence in the stress scenario, like ING (INGA.AS) or Bank of America (BAC). The NBFIs are present during a specific time period: for instance, the presence of European insurance companies occurs during the European sovereign debt crisis (2011–2012).

[INSERT FIGURE 17 HERE]

[INSERT FIGURE 18 HERE]

For the US RiS, the scenario leading to the largest average losses changes over time, while the weight in European DSIBs is more relevant before 2017, and Canadian DSIBs become more relevant to generate the worst average return in US financial institutions. This can be seen in the darker colors in Figure 20 in European and Canadian DSIBs. At the individual institution assessment, shown by Figure 19, the Canadian DSIB present in this scenario is concentrated in the Royal Bank of Canada (RY.TO), which is the largest bank in Canada in term of market capitalization.²⁷ The presence of NBFIs in this market scenario for the US is marginal, with the European insurance companies being relevant during the 2011–2012 period. Deutsche Bank (DBKGn.DE) is present in the stress scenario before the GFC and the European sovereign debt crisis, but not afterward.

²⁷https://financialpost.com/feature/how-rbc-became-canada-biggest-bank

[INSERT FIGURE 19 HERE]

[INSERT FIGURE 20 HERE]

The RiS for Europe is generated by a scenario where the stress is shared by Canadian and US DSIBs, with a more relevant presence of US NBFI institutions, as shown by Figure 22. The presence of other DTIs in the scenario occurs for the US but not for Canada. The stress during early 2023, when the SVB crisis occurred, is reflected in other DTIs being included in the scenario, but with the stress, measured in terms of quantiles, being lower than in US DSIBs, showing that the US DSIBs work as a market transmission with international markets. Also, the international market connection of SVB is lower than other DTIs, like PNC, as shown by Figure 21. The role of Japanese institutions is marginal for international stress scenarios for Canada, the US, and Europe.

[INSERT FIGURE 21 HERE]

[INSERT FIGURE 22 HERE]

For the Japanese RiS, the connection with foreign financial institutions is weaker, which explains the larger number of institutions under the 5% probability scenario compared to the number of institutions for the scenarios in Canada, the US, and Europe. The stress is mainly focused on DSIBs, with the presence of NBFIs just for the US region, as shown by Figure 24. Figure 23 shows that Société Générale (SOGN.PA) and Morgan Stanley (MS) are more relevant, in terms of being in a lower quantile, at the beginning of the sample, while Bank of America (BAC) and Royal Bank of Canada (RY.TO) are more relevant at the end of the sample. JP Morgan (JPM) and BNP Paribas (BNPP.PA) are continuously present in the scenario over the full period.

[INSERT FIGURE 23 HERE]

[INSERT FIGURE 24 HERE]

4.3.2 Expected Shortfall Allocation

We divide the Expected Shortfall for each financial institution into four categories, depending on if those tail losses are happening or not at the same time as left tail realizations on the latent domestic and foreign factor.²⁸ This decomposition allows us to identify an idiosyncratic section, where only the financial institution under analysis is at the tail; a domestic section, where tail returns for the institution under analysis is happening at the same time as left tail realizations for the domestic sector but not for any foreign sector; a foreign sector, which would indicate the opposite; and a global section, where the tail returns are happening for domestic and foreign sectors, too.

Figure 25 presents the ESA of a Japanese financial firm (left axis), the correlation of the financial institution with the regional factor (black line, right axis), and the correlation between the Japanese latent factor and the global latent factor (red line, right axis). We distinguish three different combinations of correlations that generate a different decomposition of the Expected Shortfall. Before 2010, correlation between the Japanese factor and the global factor is above 50%, but the correlation between the Japanese firm and the regional factor is close to zero, which makes the idiosyncratic sector of the Expected Shortfall close to 70% and the global section slightly above 10%. In 2019, both series of correlations are close to their historical maximum: the idiosyncratic sector around 25%, the global section 30%, and the domestic section 35%. At the beginning of 2024, the correlation between the regional factor and the global factor is close to zero,

 $^{^{28}}$ We also perform this exercise with a certain number of institutions being at the tail, e.g., a domestic tail event would be an event in which at least N domestic institutions are in their tail, similar to the approach used by Gravelle and Li (2013). Results are similar if the number of institutions under stress is 4 or more. This comparison allows us to better understand what the tail event for the latent factor implies.

while the correlation between the firm and the regional factor is still at its maximum. This is reflected in a 40% share of the domestic section, a 30% share of both idiosyncratic and global portions, and a 25% share of the global part. This representation shows how the evolution of the dependence structure is captured by the changes in the *Expected Shortfall Allocation*.

[INSERT FIGURE 25 HERE]

Figures 26 to 29 present the shares of the Expected Shortfall (left axis) and the actual Expected Shortfall (right axis) of the DSIBs and DTIS (left charts) and NBFI (right charts) aggregated by market weight for the four different regions. Canadian and European NBFIs show a more volatile pattern of the Expected Shortfall than for DSIBs and DTIs in the same region, while for the US and Japan, the opposite is true. One insight that we can appreciate in all the regions is a higher share of the idiosyncratic part in NBFIs than in DTIs, which implies a higher tail co-movement between DTIs and foreign financial systems. The domestic share is usually larger than the global share, which indicates a "home bias" feature, meaning that cross-country contribution to the Expected Shortfall tends to be smaller than domestic risk contribution, aligned with the results found by Gravelle and Li (2013) for Canada.

[INSERT FIGURE 26 HERE]

[INSERT FIGURE 27 HERE]

[INSERT FIGURE 28 HERE]

[INSERT FIGURE 29 HERE]

5 Conclusion

This paper develops a flexible multivariate framework that captures tail co-movements across financial institutions to analyze international systemic risk. We propose two systemic risk measures: the Return-in-Stress (RiS), which identifies the most adverse international scenario for a domestic financial system under a fixed joint probability constraint; and the Expected Shortfall Allocation (ESA), which decomposes individual institutions' tail losses according to the presence or absence of systemic distress across domestic and foreign markets. These measures are built using a bi-factor latent Skewed-t copula model that captures non-linear dependencies, asymmetries, and time-varying features in the joint distribution of returns across a large cross-section of global financial institutions. This approach, inspired by a reverse stress-testing perspective, provides a more realistic and scenario-rich characterization of systemic risk than traditional models.

Using weekly equity returns from 2001 to 2024, we examine financial institutions from Canada, the United States, Western Europe, and Japan, including both banks and non-bank financial intermediaries (NBFIs). Our empirical findings underscore the central role of DSIBs and other deposit-taking institutions in shaping tail dependencies and international spillovers. These institutions consistently appear in scenarios that maximize conditional domestic losses and exhibit a large non-idiosyncratic share of their Expected Shortfall. While NBFIs historically played a secondary role, their systemic relevance has grown—especially in the U.S.—with insurance firms, asset managers, and mortgage finance companies showing rising co-movement with regional risk factors. Regionally, stress originating in the U.S. and Europe tends to produce the most severe international

spillovers. The systemic weight of Canada has increased since 2017, while Japan remains relatively insulated, consistent with previous findings (e.g., Gravelle and Li 2013).

The results should be interpreted with care given three important considerations. First, the use of equity data means the analysis focuses on listed firms, potentially underrepresenting parts of the financial system with limited or no market data—such as small
banks, pension funds, or other non-listed institutions. Second, the framework captures
co-movement through market prices, emphasizing confidence and information channels,
while other transmission mechanisms, such as direct exposures or funding links, might be
better captured using balance sheet data. Third, the reverse stress testing approach begins with the outcome—extreme and unlikely losses—and identifies the financial scenarios
in which these events tend to occur. This highlights the conditions most often present
when distress happens but does not imply that these conditions are the most likely to
lead to distress. The method reveals associations conditional on loss events rather than
causal drivers and, consequently, should be used to complement forward-looking risk
assessments.

This framework opens several avenues for future research. It can be extended to analyze tail risk connections among emerging markets, taking into account the role of exchange rate dynamics in shaping cross-border stress transmission. Recent work (Du et al. 2018; Ojea-Ferreiro and Reboredo 2022) emphasizes that frictions in FX markets are key to understanding how financial shocks propagate internationally, particularly in times of equity market distress. The *Return-in-Stress* methodology could also support the development of multi-institution, multi-region generalizations of *CoVaR* or *SRISK*, enhancing the systemic risk monitoring toolkit. Additionally, the *Expected Shortfall Allocation* enables the decomposition of tail risk across any grouping of interest—not only

by region, but also by institution type, asset class, or exposure category. For instance, it could be used to disentangle severe declines in banks' regulatory capital in scenarios involving mortgage defaults, market shocks, yield curve shifts, or other valuation risk factors. Adapting the model to alternative data types, such as CDS spreads or bond yields, may also provide a more comprehensive view of financial fragility. Ultimately, this approach can inform the design of macroprudential policies to limit the cross-border transmission of financial stress.

References

- Aas, K., C. Czado, A. Frigessi, and H. Bakken (2009). Pair-copula constructions of multiple dependence. *Insurance: Mathematics and Economics* 44(2), 182–198.
- Abad, J., M. D'Errico, N. Killeen, V. Luz, T. Peltonen, R. Portes, and T. Urbano (2022).

 Mapping exposures of EU banks to the global shadow banking system. *Journal of Banking & Finance* 134, 106168.
- Acemoglu, D., A. Ozdaglar, and A. Tahbaz-Salehi (2015). Systemic risk and stability in financial networks. *American Economic Review* 105(2), 564–608.
- Acharya, V., R. Engle, and M. Richardson (2012). Capital shortfall: A new approach to ranking and regulating systemic risks. *American Economic Review* 102(3), 59–64.
- Acharya, V. V., N. Cetorelli, and B. Tuckman (2024). The Growing Risk of Spillovers and Spillbacks in the Bank-NBFI Nexus. *Liberty Street Economics*.
- Acharya, V. V., L. H. Pedersen, T. Philippon, and M. Richardson (2017). Measuring systemic risk. *The Review of Financial Studies* 30(1), 2–47.
- Adrian, T. and M. K. Brunnermeier (2016). CoVaR. The American Economic Review 106(7), 1705.
- Aradillas Fernandez, A., M. Hiti, and A. Sarkar (2024). Are Nonbank Financial Institutions Systemic? *Liberty Street Economics*.
- Bank for International Settlements (2025). Banks' interconnections with non-bank financial intermediaries. Technical report d598, Bank for International Settlements.

- Bianchi, J. (2011). Overborrowing and systemic externalities in the business cycle. *American Economic Review* 101(7), 3400–3426.
- Blasques, F., S. J. Koopman, K. Łasak, and A. Lucas (2016). In-sample confidence bands and out-of-sample forecast bands for time-varying parameters in observation-driven models. *International Journal of Forecasting* 32(3), 875–887.
- Blasques, F., J. van Brummelen, S. J. Koopman, and A. Lucas (2022). Maximum likelihood estimation for score-driven models. *Journal of Econometrics* 227(2), 325–346.
- Brownlees, C. and R. F. Engle (2017). SRISK: A conditional capital shortfall measure of systemic risk. The Review of Financial Studies 30(1), 48–79.
- Brychkov, Y. A. (2016). Higher derivatives of the Bessel functions with respect to the order. *Integral Transforms and Special Functions* 27(7), 566–577.
- Cai, J. (1994). A Markov model of switching-regime arch. Journal of Business & Economic Statistics 12(3), 309–316.
- Creal, D., S. J. Koopman, and A. Lucas (2013). Generalized autoregressive score models with applications. *Journal of Applied Econometrics* 28(5), 777–795.
- Demarta, S. and A. J. McNeil (2005). The t copula and related copulas. *International Statistical Review* 73(1), 111–129.
- Demirer, M., F. X. Diebold, L. Liu, and K. Yilmaz (2018). Estimating global bank network connectedness. *Journal of Applied Econometrics* 33(1), 1–15.
- Diebold, F. X. and K. Yılmaz (2014). On the network topology of variance decomposi-

- tions: Measuring the connectedness of financial firms. *Journal of Econometrics* 182(1), 119–134.
- Du, W., A. Tepper, and A. Verdelhan (2018). Deviations from covered interest rate parity. The Journal of Finance 73(3), 915–957.
- ECB (2009, December). The concept of systemic risk. Technical report, European Central Bank.
- Elliott, M., B. Golub, and M. O. Jackson (2014). Financial networks and contagion.

 American Economic Review 104 (10), 3115–3153.
- Engle, R. and B. Kelly (2012). Dynamic equicorrelation. *Journal of Business & Economic Statistics* 30(2), 212–228.
- Financial Stability Board (2024). Global monitoring report on non-bank financial intermediation: 2024. Technical report, Financial Stability Board. 2024 edition.
- Gadea, M. D., L. Laeven, and G. Pérez-Quirós (2020). Growth-and-risk trade-off. Technical report, ECB Working Paper.
- Girardi, G. and A. T. Ergün (2013). Systemic risk measurement: Multivariate GARCH estimation of CoVaR. *Journal of Banking & Finance* 37(8), 3169–3180.
- Gonzalez-Rivera, G., J. Maldonado, and E. Ruiz (2019). Growth in stress. *International Journal of Forecasting* 35(3), 948–966.
- González-Rivera, G., C. V. Rodríguez-Caballero, and E. Ruiz (2024). Expecting the unexpected: Stressed scenarios for economic growth. *Journal of Applied Econometrics* 39(5), 926–942.

- González-Santander, J. (2018). Closed-form expressions for derivatives of Bessel functions with respect to the order. *Journal of Mathematical Analysis and Applications* 466(1), 1060–1081.
- González-Santander, J. L. (2023). Reflection formulas for order derivatives of Bessel functions. Results in Mathematics 78(1), 30.
- Gravelle, T. and F. Li (2013). Measuring systemic importance of financial institutions:

 An extreme value theory approach. *Journal of Banking & Finance* 37(7), 2196–2209.
- Hansen, B. E. (1994). Autoregressive conditional density estimation. *International Economic Review*, 705–730.
- Hurlin, C., S. Laurent, R. Quaedvlieg, and S. Smeekes (2017). Risk measure inference.

 Journal of Business & Economic Statistics 35(4), 499–512.
- Joe, H. (2014). Dependence Modeling with Copulas. Chapman & Hall/CRC Monographs on Statistics & Applied Probability. Taylor & Francis.
- Joe, H. and J. J. Xu (1996). The estimation method of inference functions for margins for multivariate models. Technical report, Department of Statistics, University of British Columbia.
- Koopman, S. J., A. Lucas, and M. Scharth (2016). Predicting time-varying parameters with parameter-driven and observation-driven models. *Review of Economics and Statistics* 98(1), 97–110.
- Krupskii, P. and H. Joe (2013). Factor copula models for multivariate data. *Journal of Multivariate Analysis 120*, 85–101.

- Krupskii, P. and H. Joe (2015). Structured factor copula models: Theory, inference and computation. *Journal of Multivariate Analysis* 138, 53–73.
- Lucas, A., B. Schwaab, and X. Zhang (2014). Conditional euro area sovereign default risk. *Journal of Business & Economic Statistics* 32(2), 271–284.
- Lucas, A., B. Schwaab, and X. Zhang (2017). Modeling financial sector joint tail risk in the euro area. *Journal of Applied Econometrics* 32(1), 171–191.
- Mainik, G. and E. Schaanning (2014). On dependence consistency of CoVaR and some other systemic risk measures. Statistics & Risk Modeling 31(1), 49–77.
- Montagna, M., G. Torri, and G. Covi (2020). On the origin of systemic risk. Technical Report 2502, ECB Working Paper.
- Oh, D. H. and A. J. Patton (2017). Modeling dependence in high dimensions with factor copulas. *Journal of Business & Economic Statistics* 35(1), 139–154.
- Oh, D. H. and A. J. Patton (2018). Time-varying systemic risk: Evidence from a dynamic copula model of CDS spreads. *Journal of Business & Economic Statistics* 36(2), 181–195.
- Oh, D. H. and A. J. Patton (2023). Dynamic factor copula models with estimated cluster assignments. *Journal of Econometrics* 237(2), 105374.
- Ojea Ferreiro, J. (2020). Disentangling the role of the exchange rate in oil-related scenarios for the European stock market. *Energy Economics* 89, 104776.
- Ojea-Ferreiro, J. (2025). Perceived interconnections under stress between Canadian banks and non-bank financial intermediaries. Staff Analitical Note Bank of Canada.

- Ojea-Ferreiro, J. and J. C. Reboredo (2022). Exchange rates and the global transmission of equity market shocks. *Economic Modelling* 114, 105914.
- Ojea-Ferreiro, J., J. C. Reboredo, and A. Ugolini (2024). Systemic risk effects of climate transition on financial stability. *International Review of Financial Analysis* 96, 103722.
- Petersen, M. A. (2008). Estimating standard errors in finance panel data sets: Comparing approaches. *The Review of Financial Studies* 22(1), 435–480.
- Romano, J. P. and A. F. Siegel (1986). Counterexamples in probability and statistics.

 CRC Press.
- Segoviano, M. A. and C. Goodhart (2010). Banking stability measures. *IMF Working Papers* 2010(09/4).
- Sklar, M. (1959). Fonctions de répartition à n dimensions et leurs marges. In *Annales de l'ISUP*, Volume 8, pp. 229–231.
- Smith, M. S. (2023). Implicit copulas: An overview. *Econometrics and Statistics* 28, 81–104.
- Stroud, A. H., D. Secrest, et al. (1966). Gaussian quadrature formulas, Volume 374.

 Prentice-Hall.
- Van Oordt, M. and C. Zhou (2019). Systemic risk and bank business models. *Journal of Applied Econometrics* 34(3), 365–384.
- Van Oordt, M. R. (2023). Calibrating the magnitude of the countercyclical capital buffer using market-based stress tests. *Journal of Money, Credit and Banking* 55(2-3), 465–501.

Yang, Z.-H. and Y.-M. Chu (2017). On approximating the modified Bessel function of the second kind. *Journal of Inequalities and Applications* 2017, 1–8.

Appendix

Tables

Table 1: Financial institutions in the sample

Code	EBET Classification	Company Common Name	Country
BAM.TO	Investment Management Companies	Brookfield Asset Management Ltd	CA
BMO.TO*	DTIs	Bank of Montreal	CA
BNS.TO*	DTIs	Bank of Nova Scotia	CA
CF.TO	Investment Dealers	Canaccord Genuity Group Inc	CA
CHW.TO	Leasing & Finance Companies	Chesswood Group Ltd	CA
CIX.TO	Investment Management Companies	CI Financial Corp	CA
CM.TO*	DTIs	Canadian Imperial Bank of Com-	CA
		merce	
CWB.TO	DTIs	Canadian Western Bank	CA
CYB.TO	Investment Management Companies	Cymbria Corp	CA
ECN.TO	Mortgage Finance Companies	ECN Capital Corp	CA
EFN.TO	Leasing & Finance Companies	Element Fleet Management Corp	CA
EQB.TO	Mortgage Finance Companies	EQB Inc	CA
FFH.TO	Insurance Companies	Fairfax Financial Holdings Ltd	CA
FN.TO	Mortgage Finance Companies	First National Financial Corp	CA
GSY.TO	Mortgage Finance Companies	goeasy Ltd	CA
GWO.TO	Insurance Companies	Great-West Lifeco Inc	CA
HCG.TO^I23	Mortgage Finance Companies	Home Capital Group Inc	CA
IAG.TO	Insurance Companies	iA Financial Corporation Inc	CA
IFC.TO	Insurance Companies	Intact Financial Corp	CA
IGM.TO	Investment Management Companies	IGM Financial Inc	CA
LB.TO	DTIs	Laurentian Bank of Canada	CA
MFC.TO	Insurance Companies	Manulife Financial Corp	CA
MKP.TO	Mortgage Finance Companies	MCAN Mortgage Corp	CA
NA.TO*	DTIs	National Bank of Canada	CA
ONEX.TO	Investment Management Companies	Onex Corp	CA
POW.TO	Insurance Companies	Power Corporation of Canada	CA
PRL.TO	Clearing Houses	Propel Holdings Inc	CA
RY.TO*	DTIs	Royal Bank of Canada	CA
SII.TO	Investment Management Companies	Sprott Inc	CA
SLF.TO	Insurance Companies	Sun Life Financial Inc	CA
TD.TO*	DTIs	Toronto-Dominion Bank	CA
TF.TO	Mortgage Finance Companies	Timbercreek Financial Corp	CA
VBNK.TO	DTIs	VersaBank	CA
X.TO	Clearing Houses	TMX Group Ltd	CA

^{*} indicates a Domestic Systemic Important Bank (DSIB) according to OSFI.

 ${\bf Table~1:~Financial~institutions~in~the~sample~(Cont.)}$

Code	EBET Classification	Company Common Name	Country
JPM*	Investment Dealers	JPMorgan Chase & Co	US
MS^*	Investment Dealers	vestment Dealers Morgan Stanley	
C^*	Investment Dealers	Citigroup Inc	US
BX	Investment Management Companies	Blackstone Inc	US
GS^*	Investment Dealers	Goldman Sachs Group Inc	US
BLK	Investment Management Companies	BlackRock Inc	US
APO	Investment Management Companies	Apollo Global Management Inc	US
KKR	Investment Management Companies	KKR & Co Inc	US
SCHW.K	Investment Management Companies	Charles Schwab Corp	US
IBKR.O	Investment Dealers	Interactive Brokers Group Inc	US
BK*	Investment Management Companies	Bank of New York Mellon Corp	US
STT*	Investment Management Companies	State Street Corp	US
MER.N^A09	Investment Dealers	Merrill Lynch & Co Inc	US
MEL^G07	Investment Management Companies	Mellon Financial Corp	US
LEHMQ.PK^C12	Investment Dealers	Lehman Brothers Holdings Inc	US
MFGLQ.PK^F13	Investment Dealers	MF Global Holdings Ltd	US
WFC*	DTIs	Wells Fargo & Co	US
USB	DTIs	US Bancorp	US
BAC*	DTIs	Bank of America Corp	US
PNC	DTIs	PNC Financial Services Group Inc	US
FCNCA.O	DTIs	First Citizens BancShares Inc	US
		(Delaware)	
FRCB.PK	DTIs	First Republic Bank	US
SIVBQ.PK	DTIs	SVB Financial Group	US
WB.N^A09	DTIs	Wachovia Corp	US
ALL	Insurance Companies	Allstate Corp	US
PGR	Insurance Companies	Progressive Corp	US
MET	Insurance Companies	MetLife Inc	US
MMC	Insurance Companies	Marsh & McLennan Companies	US
	-	Inc	
FNF	Insurance Companies	Fidelity National Financial Inc	US
AFL	Insurance Companies	Aflac Inc	US
AJG	Insurance Companies	Arthur J. Gallagher & Co.	US
TRV	Insurance Companies	Travelers Companies Inc	US
AIG	Insurance Companies	American International Group Inc	US
PRU	Insurance Companies	Prudential Financial Inc	US
	2 Insurance Companies	WMI Holdings Corp	US
AXP	Leasing & Finance Companies	American Express Co	US
ICE	Clearing Houses	Intercontinental Exchange Inc	US
CME.O	Clearing Houses	CME Group Inc	US
COF	Leasing & Finance Companies	Capital One Financial Corp	US
DFS	Leasing & Finance Companies	Discover Financial Services	US
SYF	Mortgage Finance Companies	Synchrony Financial	US
UWMC.K	Mortgage Finance Companies	UWM Holdings Corp	US

WMC.K Mortgage Finance Companies UWM Holdings Corp
* indicates a Domestic Systemic Important Bank (DSIB) according to OFR, FSB or BIS.

Table 1: Financial institutions in the sample (Cont.)

Code	EBET Classification	Company Common Name	Country
HSBA.L*	DTIs	HSBC Holdings PLC	GB
SAN.MC*	DTIs	Banco Santander SA	ES
BNPP.PA*	DTIs	BNP Paribas SA	FR
ISP.MI*	DTIs	Intesa Sanpaolo SpA	IT
CRDI.MI*	DTIs	UniCredit SpA	IT
INGA.AS*	DTIs	ING Groep NV	NL
LLOY.L*	DTIs	Lloyds Banking Group PLC	GB
CAGR.PA*	DTIs	Credit Agricole SA	FR
BARC.L*	DTIs	Barclays PLC	GB
NDAFI.HE*	DTIs	Nordea Bank Abp	FI
NWG.L*	DTIs	NatWest Group PLC	GB
DBKGn.DE*	DTIs	Deutsche Bank AG	DE
KBC.BR*	DTIs	Kbc Groep NV	BE
STAN.L*	DTIs	Standard Chartered PLC	GB
ERST.VI*	DTIs	Erste Group Bank AG	AT
CBKG.DE*	DTIs	Commerzbank AG	DE
SOGN.PA*	DTIs	Societe Generale SA	FR
HBOS.L^A09	DTIs	HBOS Plc	GB
BIRG.I*	DTIs	Bank of Ireland Group PLC	ΙE
NBGr.AT*	DTIs	National Bank of Greece SA	GR
BMPS.MI	DTIs	Banca Monte dei Paschi di Siena	IT
		SpA	
CSGN.S^F23	DTIs	Credit Suisse Group AG	СН
POP.MC^F17	DTIs	Banco Popular Espanol SA	ES
WTW.O	Insurance Companies	Willis Towers Watson PLC	GB
PRU.L	Insurance Companies	Prudential PLC	GB
AV.L	Insurance Companies	Aviva PLC	GB
СВ	Insurance Companies	Chubb Ltd	СН
ZURN.S	Insurance Companies	Zurich Insurance Group AG	СН
ALVG.DE	Insurance Companies	Allianz SE	DE
AXAF.PA	Insurance Companies	AXA SA	FR
AON	Insurance Companies	Aon PLC	ΙE
UBSG.S	Investment Management Companies	UBS Group AG	СН
PGHN.S	Investment Management Companies	Partners Group Holding AG	СН
III.L	Investment Management Companies	3i Group PLC	GB
LGEN.L	Investment Management Companies	Legal & General Group PLC	GB
AMUN.PA	Investment Management Companies	Amundi SA	FR
LSEG.L	Clearing Houses	London Stock Exchange Group PLC	GB
DB1Gn.DE	Clearing Houses	Deutsche Boerse AG	DE
ENX.PA	Clearing Houses	Euronext NV	NL
SQN.S	Clearing Houses	Swissquote Group Holding SA	СН
BBVA.MC	DTIs	Banco Bilbao Vizcaya Argentaria	ES
		SA	
DEXI.BR^L19	Mortgage Finance Companies	Dexia holding SA	BE

^{*} indicates a Domestic Systemic Important Bank (DSIB) according to FINMA, FSB, EBA, BoE or BIS.

Table 1: Financial institutions in the sample (Cont.)

Code	EBET Classification	Company Common Name	Country
8306.T*	DTIs Mitsubishi UFJ Financial Grou		JP
		Inc	
8316.T*	DTIs	Sumitomo Mitsui Financial Group	JP
		Inc	
8411.T*	DTIs	Mizuho Financial Group Inc	JP
7182.T	DTIs	Japan Post Bank Co Ltd	JP
8308.T	DTIs	Resona Holdings Inc	JP
7186.T	DTIs	Concordia Financial Group Ltd	JP
8331.T	DTIs	Chiba Bank Ltd	JP
5830.T	DTIs	Iyogin Holdings Inc	JP
7163.T	DTIs	SBI Sumishin Net Bank Ltd	JP
8334.T	DTIs	Gunma Bank Ltd	JP
5831.T	DTIs	Shizuoka Financial Group Inc	JP
8418.T	DTIs	Yamaguchi Financial Group Inc	JP
7180.T	DTIs	Kyushu Financial Group Inc	JP
8354.T	DTIs	Fukuoka Financial Group Inc	JP
8304.T	DTIs	Aozora Bank Ltd	JP
5844.T	DTIs	Kyoto Financial Group Inc	JP
8410.T	DTIs	Seven Bank Ltd	JP
8766.T	Insurance Companies Tokio Marine Holdings In-		JP
8725.T	Insurance Companies	MS&AD Insurance Group Hold-	JP
		ings Inc	
6178.T	Insurance Companies	Japan Post Holdings Co Ltd	JP
8750.T	Insurance Companies	Dai-ichi Life Holdings Inc	JP
8630.T	Insurance Companies	Sompo Holdings Inc	JP
8604.T*	Investment Dealers	Nomura Holdings Inc	JP
8601.T*	Investment Dealers	Daiwa Securities Group Inc	JP
8473.T	Investment Dealers	SBI Holdings Inc	JP
8628.T	Investment Dealers	Matsui Securities Co Ltd	JP
8698.T	Investment Dealers	Monex Group Inc	JP
8609.T	Investment Dealers	Okasan Securities Group Inc	JP
8591.T	Leasing & Finance Companies	ORIX Corp	JP
8593.T	Leasing & Finance Companies	Mitsubishi HC Capital Inc	JP
$8252.\mathrm{T}$	Leasing & Finance Companies	Marui Group Co Ltd	JP
8439.T	Leasing & Finance Companies	Tokyo Century Corp	JP
8424.T	Leasing & Finance Companies	Fuyo General Lease Co Ltd	JP
8425.T	Leasing & Finance Companies	Mizuho Leasing Co Ltd	JP

 $^{^{\}ast}$ indicates a Domestic Systemic Important Bank (DSIB) according to BIS.

Table 2: Table of estimates for the long-run correlation with the regional latent factor

CAN	ADA	US		WESTERN E	UROPE	JA	PAN
Code	$ar{ ho}$	Code	$\bar{ ho}$	Code	$\bar{ ho}$	Code	$ar{ ho}$
BAM.TO	0.77 $[0.68, 0.80]$	JPM*	0.88 [0.79,0.88]	HSBA.L*	0.66 $[0.64, 0.68]$	8306.T*	0.89 $[0.79, 0.90]$
BMO.TO*	0.80	MS*	0.83	SAN.MC*	0.83	8316.T*	0.88
BNS.TO*	$\begin{bmatrix} 0.70, 0.82 \\ 0.82 \end{bmatrix}$	C*	$\begin{bmatrix} 0.77, 0.84 \\ 0.84 \end{bmatrix}$	BNPP.PA*	[0.80, 0.83] 0.88	8411.T*	$[0.79, 0.89] \\ 0.87$
CF.TO	$\begin{bmatrix} 0.73, 0.84 \\ 0.44 \end{bmatrix}$	BX	$[0.77, 0.85] \ 0.61$	ISP.MI*	[0.85, 0.88] 0.79	7182.T	$\begin{bmatrix} 0.81, 0.88 \\ 0.74 \end{bmatrix}$
CHW.TO	$\begin{bmatrix} 0.30, 0.53 \\ 0.21 \end{bmatrix}$	GS*	$\begin{bmatrix} 0.56, 0.63 \\ 0.82 \end{bmatrix}$	CRDI.MI*	$[0.76, 0.80] \\ 0.79$	8308.T	$\begin{bmatrix} 0.65, 0.77 \\ 0.81 \end{bmatrix}$
	[0.07, 0.31]		[0.76, 0.83]		[0.76, 0.80]		[0.70, 0.83]
CIX.TO	0.55 $[0.44, 0.60]$	BLK	0.67 [0.60,0.69]	INGA.AS*	$0.87 \\ [0.84, 0.87]$	7186.T	0.86 [0.77,0.88]
CM.TO*	0.80 [0.71,0.83]	APO	0.53 $[0.49, 0.55]$	LLOY.L*	0.72 [0.70,0.73]	8331.T	0.79 [0.73,0.82]
CWB.TO	$\begin{bmatrix} 0.62 \\ [0.53, 0.66] \end{bmatrix}$	KKR	$\begin{bmatrix} 0.61 \\ [0.52, 0.62] \end{bmatrix}$	CAGR.PA*	$\begin{bmatrix} 0.84 \\ [0.81, 0.85] \end{bmatrix}$	5830.T	$\begin{bmatrix} 0.74 \\ [0.65, 0.78] \end{bmatrix}$
CYB.TO	0.33	SCHW.K	0.74	BARC.L*	0.78	7163.T	0.50
ECN.TO	$\begin{bmatrix} 0.20, 0.41 \\ 0.41 \\ \end{bmatrix}$	IBKR.O	$\begin{bmatrix} 0.68, 0.76 \\ 0.53 \\ 0.53 \end{bmatrix}$	NDAFI.HE*	$\begin{bmatrix} 0.75, 0.79 \\ 0.72 \\ \vdots \\ 0.72 \end{bmatrix}$	8334.T	$\begin{bmatrix} 0.41, 0.56 \\ 0.75 \\ 0.75 \end{bmatrix}$
EFN.TO	$\begin{bmatrix} 0.31, 0.48 \\ 0.39 \end{bmatrix}$	BK*	$\begin{bmatrix} 0.48, 0.56 \\ 0.80 \end{bmatrix}$	NWG.L*	$\begin{bmatrix} 0.69, 0.73 \\ 0.73 \end{bmatrix}$	5831.T	$\begin{bmatrix} 0.67, 0.78 \\ 0.77 \end{bmatrix}$
EQB.TO	$\begin{bmatrix} 0.27, 0.47 \\ 0.38 \end{bmatrix}$	STT*	$\begin{bmatrix} 0.75, 0.82 \\ 0.79 \end{bmatrix}$	DBKGn.DE*	$\begin{bmatrix} 0.70, 0.74 \\ 0.83 \end{bmatrix}$	8418.T	$\begin{bmatrix} 0.69, 0.80 \\ 0.74 \end{bmatrix}$
FFH.TO	$\begin{bmatrix} 0.22, 0.45 \\ 0.29 \end{bmatrix}$	MER.N^A09	$[0.72, 0.80] \\ 0.82$	KBC.BR*	[0.80, 0.84] 0.77		$\begin{bmatrix} 0.64, 0.77 \\ 0.79 \end{bmatrix}$
	[0.15, 0.39]		[0.74, 0.83]		[0.75, 0.78]	7180.T	[0.69, 0.81]
FN.TO	$0.35 \\ [0.24, 0.43]$	MEL^G07	0.75 $[0.69, 0.76]$	STAN.L*	0.68 [0.64,0.69]	8354.T	0.77 $[0.68, 0.80]$
GSY.TO	0.26 [0.13,0.37]	LEHMQ.PK^C12	$\begin{bmatrix} 0.62 \\ [0.62, 0.68] \end{bmatrix}$	ERST.VI*	0.68 [0.66,0.70]	8304.T	0.67 [0.60,0.71]
GWO.TO	$\begin{bmatrix} 0.69 \\ [0.57, 0.74] \end{bmatrix}$	MFGLQ.PK^F13	$\begin{bmatrix} 0.52 \\ [0.45, 0.54] \end{bmatrix}$	CBKG.DE*	$\begin{bmatrix} 0.77 \\ [0.73, 0.77] \end{bmatrix}$	5844.T	$\begin{bmatrix} 0.77 \\ [0.67, 0.79] \end{bmatrix}$
HCG.TO^I23	0.41	WFC*	0.81	SOGN.PA*	0.87	8410.T	0.54
IAG.TO	$\begin{bmatrix} 0.27, 0.47 \\ 0.61 \\ 0.61 \end{bmatrix}$	USB	[0.75, 0.82] 0.81	HBOS.L^A09	[0.84, 0.88] 0.67	8766.T	$\begin{bmatrix} 0.42, 0.59 \\ 0.76 \\ 0.25, 0.76 \end{bmatrix}$
IFC.TO	$\begin{bmatrix} 0.51, 0.66 \\ 0.33 \end{bmatrix}$	BAC*	[0.75, 0.82] 0.86	BIRG.I*	[0.64, 0.68] 0.62	8725.T	[0.67, 0.78] 0.76
IGM.TO	$\begin{bmatrix} 0.22, 0.44 \\ 0.66 \end{bmatrix}$	PNC	$[0.79, 0.86] \\ 0.83$	NBGr.AT*	[0.59, 0.63] 0.49	6178.T	$\begin{bmatrix} 0.66, 0.78 \\ 0.73 \end{bmatrix}$
LB.TO	$\begin{bmatrix} 0.57, 0.70 \\ 0.57 \end{bmatrix}$	FCNCA.O	$\begin{bmatrix} 0.77, 0.83 \\ 0.61 \end{bmatrix}$	BMPS.MI	$\begin{bmatrix} 0.45, 0.51 \\ 0.65 \end{bmatrix}$	8750.T	$\begin{bmatrix} 0.65, 0.76 \\ 0.82 \end{bmatrix}$
MFC.TO	$\begin{bmatrix} 0.47, 0.64 \\ 0.73 \end{bmatrix}$	FRCB.PK	$\begin{bmatrix} 0.54, 0.63 \\ 0.66 \end{bmatrix}$	CSGN.S^F23	$\begin{bmatrix} 0.62, 0.66 \\ 0.79 \end{bmatrix}$	8630.T	$\begin{bmatrix} 0.74, 0.84 \\ 0.75 \end{bmatrix}$
	[0.63, 0.77]		[0.60, 0.68]		[0.79, 0.81]		[0.66, 0.78]
MKP.TO	$ \begin{array}{c} 0.30 \\ [0.22, 0.40] \end{array} $	SIVBQ.PK	0.72 [0.67,0.74]	POP.MC^F17	0.67 [0.64,0.68]	8604.T*	0.82 [0.72,0.84]
NA.TO*	0.74 [0.64,0.78]	WB.N^A09	$\begin{bmatrix} 0.72 \\ [0.72, 0.76] \end{bmatrix}$	WTW.O	0.33 [0.29,0.34]	8601.T*	0.82 [0.72,0.84]
ONEX.TO	$\begin{bmatrix} 0.46 \\ [0.36, 0.54] \end{bmatrix}$	ALL	$\begin{bmatrix} 0.60 \\ [0.52, 0.63] \end{bmatrix}$	PRU.L	$\begin{bmatrix} 0.73 \\ [0.70, 0.73] \end{bmatrix}$	8473.T	$\begin{bmatrix} 0.69 \\ [0.59, 0.73] \end{bmatrix}$
POW.TO	0.74 [0.66,0.77]	PGR	$\begin{bmatrix} 0.51 \\ [0.46, 0.54] \end{bmatrix}$	AV.L	$\begin{bmatrix} 0.76 \\ [0.73, 0.76] \end{bmatrix}$	8628.T	$\begin{bmatrix} 0.72 \\ [0.62, 0.77] \end{bmatrix}$
PRL.TO	0.46	MET	0.79	СВ	0.42	8698.T	0.62
RY.TO*	$\begin{bmatrix} 0.36, 0.50 \\ 0.82 \end{bmatrix}$	MMC	$\begin{bmatrix} 0.72, 0.81 \\ 0.58 \end{bmatrix}$	ZURN.S	$\begin{bmatrix} 0.38, 0.44 \\ 0.72 \\ \end{bmatrix}$	8609.T	$\begin{bmatrix} 0.53, 0.66 \\ 0.78 \end{bmatrix}$
SII.TO	$[0.73, 0.84] \\ 0.17$	FNF	$[0.53, 0.62] \ 0.46$	ALVG.DE	$[0.69, 0.73] \\ 0.79$	8591.T	[0.68, 0.81] 0.74
SLF.TO	$\begin{bmatrix} 0.02, 0.27 \\ 0.71 \end{bmatrix}$	AFL	$\begin{bmatrix} 0.40, 0.49 \\ 0.62 \end{bmatrix}$	AXAF.PA	[0.76, 0.80] 0.84	8593.T	$\begin{bmatrix} 0.63, 0.77 \\ 0.71 \end{bmatrix}$
TD.TO*	$\begin{bmatrix} 0.63, 0.74 \\ 0.81 \end{bmatrix}$	AJG	$[0.55, 0.66] \ 0.51$	AON	[0.80, 0.85] 0.33	8252.T	$\begin{bmatrix} 0.62, 0.74 \\ 0.59 \end{bmatrix}$
TF.TO	$\begin{bmatrix} 0.72, 0.83 \\ 0.48 \end{bmatrix}$	TRV	$\begin{bmatrix} 0.47, 0.55 \\ 0.58 \end{bmatrix}$	UBSG.S	$\begin{bmatrix} 0.31, 0.36 \\ 0.82 \end{bmatrix}$	8439.T	$[0.49, 0.66] \\ 0.66$
	[0.33, 0.54]		[0.54, 0.62]		[0.78, 0.82]		[0.57, 0.69]
VBNK.TO	$\begin{bmatrix} 0.21 \\ [0.09, 0.30] \end{bmatrix}$	AIG	$\begin{bmatrix} 0.70 \\ [0.63, 0.72] \end{bmatrix}$	PGHN.S	0.53 $[0.51, 0.54]$	8424.T	$\begin{bmatrix} 0.65 \\ [0.54, 0.70] \end{bmatrix}$
X.TO	0.39 $[0.27, 0.46]$	PRU	0.83 [0.76,0.84]	III.L	0.63 [0.60,0.65]	8425.T	0.69 $[0.60, 0.71]$
		WAMUQ.PK^C12	0.58 [0.52,0.60]	LGEN.L	0.73 $[0.70, 0.74]$		
		AXP	$\begin{bmatrix} 0.75 \\ [0.70, 0.77] \end{bmatrix}$	AMUN.PA	$\begin{bmatrix} 0.69 \\ [0.66, 0.70] \end{bmatrix}$		
		ICE	$\begin{bmatrix} 0.70, 0.77 \\ 0.47 \\ [0.41, 0.50] \end{bmatrix}$	LSEG.L	$\begin{bmatrix} 0.48 \\ 0.45, 0.49 \end{bmatrix}$		
		CME.O	0.43	DB1Gn.DE	0.48		
		COF	$\begin{bmatrix} 0.37, 0.48 \\ 0.78 \\ 0.78 \\ 0.78 \\ 0.00 \end{bmatrix}$	ENX.PA	$ \begin{bmatrix} 0.44, 0.50 \\ 0.40 \\ 0.27, 0.42 \end{bmatrix} $		
		DFS	$\begin{bmatrix} 0.72, 0.80 \\ 0.75 \end{bmatrix}$	SQN.S	$\begin{bmatrix} 0.37, 0.42 \\ 0.42 \end{bmatrix}$		
		SYF	$\begin{bmatrix} 0.68, 0.76 \\ 0.72 \end{bmatrix}$	BBVA.MC	$\begin{bmatrix} 0.39, 0.43 \\ 0.83 \end{bmatrix}$		
		UWMC.K	$\begin{bmatrix} 0.65, 0.74 \\ 0.36 \end{bmatrix}$	DEXI.BR^L19	[0.80, 0.84] 0.68		
		tes of the long-run correla	[0.28, 0.39]		[0.68, 0.72]		

This table presents the estimates of the long-run correlation of each financial institution with the regional latent factor. Top values indicates the estimates using the original data. Bottom values between brackets indicates the 90% confidence interval for the estimates using Monte Carlo simulation. We simulate 200 paths of the data assuming that the original estimated model is the true generating data process. We reestimate the model 200 times using the simulated data and we present in the brackets percentile 5 and 95 for each parameter. Note that, because we are simulating returns, the confidence interval of the dependence estimates includes the uncertainty about the true estimates from the marginal distribution. More information about this method can be found in chapter 5 from Joe (2014).

* indicates a Domestic Systemic Important Bank (DSIB). See Table 1.

Table 3: Table of estimates for the copula structure and the GAS dynamics

	λ_1	λ_2	ν	α	β	$ar{ ho}$
$\overline{\text{CA}}$	-0.16	-0.23	5.19	0.027	0.995	0.72
	[-0.20, -0.09]	[-0.28, -0.18]	[5.14, 5.48]	[0.022, 0.030]	[0.988, 0.995]	[0.63, 0.73]
US	-0.12	-0.16	5.02	0.044	0.988	0.79
	[-0.14, -0.06]	[-0.21, -0.11]	[4.94, 5.25]	[0.038, 0.049]	[0.981, 0.989]	[0.70, 0.80]
WE	-0.12	-0.15	4.99	0.041	0.966	0.78
	[-0.13, -0.07]	[-0.18, -0.10]	[4.95, 5.20]	[0.034, 0.047]	[0.952, 0.973]	[0.68, 0.78]
$_{ m JP}$	-0.12	-0.09	5.00	0.055	0.991	0.30
	[-0.17, -0.07]	[-0.14, -0.03]	[4.78, 5.22]	[0.049, 0.061]	[0.986, 0.992]	[0.25, 0.33]
GL	-1.04	-0.98	6.28	0.073	0.989	
	[-1.07, -0.81]	[-1.01, -0.76]	[6.25, 7.04]	[0.053, 0.118]	[0.974, 0.994]	

This table presents the estimates of the long-run correlation of each financial institution with the regional latent factor. Top values indicates the estimates using the original data. Bottom values between brackets indicates the 90% confidence interval for the estimates using Monte Carlo simulation (W=200). λ_1 and λ_2 are the skewness parameters, ν is the number of degrees of freedom, α and β are the parameters of the GAS dynamics, $\bar{\rho}$ is the long-term correlation between the latent regional factors and the latent global factor.

Table 4: Variables influencing the regional latent factor

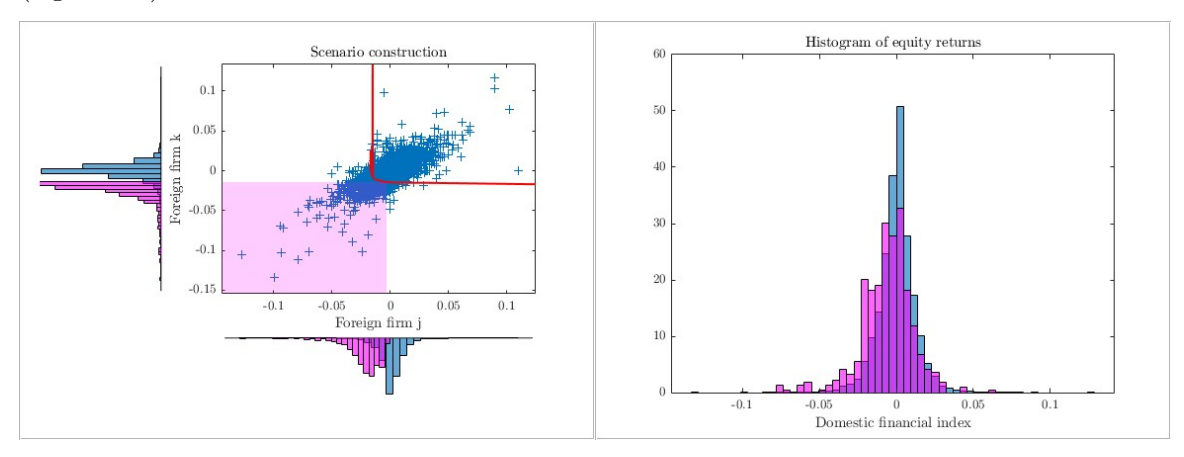
	Distribution of	of the regional	latent factor
	Bottom 10%	Middle 10%	Top 10%
Effective Exchange Rate return	-0.286*	0.882	1.476
	(0.109)	(1.350)	(1.526)
Change in Yield Slope	-0.026	0.082	0.145
	(0.020)	(0.081)	(0.086)
Bond return	-0.396	-3.783*	-4.760**
	(0.345)	(1.295)	(1.420)
Stock return	1.661**	10.41***	11.85***
	(0.287)	(0.769)	(0.715)
Commodity return	0.329	0.104	-1.472
	(0.712)	(3.593)	(4.052)
Energy return	-0.331	-0.645	0.527
	(0.554)	(2.714)	(3.053)
Commodity non-energy return	-0.024	0.181	0.583
	(0.213)	(1.214)	(1.339)
Observations	4,896	4,896	4,896
R-squared	0.163	0.272	0.287

Robust standard errors in parentheses *** p<0.01, ** p<0.05, * p<0.1 This table presents the estimates of Eq. (7) to explain the change in the bottom 10%, middle 10%, or top 10% of the latent factor distribution.

Figures

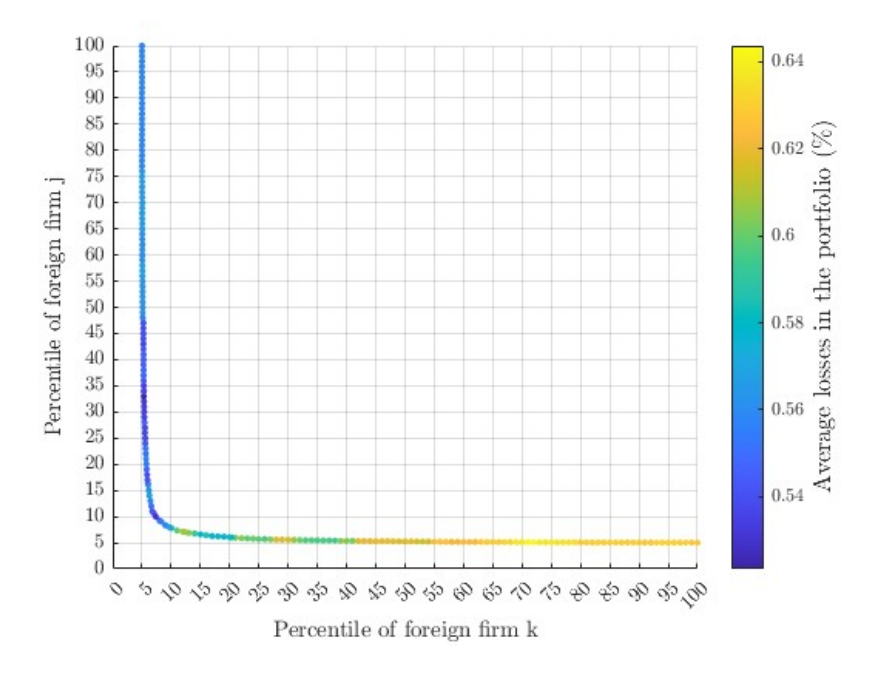
Figure 1: Computation of the Return-in-Stress (RiS)

(a) Effects of a stress scenario (left side) on a distribution of the domestic financial index (right side)



Left side represents the scenario construction that impacts on the returns' distribution of the domestic index on the right side. On the left side, the purple squared area indicates a joint scenario for foreign firms j and k with probability 5% that modifies the distribution of the domestic index returns on the right side from the blue bar to the purple bars. The red line on the left side indicates the upper threshold for firm j and k, below which the probability is 5%. This line is shown in subfigure 1b in terms of percentiles instead of returns.

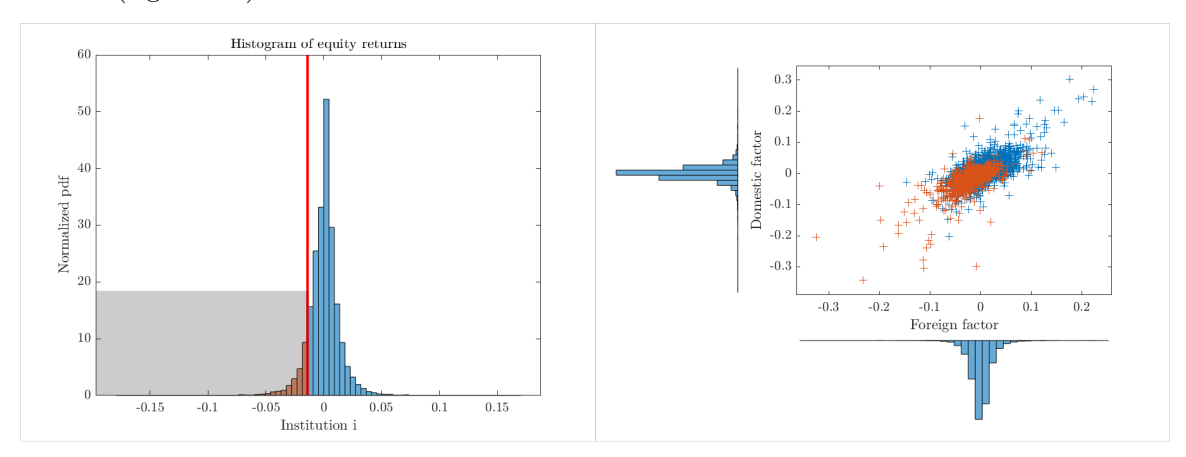
(b) Combination of stress scenarios with probability 5% for two foreign firms.



This graph represents the combination of scenarios built from the percentiles of foreign firm k and j with 5% probability. The color of the line indicates the average loss in the corresponding conditional distribution of the domestic index return.

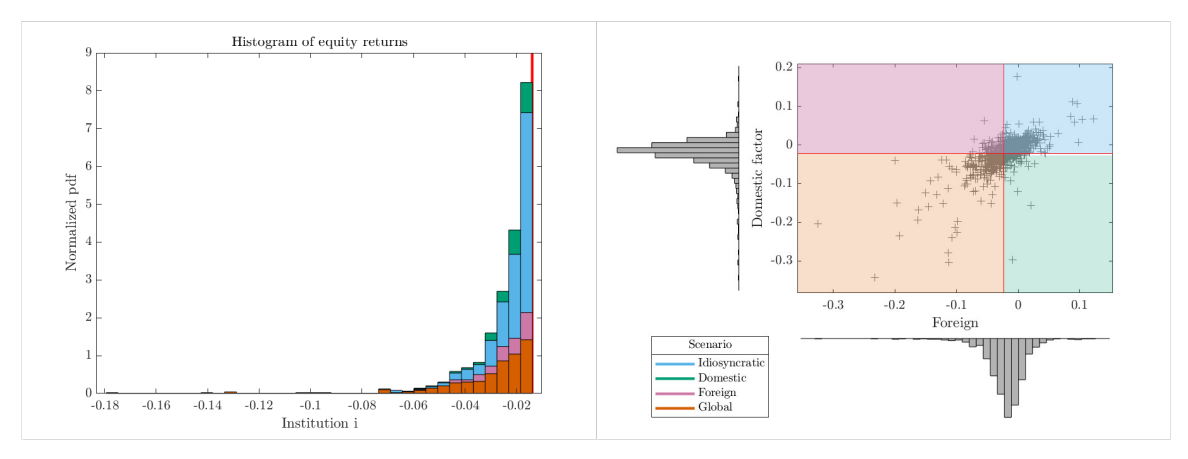
Figure 2: Shares of Expected Shortfall in common tail scenarios

(a) Histogram of returns for institution i (left side) and scatter plot of domestic and foreign factors (right side)



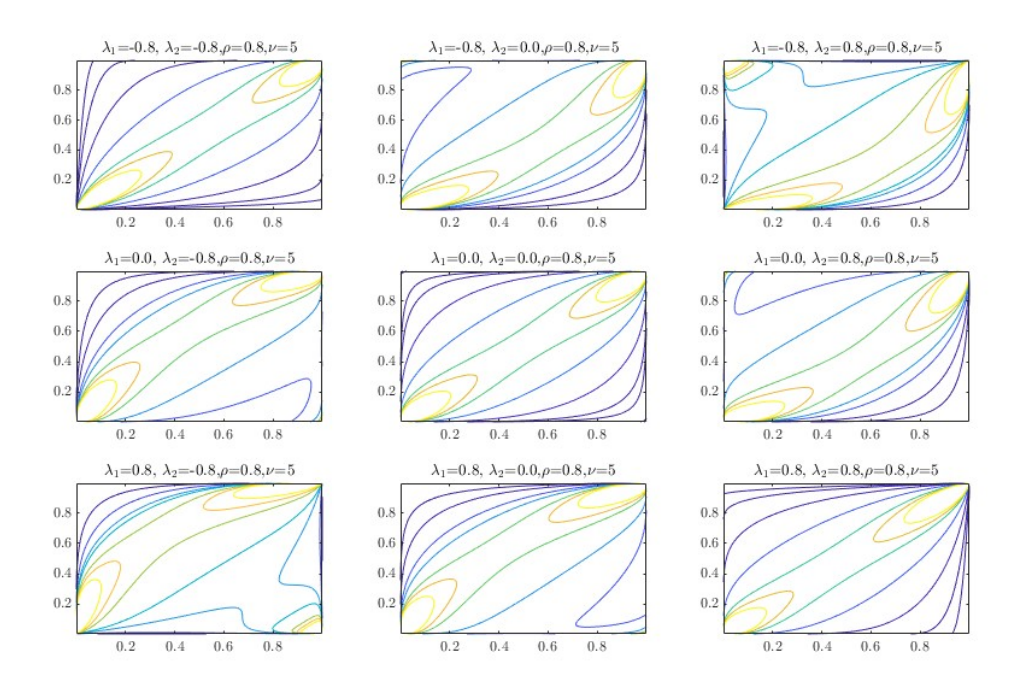
Left side shows the histogram of equity returns for institution i. The tail returns are defined as those below the red threshold (orange bars). Those extreme realizations for institution i are occurring at the same time as the realizations of the domestic and foreign factors shown by the orange dots.

(b) Expected Shortfall Allocation for institution i as the combination of tail scenarios for domestic and foreign factors.



Right scatter plot shows the realizations of domestic and foreign factors when institution i is experiencing tail returns. We divide the area depending on domestic and foreign factors experiencing tail returns. That division allows us to see tail returns of institution i in terms of tail returns for the other factors.

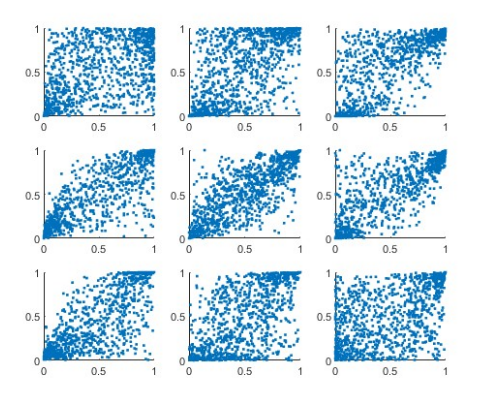
Figure 3: Copula density for different values of λ_1 and λ_2

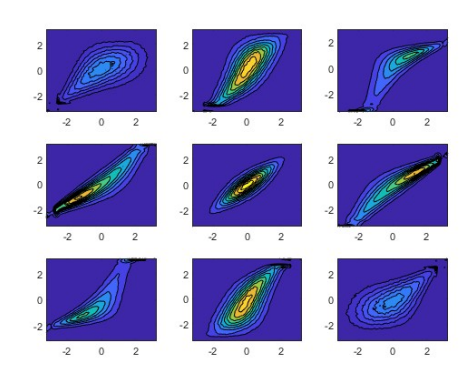


These figures show the density copula of a Skewed Student-t copula with $\rho=0.8$, $\nu=5$ and different values for the asymmetric parameters as shown above each picture

Figure 4: Simulation of a Skewed t copula

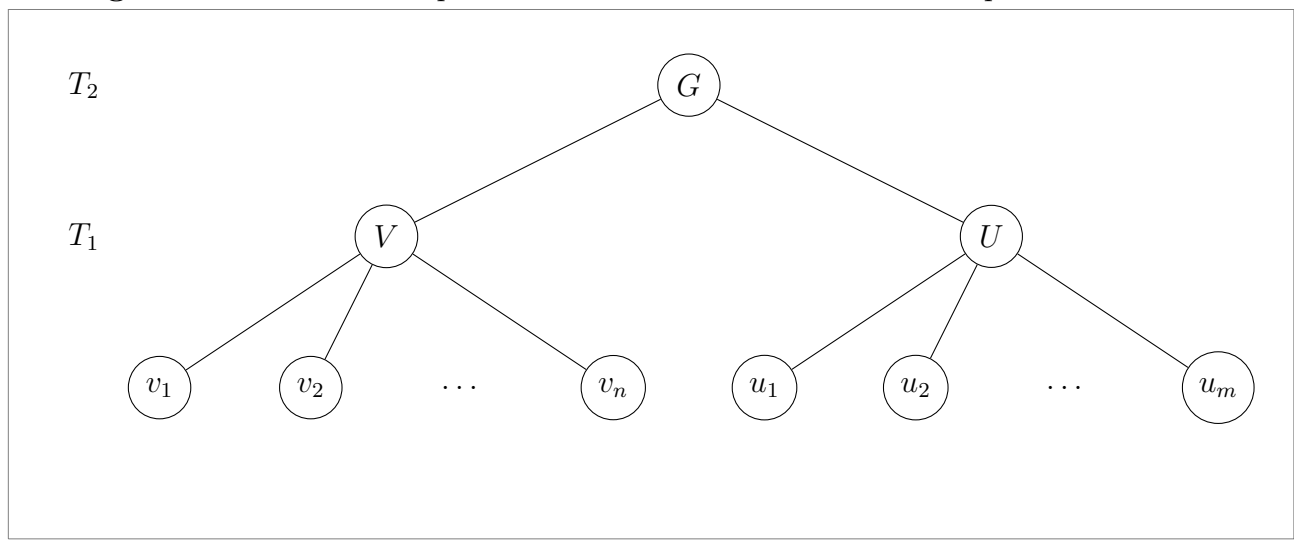
- (a) Simulation of uniform variables with a Skewed-t dependence structure
- (b) Isoquants of normal distributed variables with a Skewed-t dependence structure



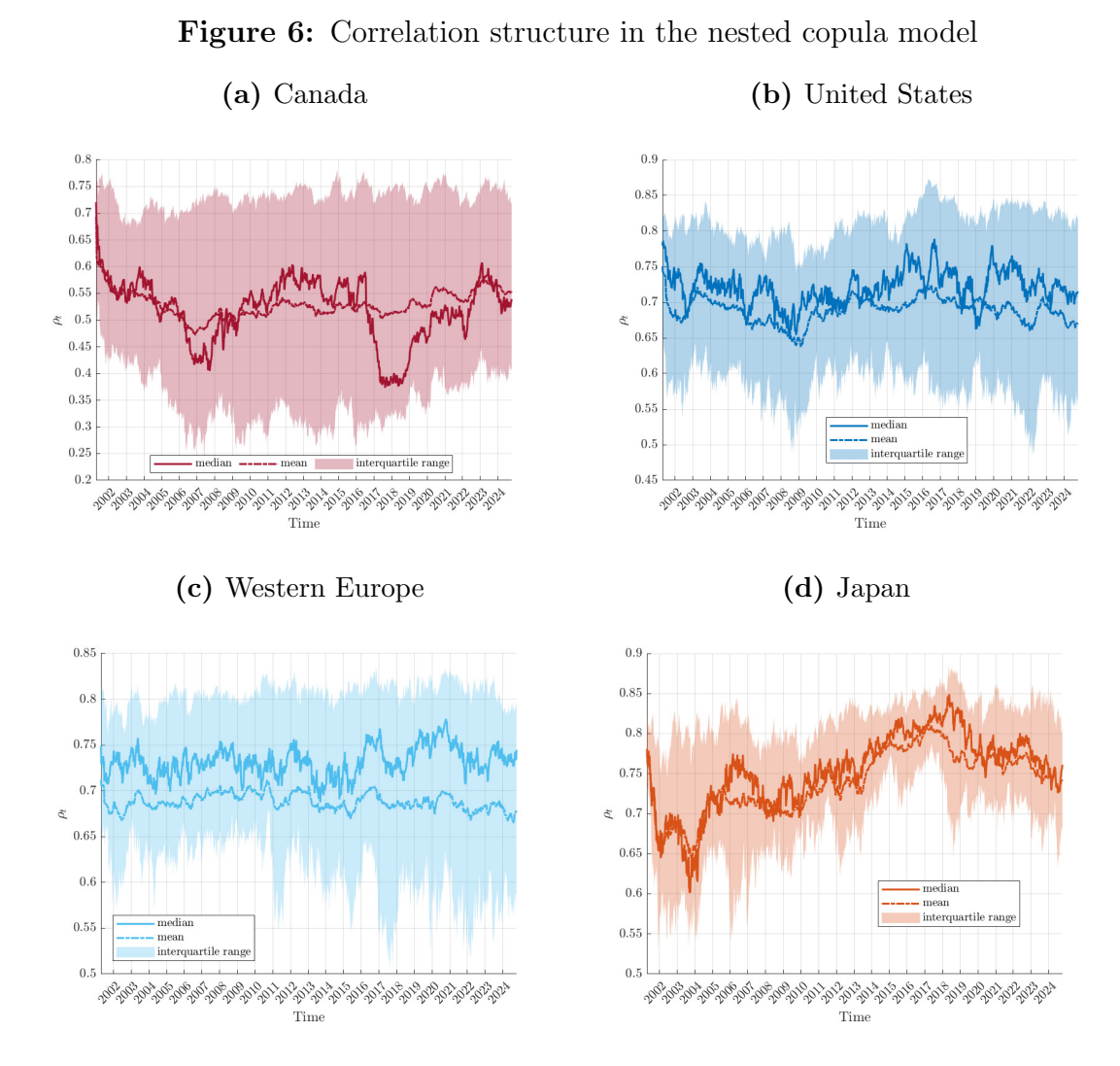


These figures show the simulation from a Skewed Student-t copula with uniform marginals (Figure 4a) and Gaussian marginals (Figure 4b). The parameters selected for the Skewed-t copula are the same as in Figure 3.

Figure 5: Hierarchical dependence structure of a nested factor copula model.

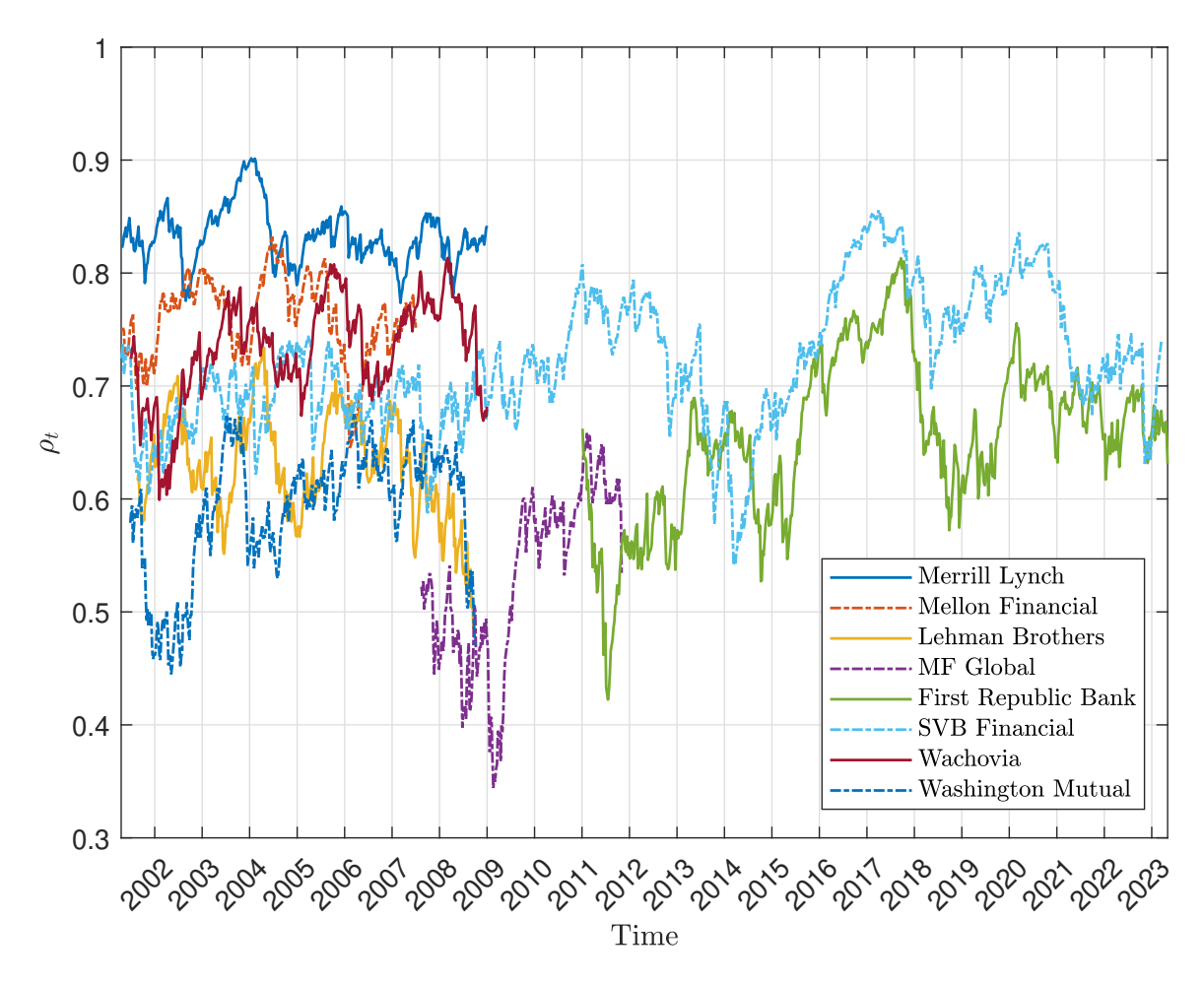


This figure shows the structure of hierarchical dependence for a nested bivariate copula. For variables in the bottom the dependence is always explained by a one-factor model (either factor V or U), and the dependence between the variables with a different factor comes from the dependence between those factors via a second factor, i.e., global factor G, that drives the comovement between factor C and factor U. The estimation process starts with the estimation of the dependence of the bottom layer T_1 , followed by the dependence in the top layer T_2 .



These charts show the interquartile range (area), the median (solid line) and the mean (dashed-dotted line) correlation of the financial institutions in each region with the corresponding latent factor.

Figure 7: Correlation of defaulted financial institutions in United States with the US latent factor



This chart shows the correlation link of eight defaulted or merged financial firms with the US latent factor. The correlation starts when the financial institution starts being quoted and ends when it stops being quoted, increasing and decreasing the matrix correlation between financial institutions in United States.

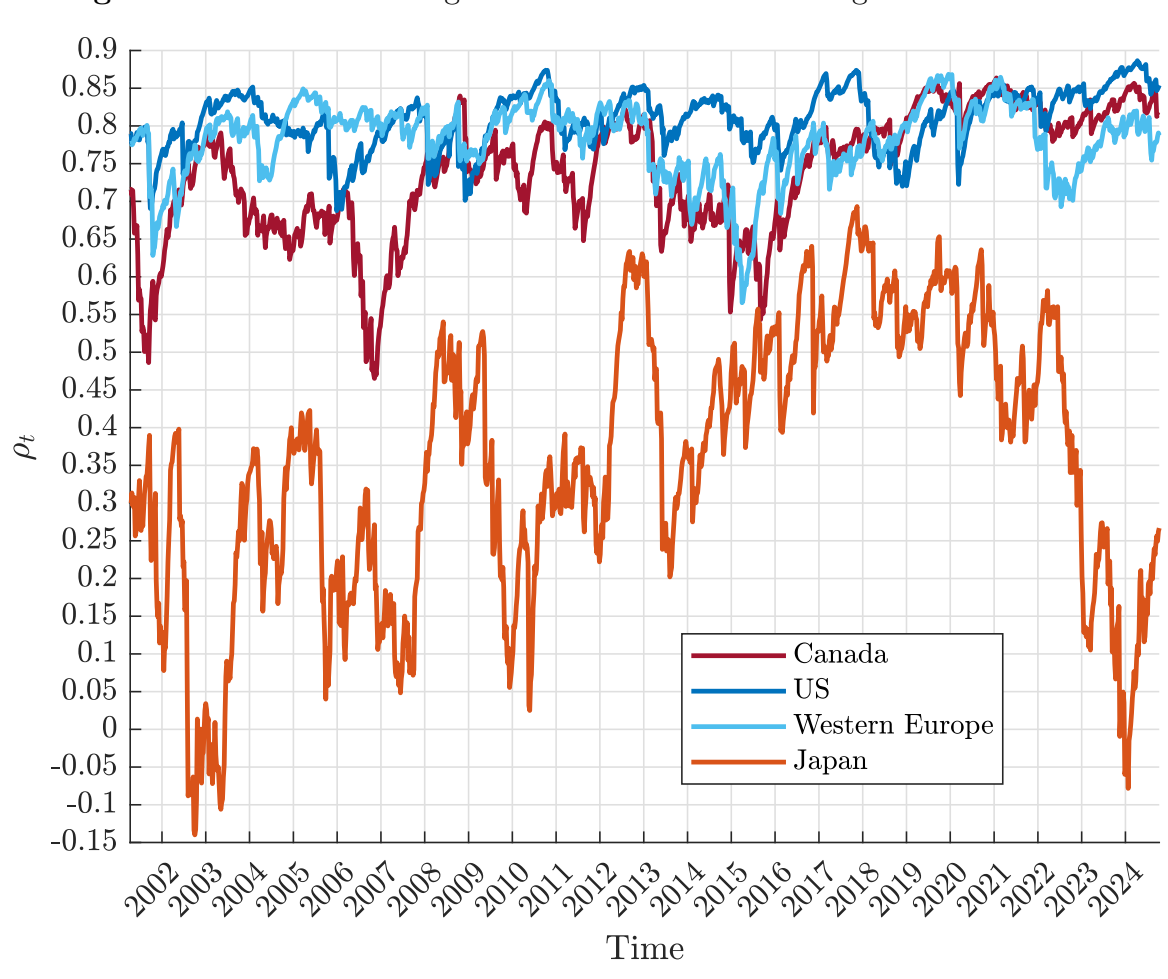
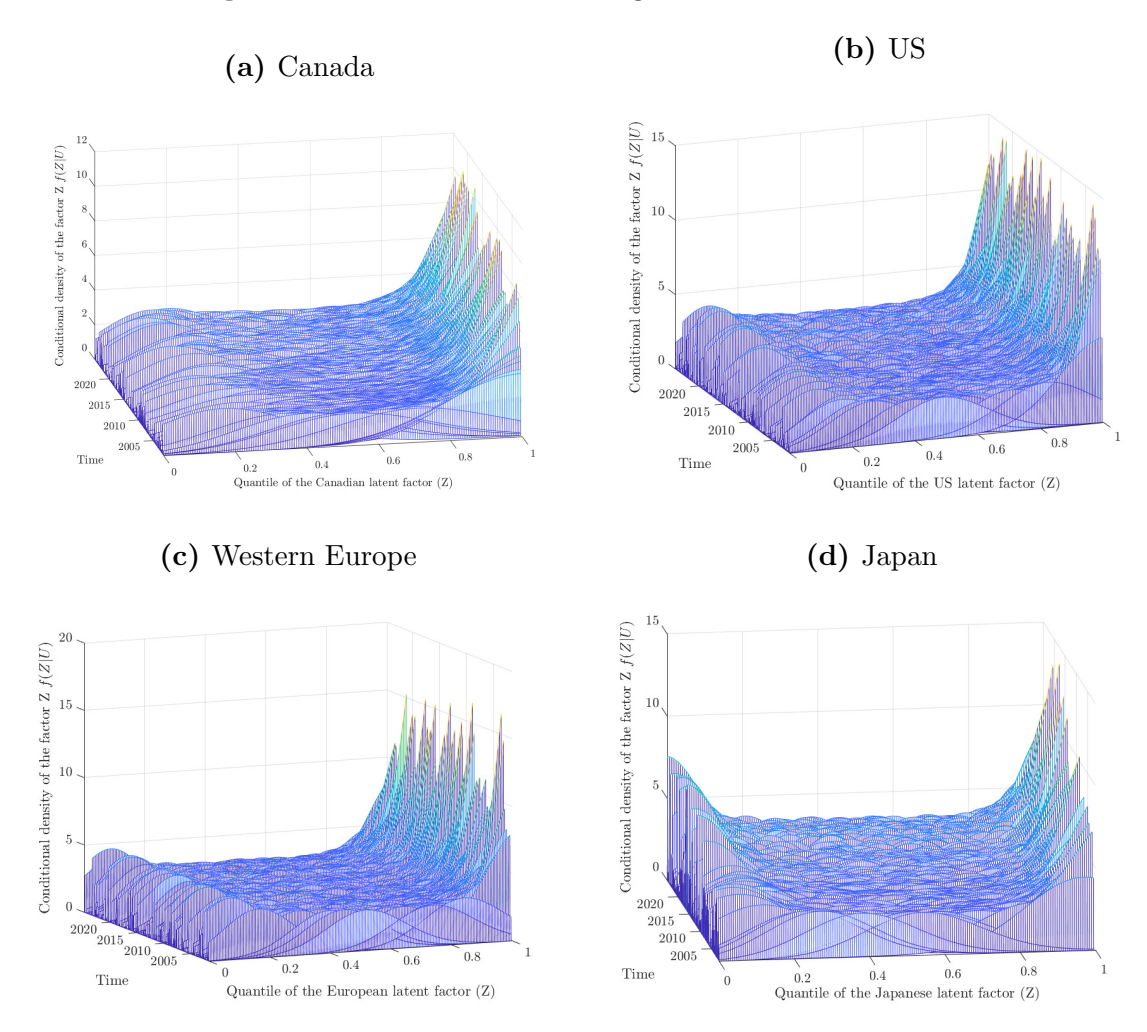


Figure 8: Correlation of regional latent factors with the global latent factor

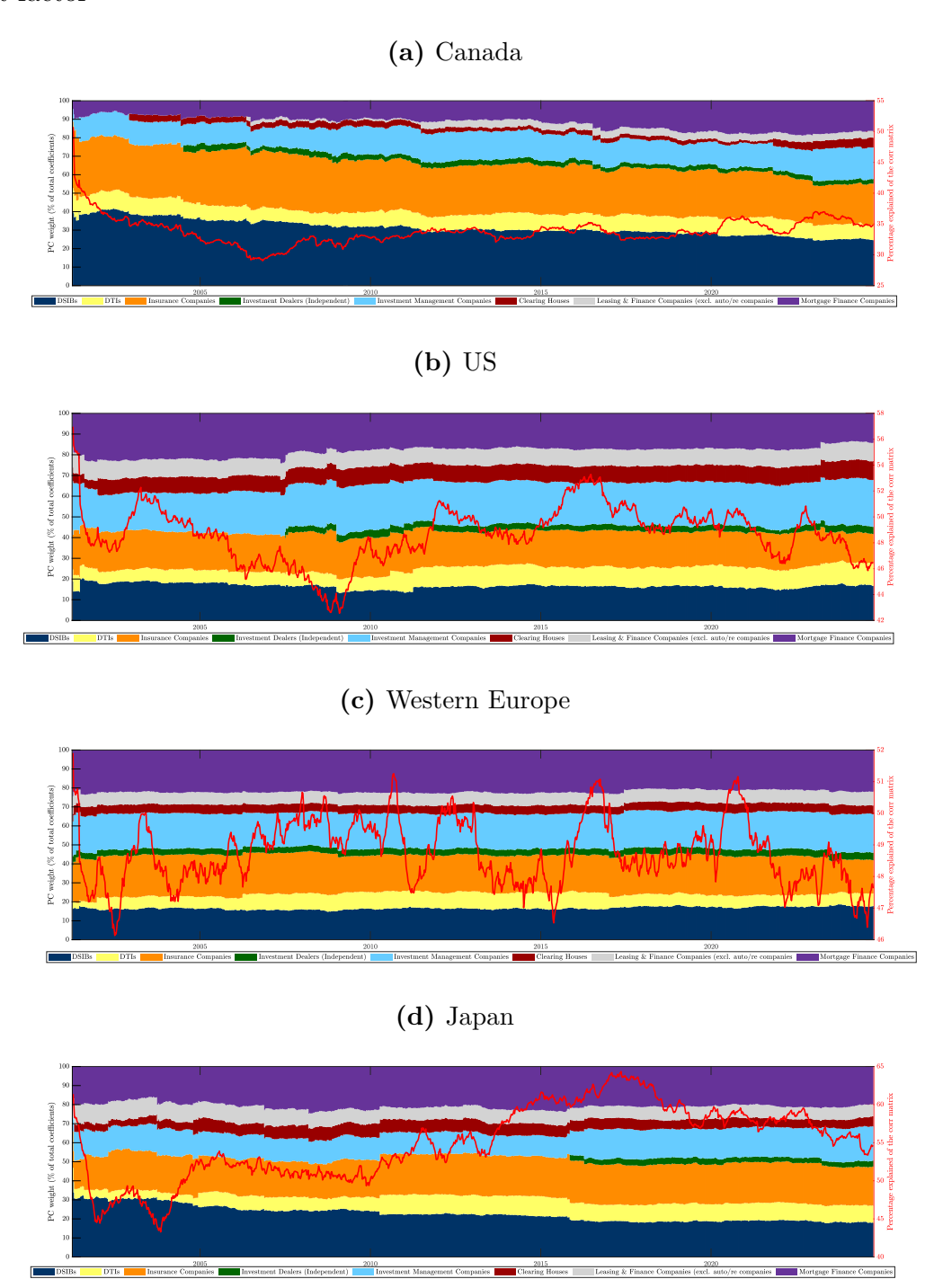
This chart shows the correlation linkage between different regional latent factors with the global latent factor.

Figure 9: Conditional latent regional factor distribution



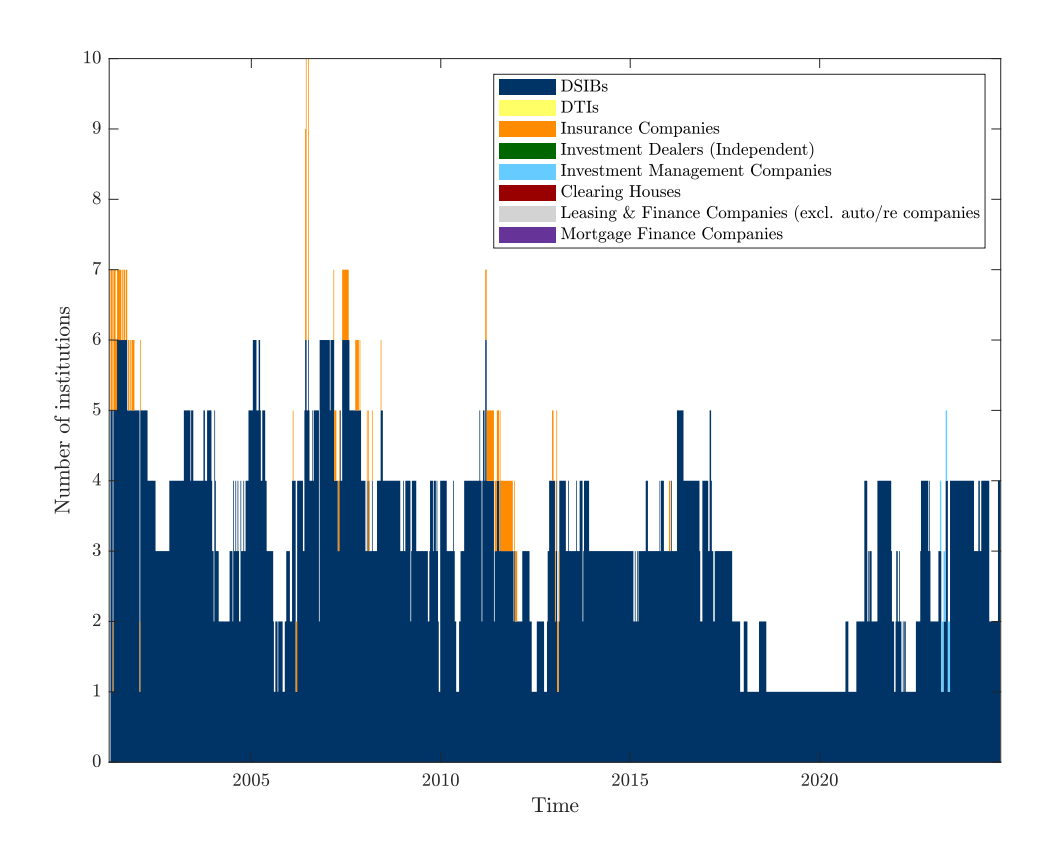
These figures show the conditional distribution of the quantiles of the latent factor (Z) on the realization of quantiles of the FIs (U) within each region, i.e., $f(Z|U) = c(Z|U) = \frac{c(Z,U)}{c(U)} = \frac{c(Z,U)}{\int_0^1 c(Z,U)dZ}$, where U,Z are uniformly distributed (0,1) and c(...) is the density copula of the Skewed-t distribution estimated for that region.

Figure 10: First principal component of the correlation matrix obtained from the latent factor



These figures show the contribution of each type of institution to the first principal component of the regional correlation matrix obtained from the latent factor structure. Correlation is obtained as $\rho_{ij,t} = E(u_{i,t},u_{j,t}) - E(u_{i,t})E(u_{j,t})$, where $E(u_{i,t},u_{j,t}) = \int_0^1 \int_0^1 u_i u_j c_t(u_i,u_j) du_i du_j$ and $c_t(u_i,u_j) = \int_0^1 c(u_i,z;\rho_{i,t})c(u_j,z;\rho_{j,t})dz$ with z being the latent regional factor. Note that the principal component analysis (PCA) fails to capture the rich dependence structure from the latent link. In the best case, PCA captures 2/3 of the correlation structure (Japan), but it explains between 1/2 and 1/3 of the correlation structure for most of the regions.

Figure 11: Top bucket (95% confidence level) of FIs with highest correlation with the Canadian latent factor



(b) 95% confidence interval for the correlation bucket

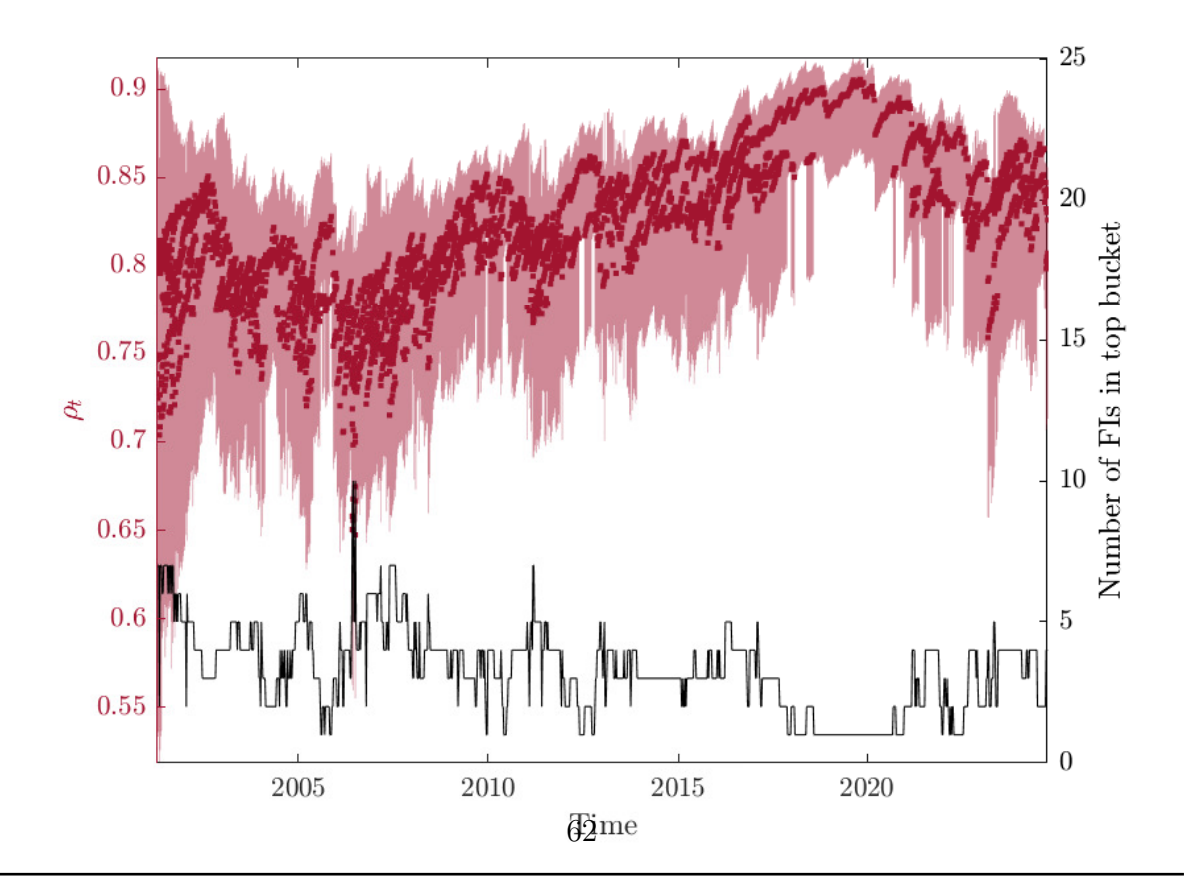
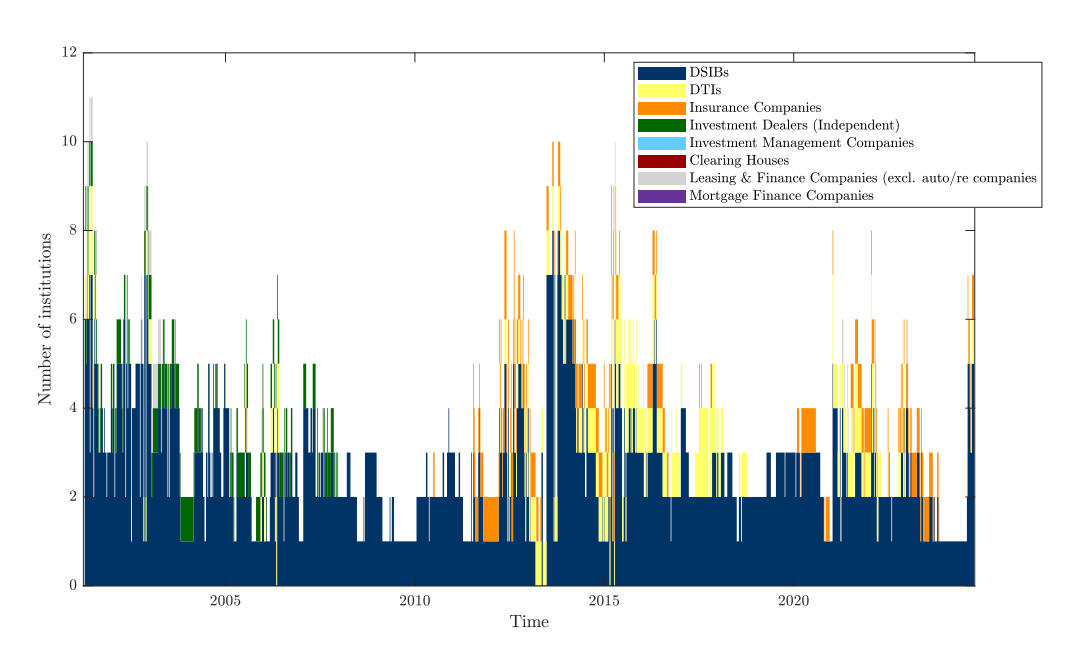


Figure 12: Top bucket (95% confidence level) of FIs with highest correlation with the US latent factor



(b) 95% confidence interval for the correlation bucket

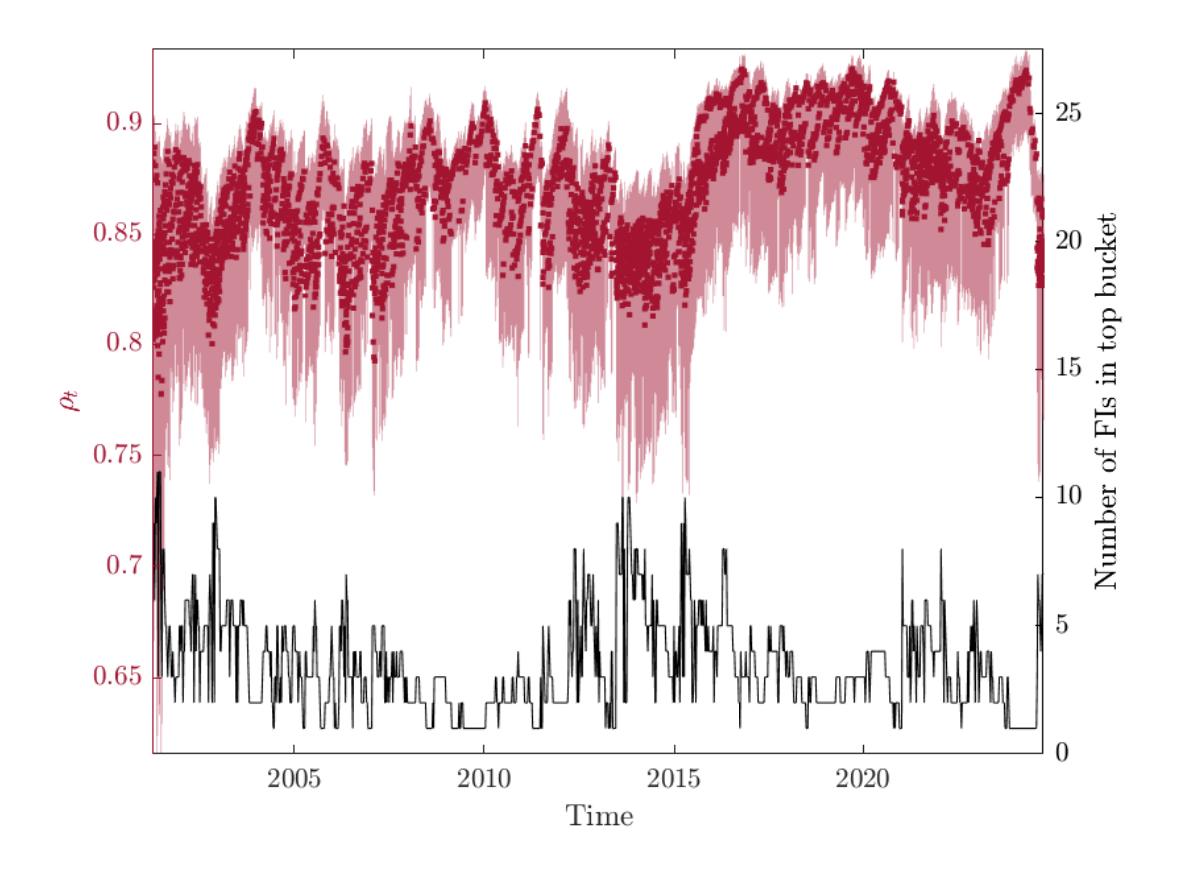
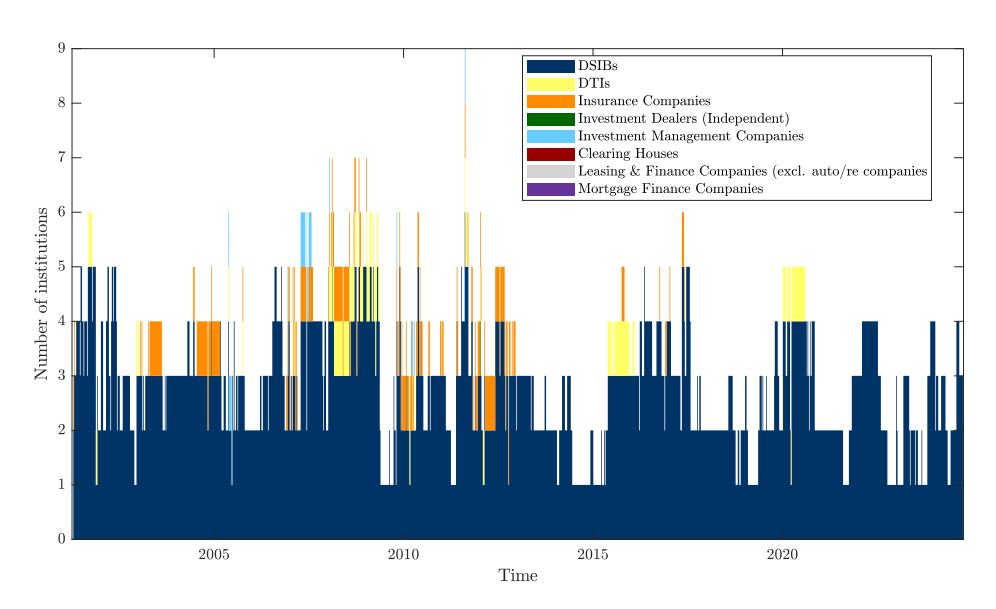


Figure 13: Top bucket (95% confidence level) of FIs with highest correlation with the European latent factor



(b) 95% confidence interval for the correlation bucket

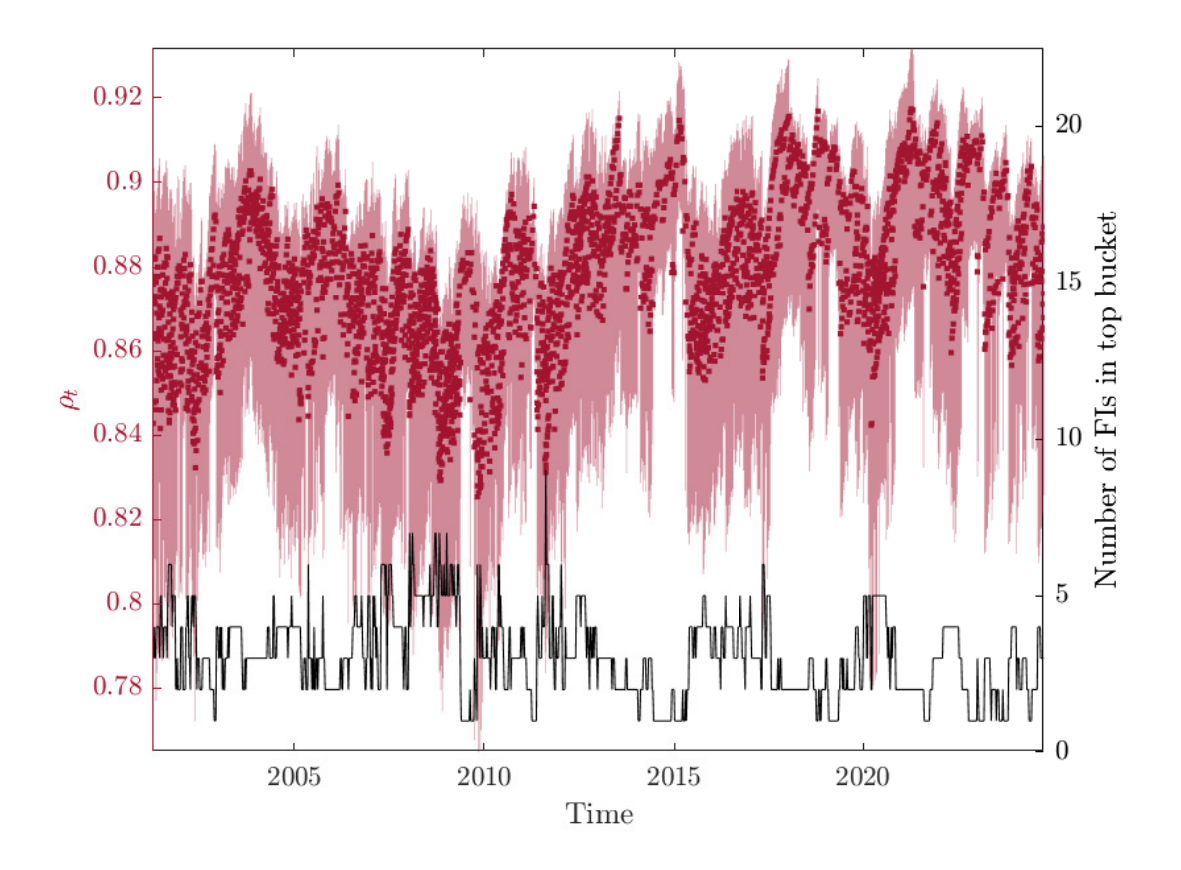
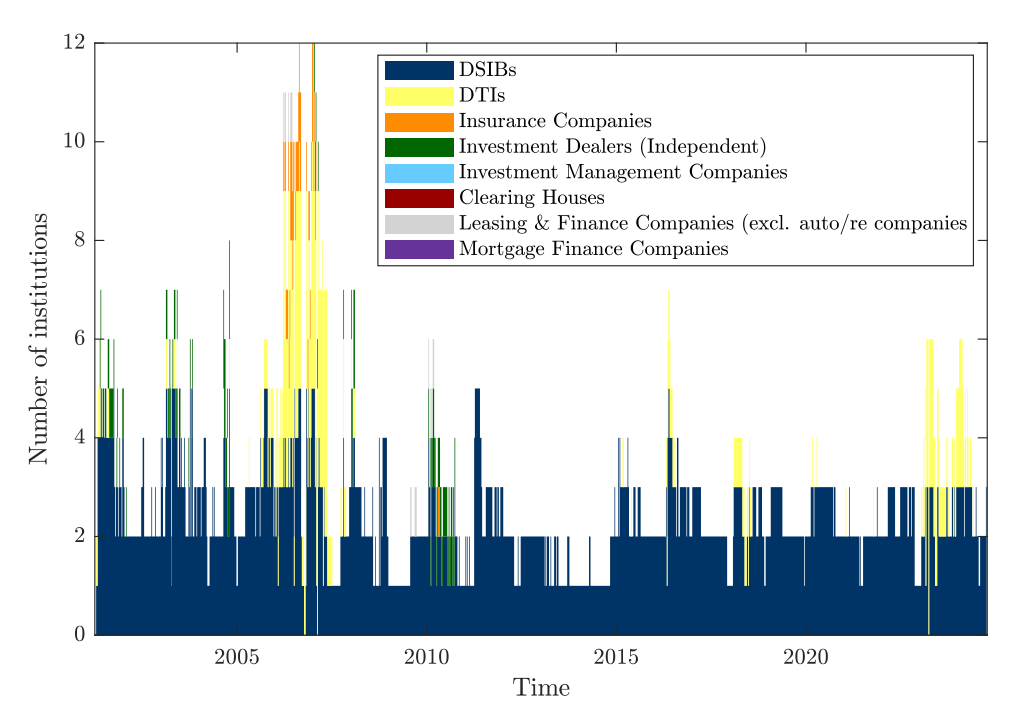


Figure 14: Top bucket (95% confidence level) of FIs with highest correlation with the Japanese latent factor



(b) 95% confidence interval for the correlation bucket

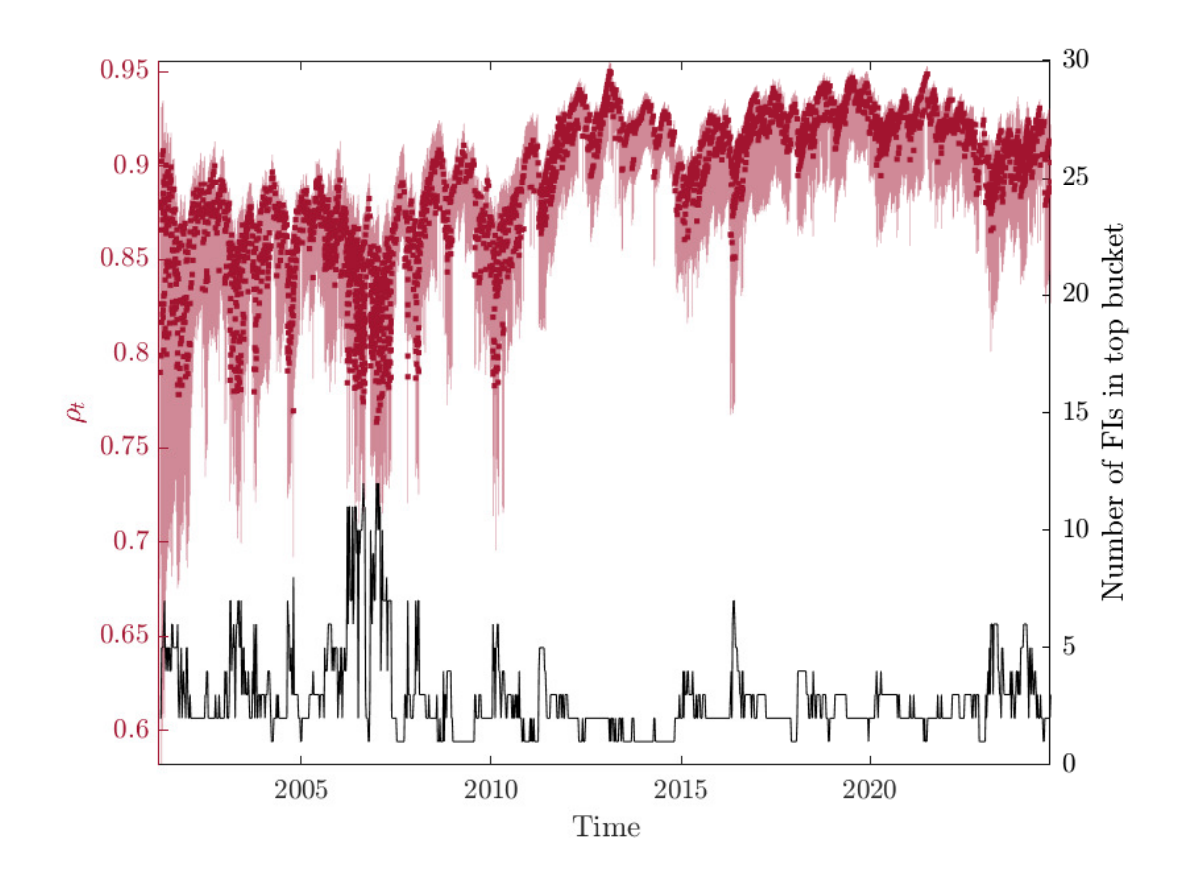


Figure 15: $Return-in-Stress\ (RiS)$ for the different financial institutions

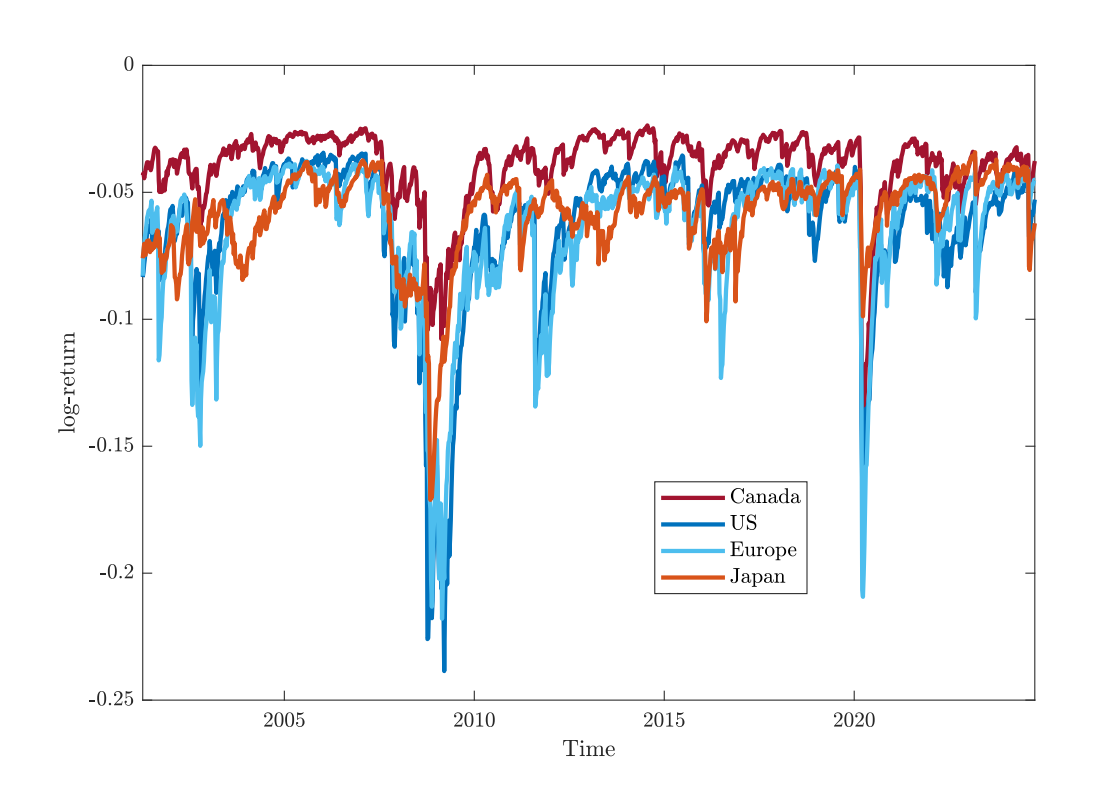
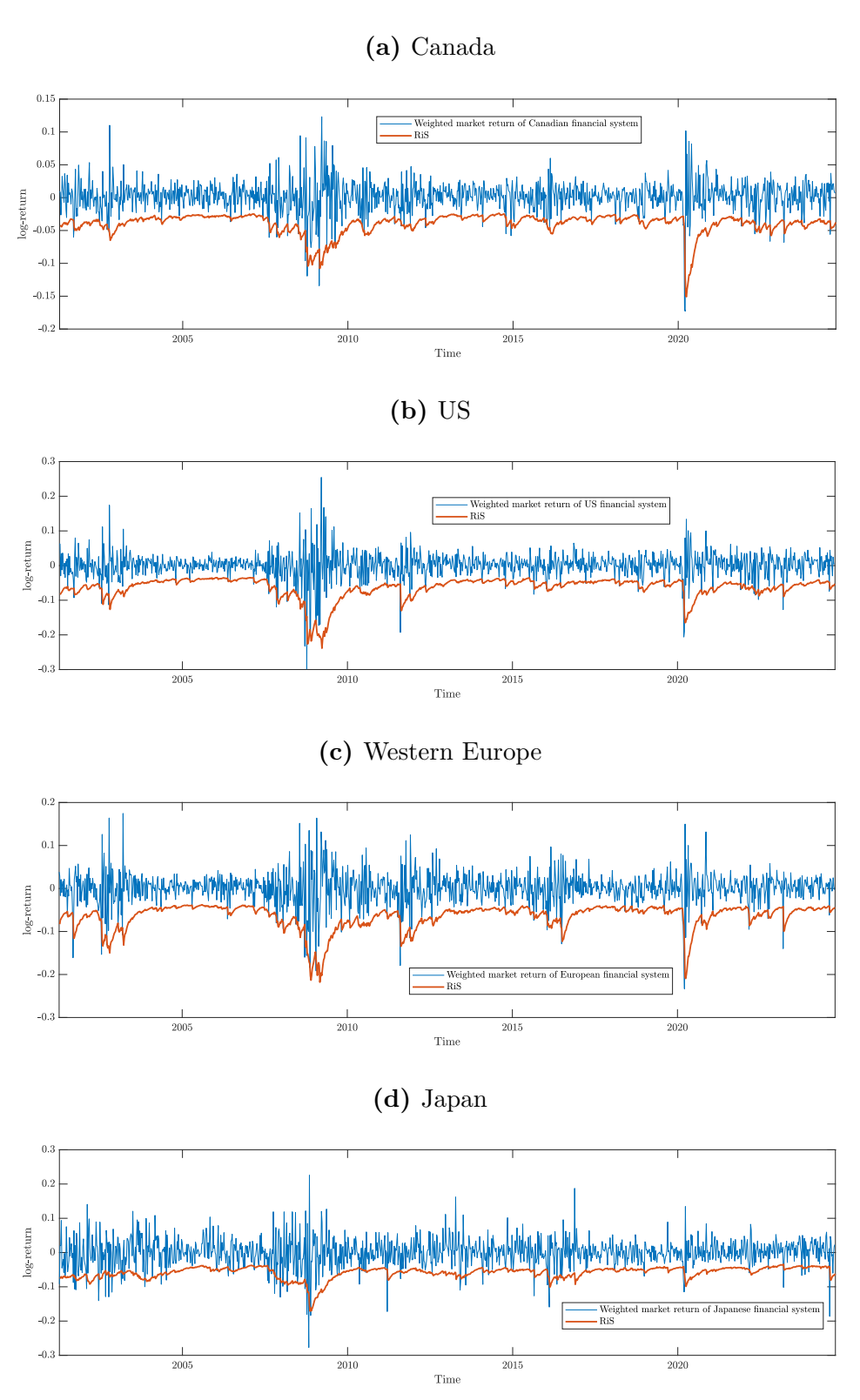
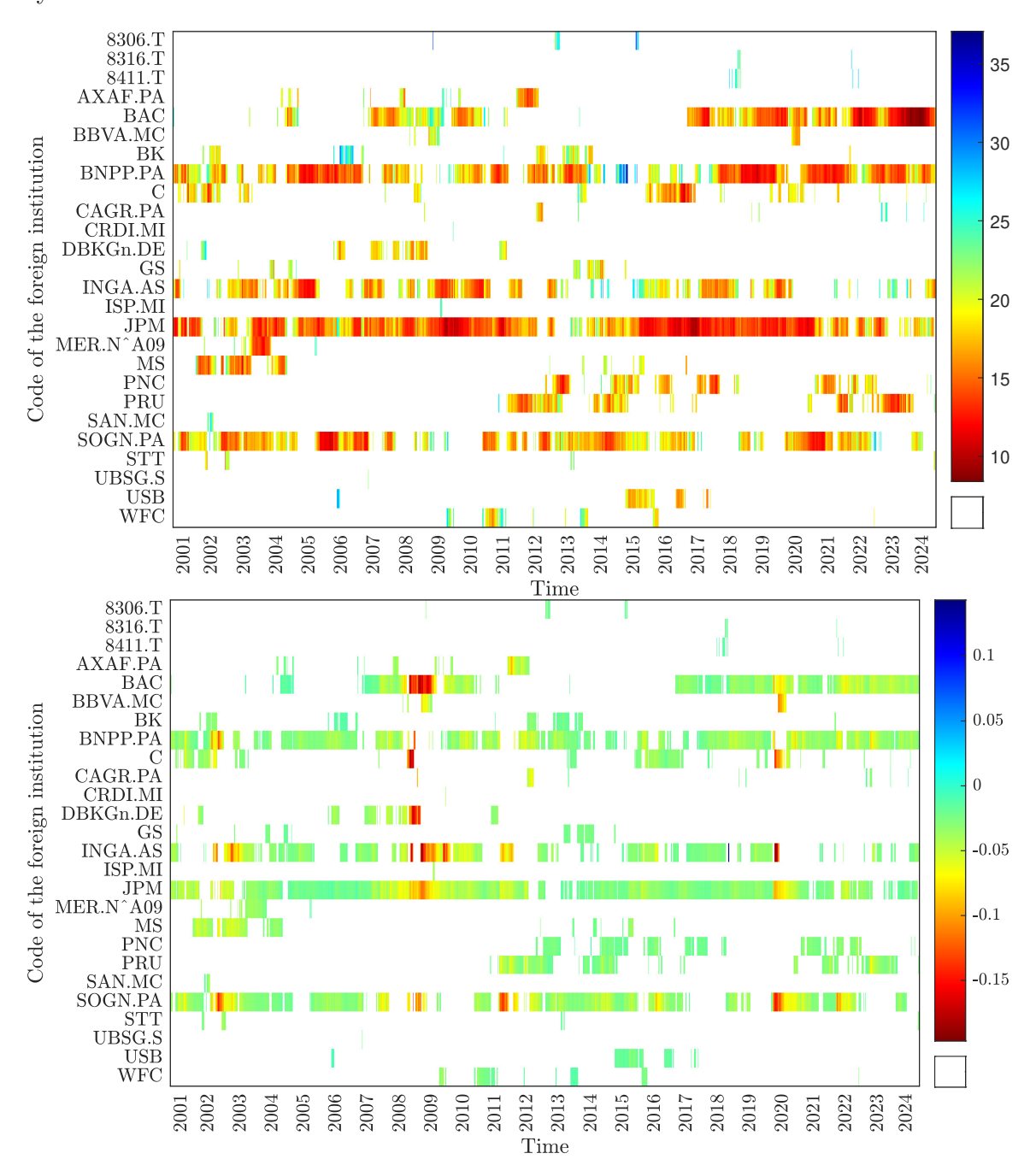


Figure 16: $Return-in-Stress\ (RiS)$ and weighted-averaged log-return of each financial system



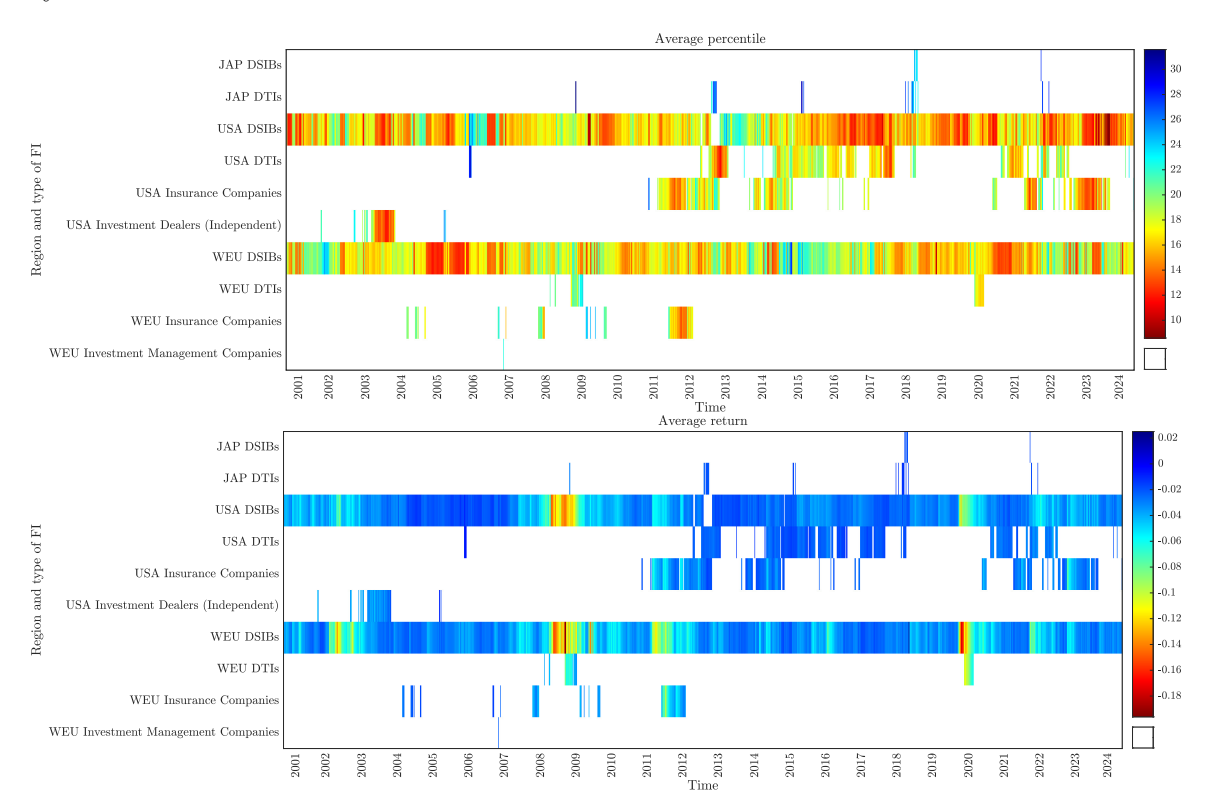
These figures show the log-returns of the weighted-market financial index for each region (European index is computed in EUR) together with the Return-in-Stress~(RiS). The number of exceedances in RiS is similar to a Value-at-Risk with a 95% confidence level (minimum percentage of exceedances is 3.6% of the sample for Canada and maximum percentage of exceedances is 5.5% of the sample for Japan.)

Figure 17: Scenario generating *Return-in-Stress* (*RiS*) for the Canadian financial system



This chart shows the scenario generating the Return-in-Stress (RiS) for the market-weighted average Canadian financial return. We consider the 5% probability foreign scenario with the highest negative impact on the average Canadian financial returns. Top (Bottom) figure indicates the distribution of stress across international FIs in terms of quantile (returns) as an upper bound for the scenario. The same quantile is translated into a different return, as the conditional distribution of foreign institutions evolves over time.

Figure 18: RiS Scenario (aggregated by type and region) for the Canadian financial system



This chart summarizes the scenario generating the $Return-in-Stress\ (RiS)$ for the market-weighted average Canadian financial return. We consider the 5% probability foreign scenario with the highest negative impact on the average Canadian financial returns. Top (Bottom) figure indicates the average distribution of stress across regions and type of FIs in terms of quantile (returns) as an upper bound for the scenario. JAP: Japan. USA: United States. WEU: Western Europe.

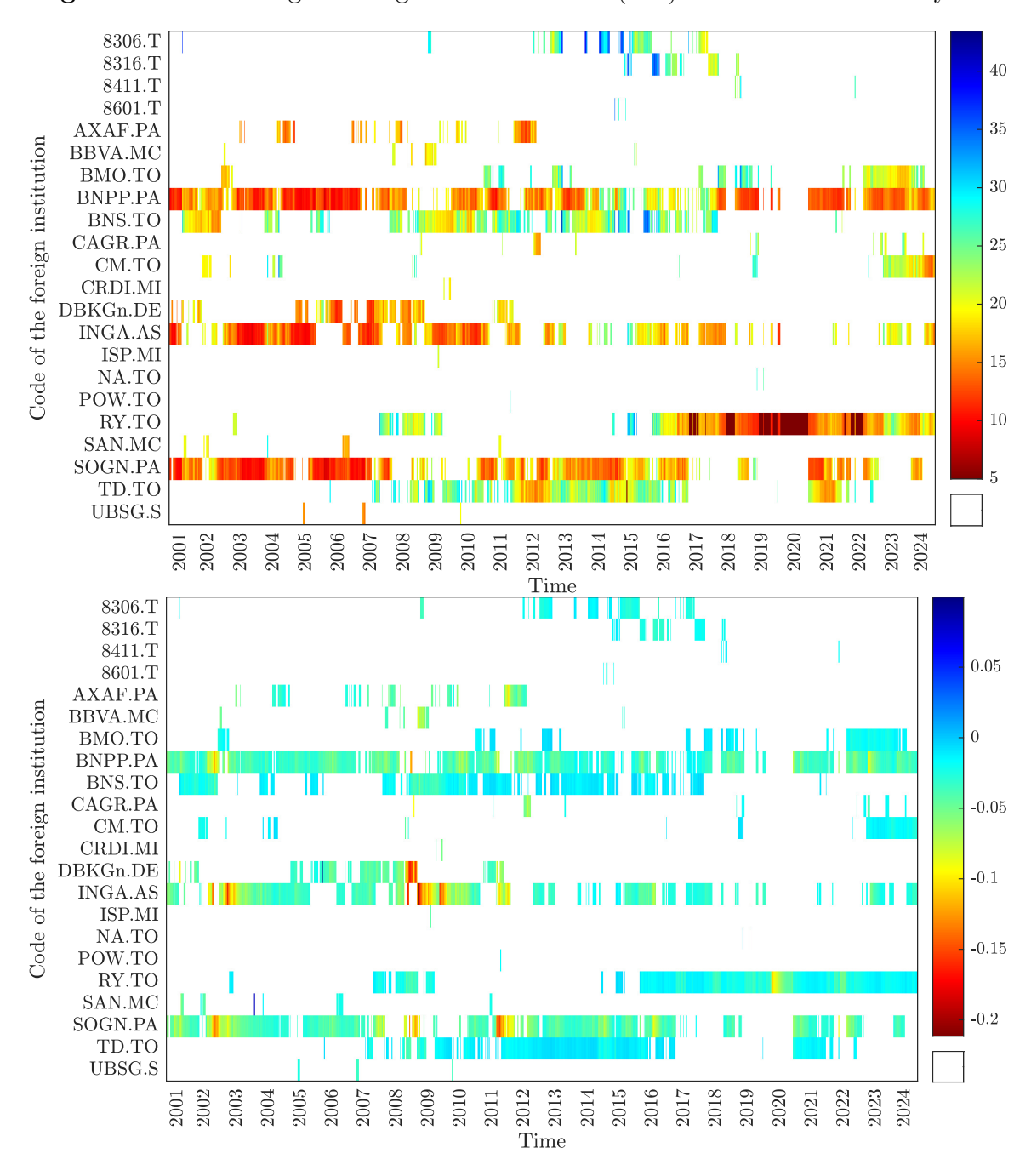


Figure 19: Scenario generating Return-in-Stress (RiS) for the US financial system

This chart shows the scenario generating the Return-in-Stress (RiS) for the market-weighted average US financial return. We consider the 5% probability foreign scenario with the highest negative impact on the average US financial returns. Top (Bottom) figure indicates the distribution of stress across international FIs in terms of quantile (returns) as an upper bound for the scenario. The same quantile is translated into a different return, as the conditional distribution of foreign institutions evolves over time.

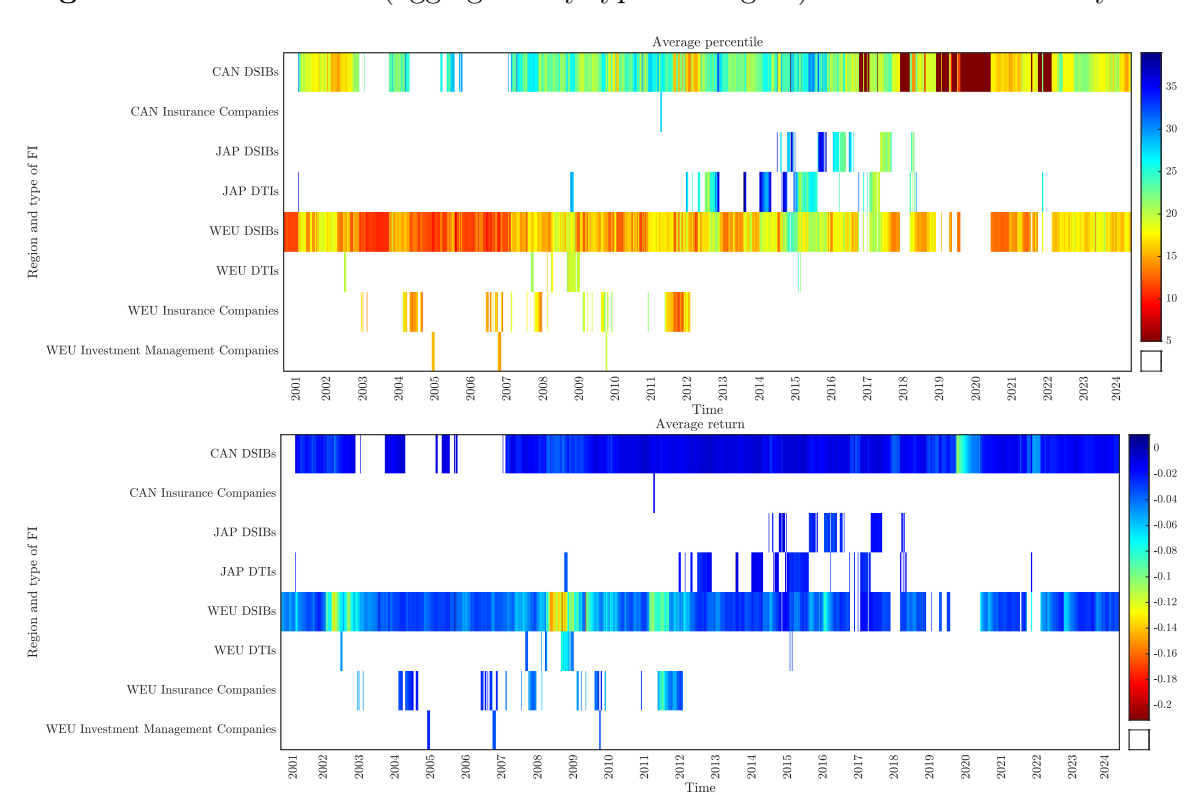
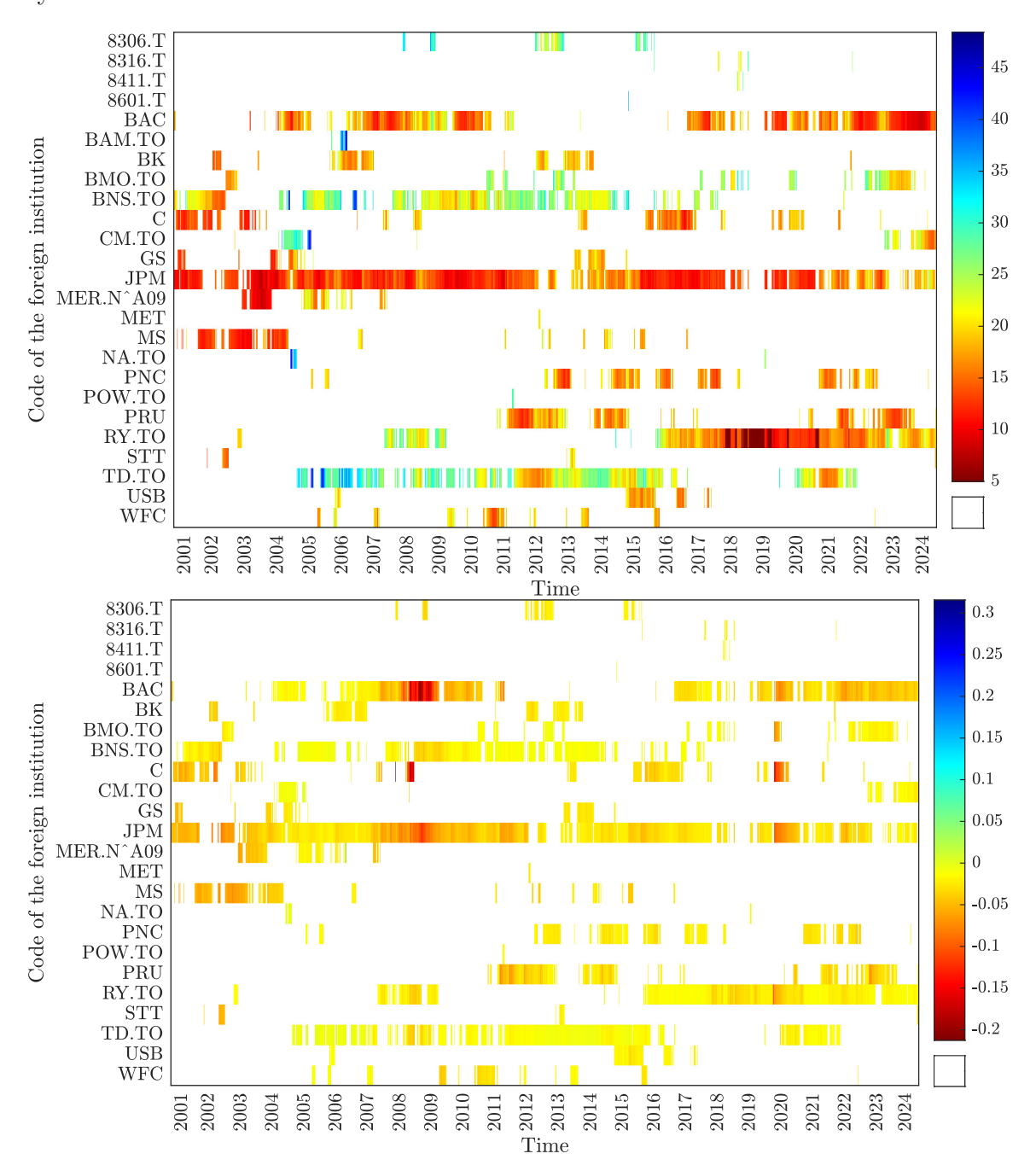


Figure 20: RiS Scenario (aggregated by type and region) for the US financial system

This chart summarizes the scenario generating the Return-in-Stress (RiS) for the market-weighted average US financial return. We consider the 5% probability foreign scenario with the highest negative impact on the average US financial returns. Top (Bottom) figure indicates the average distribution of stress across regions and type of FIs in terms of quantile (returns) as an upper bound for the scenario.

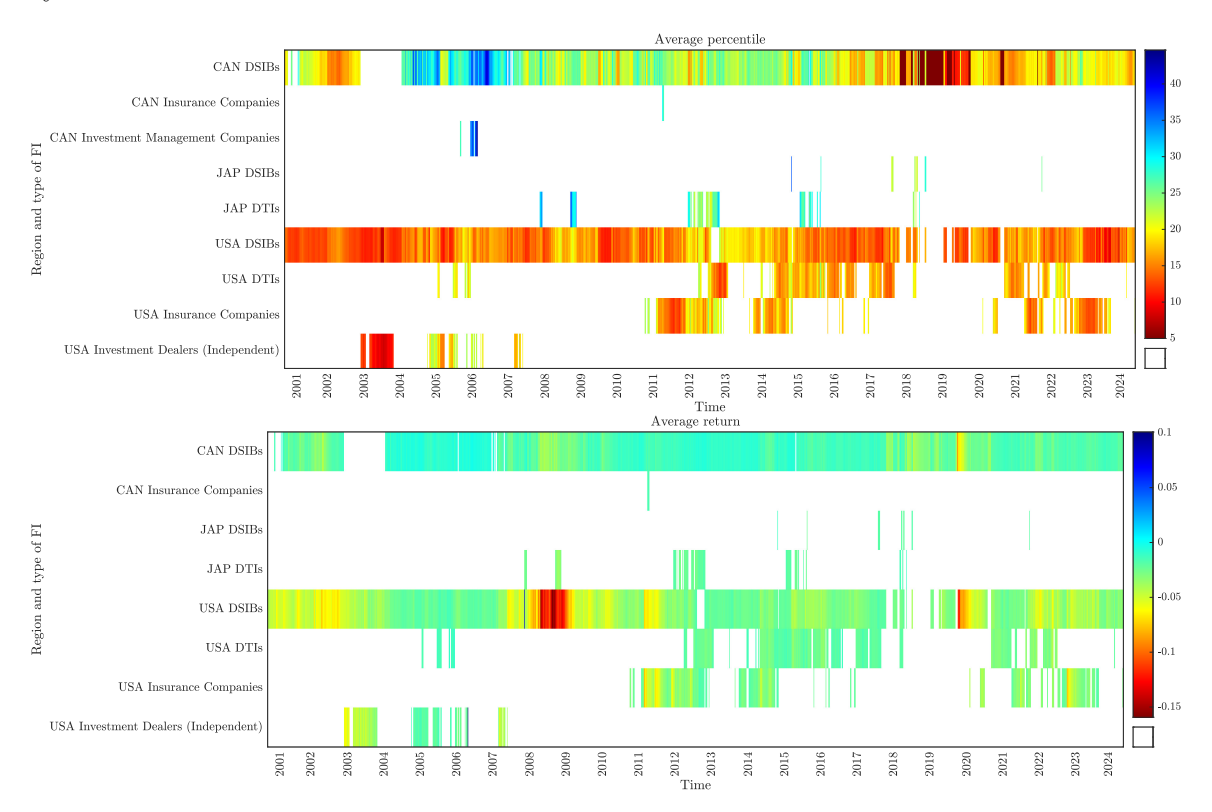
JAP: Japan. CAN: Canada. WEU: Western Europe.

Figure 21: Scenario generating $Return-in-Stress\ (RiS)$ for the European financial system



This chart shows the scenario generating the Return-in-Stress (RiS) for the market-weighted average European financial return. We consider the 5% probability foreign scenario with the highest negative impact on the average European financial returns. Top (Bottom) figure indicates the distribution of stress across international FIs in terms of quantile (returns) as an upper bound for the scenario. The same quantile is translated into a different return, as the conditional distribution of foreign institutions evolves over time.

Figure 22: RiS Scenario (aggregated by type and region) for the European financial system



This chart summarizes the scenario generating the *Return-in-Stress* (*RiS*) for the market-weighted average European financial return. We consider the 5% probability foreign scenario with the highest negative impact on the average European financial returns. Top (Bottom) figure indicates the average distribution of stress across regions and type of FIs in terms of quantile (returns) as an upper bound for the scenario. JAP: Japan. USA: United States. CAN: Canada.

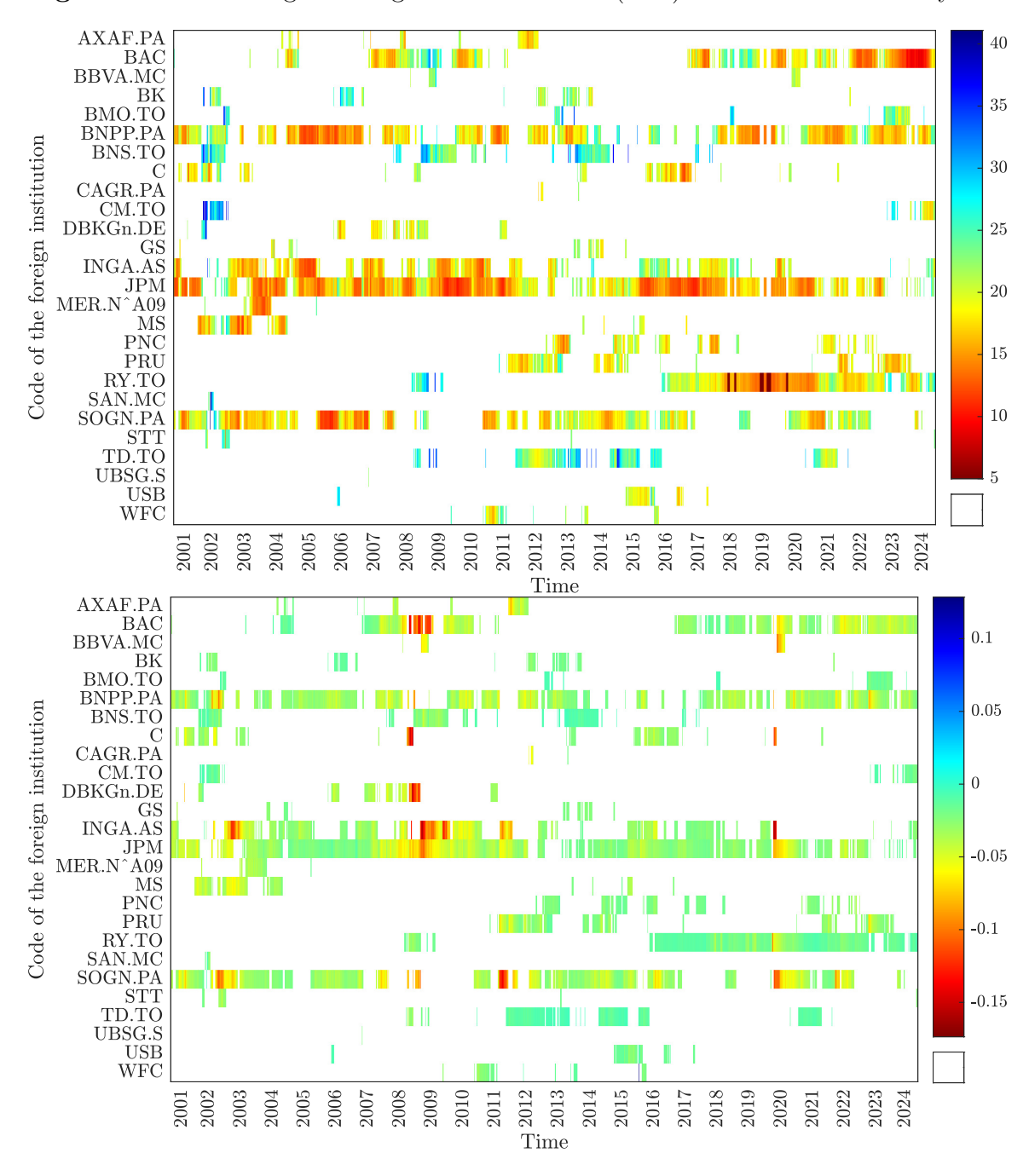
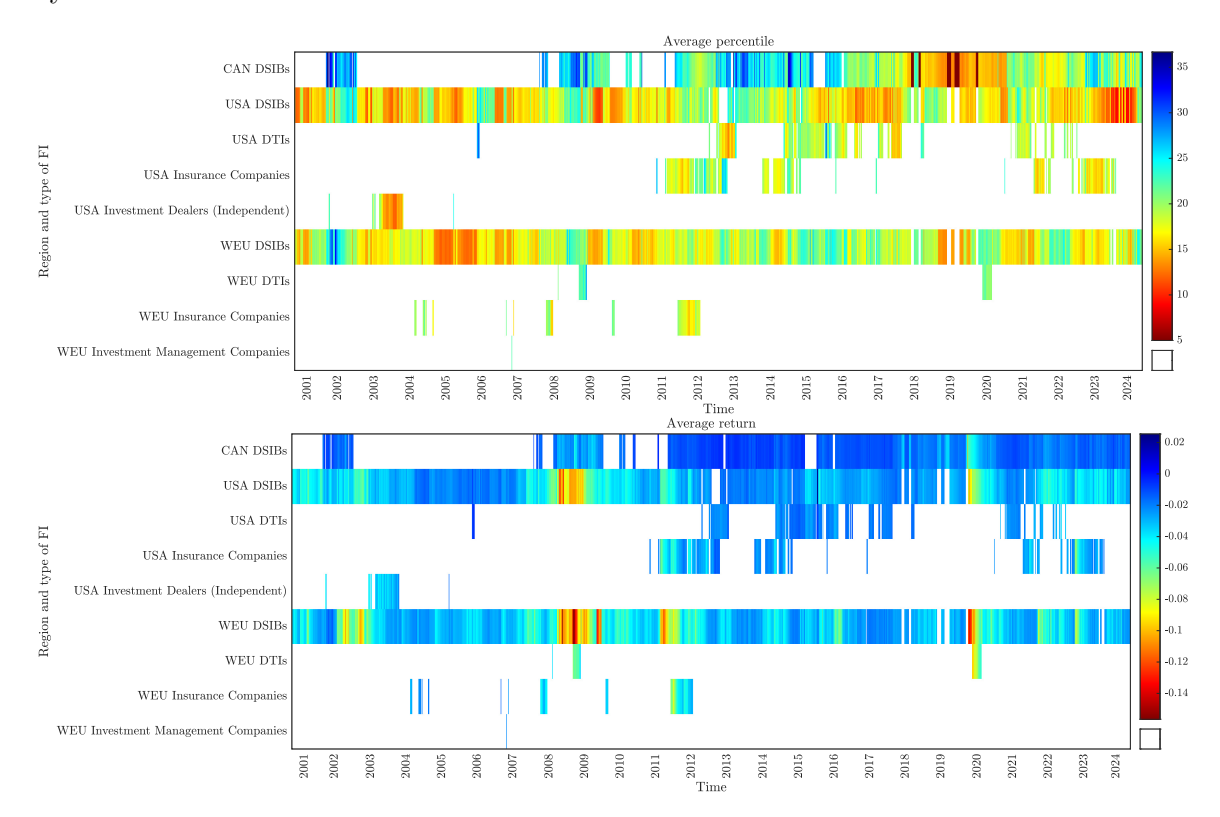


Figure 23: Scenario generating Return-in-Stress (RiS) for the US financial system

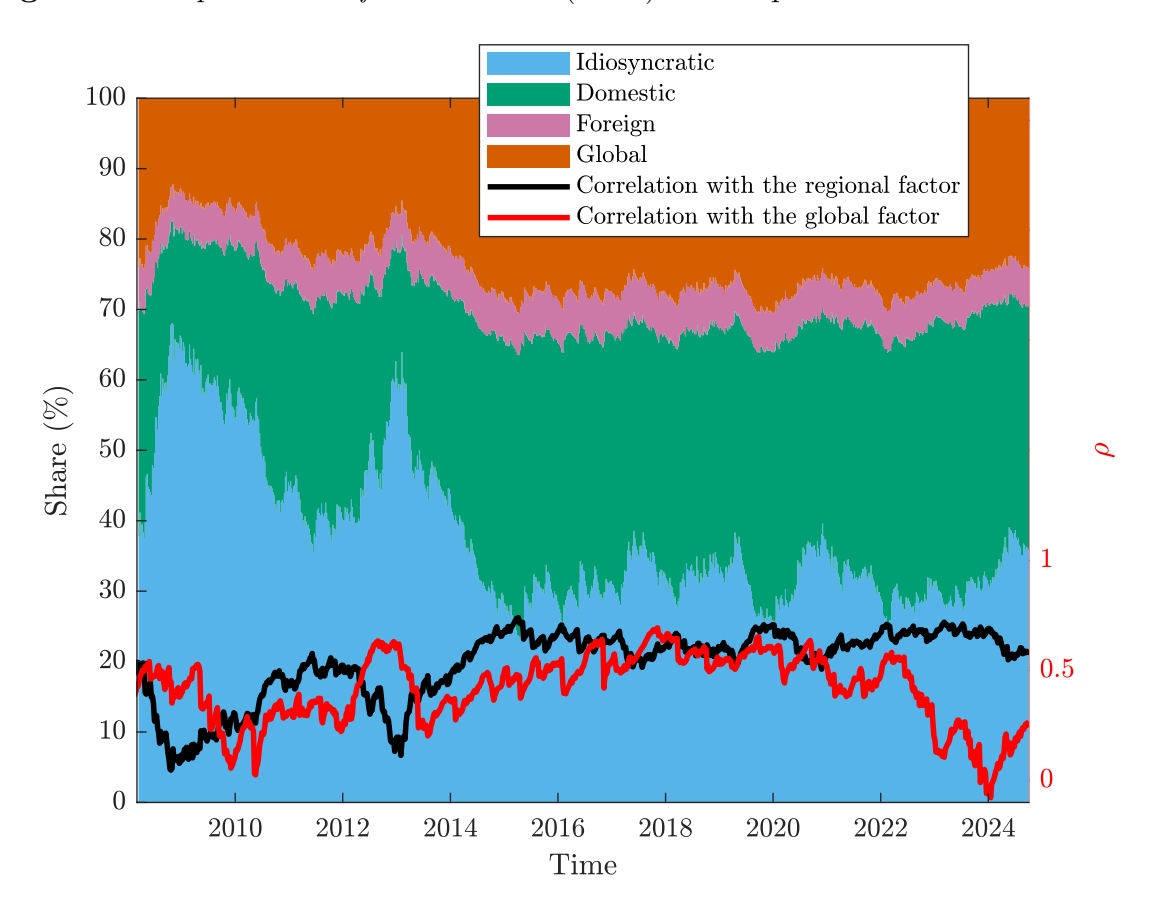
This chart shows the scenario generating the Return-in-Stress (RiS) for the market-weighted average Japanese financial return. We consider the 5% probability foreign scenario with the highest negative impact on the average Japanese financial returns. Top (Bottom) figure indicates the distribution of stress across international FIs in terms of quantile (returns) as an upper bound for the scenario. The same quantile is translated into a different return, as the conditional distribution of foreign institutions evolves over time.

Figure 24: RiS Scenario (aggregated by type and region) for the Japanese financial system



This chart summarizes the scenario generating the *Return-in-Stress* (*RiS*) for the market-weighted average Japanese financial return. We consider the 5% probability foreign scenario with the highest negative impact on the average Japanese financial returns. Top (Bottom) figure indicates the average distribution of stress across regions and type of FIs in terms of quantile (returns) as an upper bound for the scenario. WEU: Western Europe. USA: United States. CAN: Canada.

Figure 25: Expected Shortfall Allocation (ESA) for a Japanese financial institution

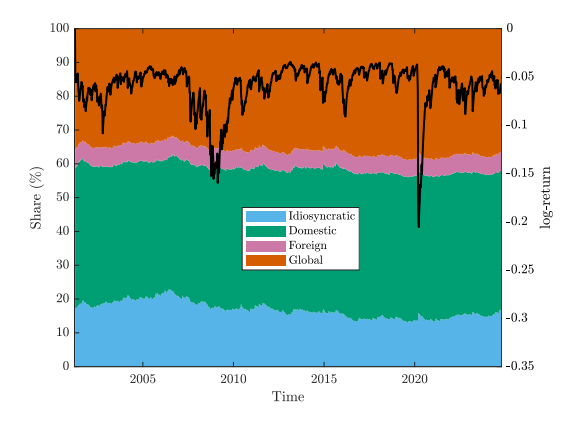


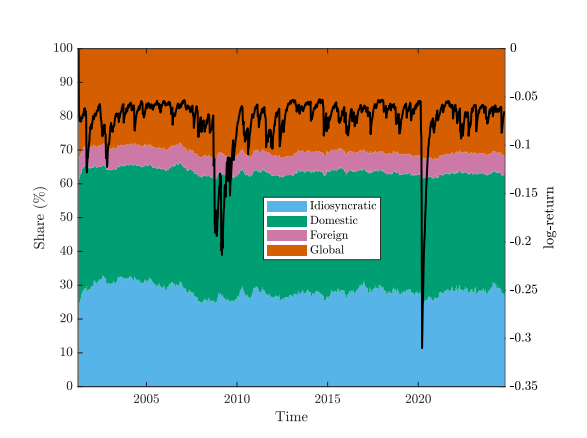
This chart shows the shares (left axis) of Expected Shortfall for a Japanese financial institution happening (or not) at the same time as tail returns in other Japanese or foreign FIs. The right axis shows the correlation of that financial institution with the regional latent factor (black line) and the correlation of the regional latent factor with the global latent factor (red line).

Figure 26: Expected Shortfall Allocation (ESA) for the DTIs and NBFIs in Canada

(a) DSIBs and other DTIs

(b) NBFIs



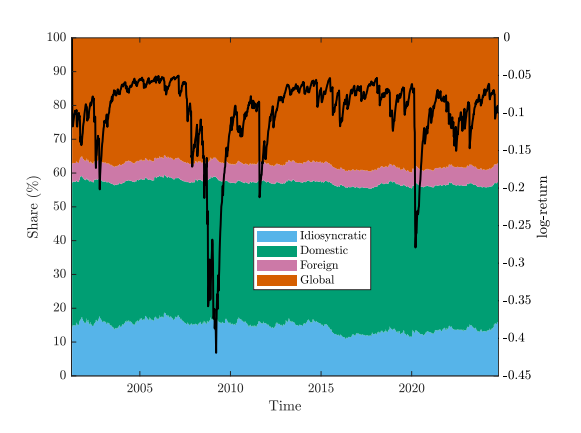


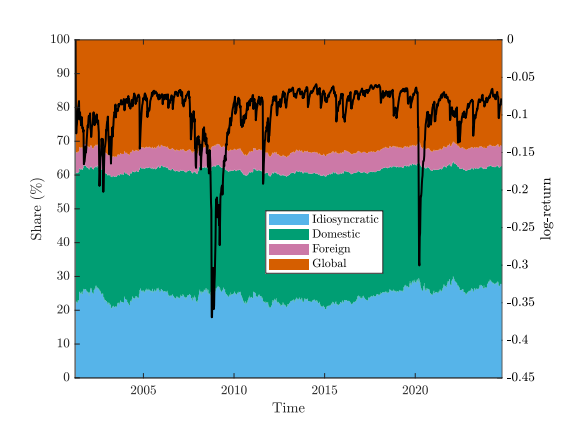
This chart shows in the right axis the weighted-average Expected Shortfall of the set of institutions which are Deposit-Taking Institutions (left figure) or Non-Banking Financial Institutions (right figure). The left axis indicates the share of the Expected Shortfall happening under four different scenarios.

Figure 27: Expected Shortfall Allocation (ESA) for the DTIs and NBFIs in US

(a) DSIBs and other DTIs

(b) NBFIs



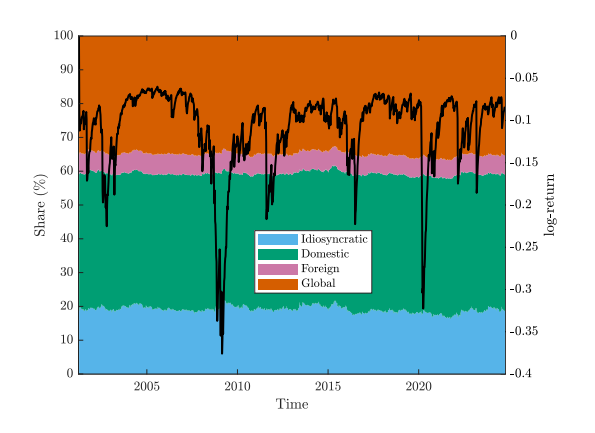


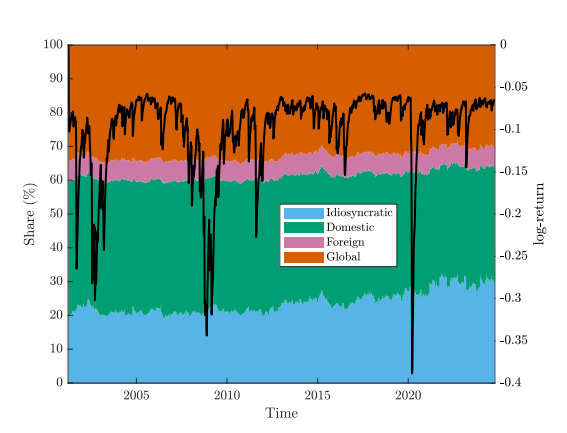
This chart shows in the right axis the weighted-average Expected Shortfall of the set of institutions which are Deposit-Taking Institutions (left figure) or Non-Banking Financial Institutions (right figure). The left axis indicates the share of the Expected Shortfall happening under four different scenarios.

Figure 28: Expected Shortfall Allocation (ESA) for the DTIs and NBFIs in Europe

(a) DSIBs and other DTIs

(b) NBFIs



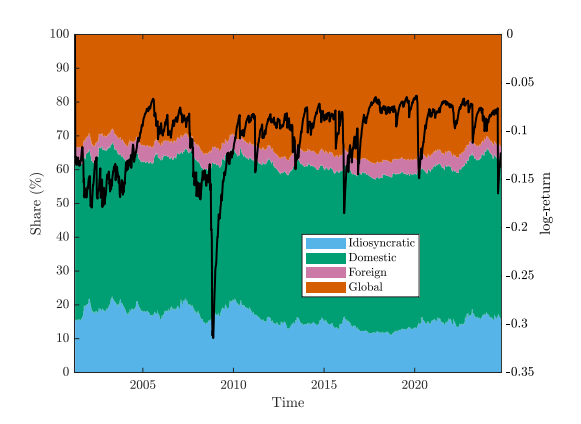


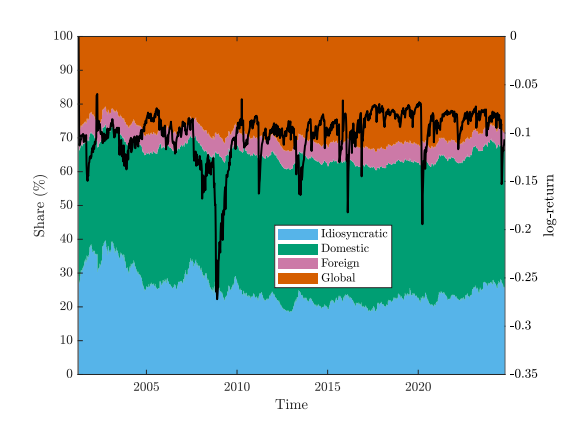
This chart shows in the right axis the weighted-average Expected Shortfall of the set of institutions which are Deposit-Taking Institutions (left figure) or Non-Banking Financial Institutions (right figure). The left axis indicates the share of the Expected Shortfall happening under four different scenarios. The Expected Shortfall is computed in euros.

Figure 29: Expected Shortfall Allocation (ESA) for the DTIs and NBFIs in Japan

(a) DSIBs and other DTIs

(b) NBFIs





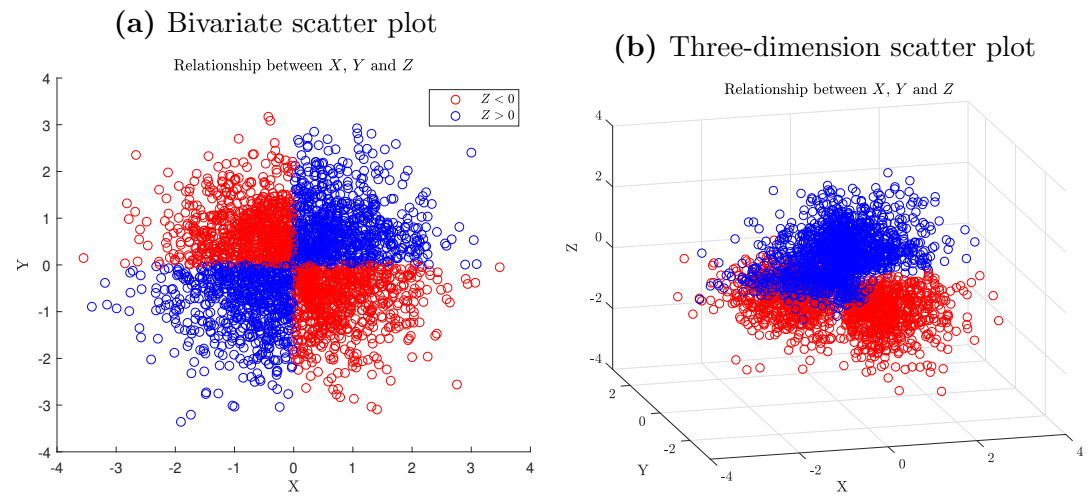
This chart shows in the right axis the weighted-average Expected Shortfall of the set of institutions which are Deposit-Taking Institutions (left figure) or Non-Banking Financial Institutions (right figure). The left axis indicates the share of the Expected Shortfall happening under four different scenarios.

Pairwise and mutual dependence.

Mutual independence is a stronger condition than pairwise independence. Pairwise independence implies that two events for a couple of variables are independent. For instance, events A and B for variables X and Y are pairwise independent if $P_X, Y(A, B) =$ $P_X(A)P_Y(B)$. Mutual independence implies that any set or combination of events for a
group of variables are independent from each other, which go further than the bivariate
dependence. Modeling and building metrics that account for the multivariate distribution of X, Y, and Z provide further information, preventing us from misleading pairwise
independence from mutual independence.

Romano and Siegel (1986) provides an example to illustrate the pairwise independence and the existence of mutual dependence. Let us assume we have three independent random variables which are normally distributed, i.e., $X \sim N(0,1)$, $Y \sim N(0,1)$, and $Z_0 \sim N(0,1)$. Let us define $Z = |Z_0| sign(XY)$. We would have that each variable is independent from the other two, i.e., independent pairwise, but it is dependent given the other two variables. Figure 30 presents a scatter plot of these variables, taking into account that three of them instead of two provides more information about the multivariate structure and increases the knowledge about the conditional distribution of X given any combination of Y and Z.

Figure 30: Example of a pairwise independence and mutual dependence



These figures show the scatter plot between X, Y, and Z. Note that X does not provide any information about Y unless it is combined with the information obtained from Z. This helps motivate the use of the multivariate scenario because although we could have pairwise independence, we must be aware of the existence of lack of mutual independence. This example is taken from Romano and Siegel (1986), where $X \sim N(0,1)$, $Y \sim N(0,1)$, and $Z \sim N(0,1)$, we have pairwise independence, i.e., $\rho_{X,Y} = 0$, $\rho_{X,Z} = 0$ and $\rho_{Y,Z} = 0$. $Z = |Z_0| sign(XY)$ where $Z_0 \sim N(0,1)$.

The Skewed t Distribution

The bivariate skewed t distribution discussed in Demarta and McNeil (2005) has the following stochastic representation:

$$X = \mu + \lambda W + \sqrt{W}Z, \tag{8}$$

where μ and λ are the mean and asymmetry vector parameter respectively, W is an inverse gamma distributed random variable $W \sim IG(\frac{\nu}{2}, \frac{\nu}{2})$ with ν being the number of degrees of freedom, and Z is a multivariable normal random variable $Z \sim N(0, P)$ independent of W with $P = \begin{bmatrix} 1 & \rho \\ \rho & 1 \end{bmatrix}$, i.e., $Z = L\varepsilon$ with $\varepsilon \sim N(0, I)$ and $L = \begin{bmatrix} L_{11} & 0 \\ L_{12} & L_{22} \end{bmatrix} = 0$

$$\left[\begin{array}{cc} 1 & 0 \\ \rho & \sqrt{1-\rho^2} \end{array}\right].$$

Note that $E(X) = \mu + \frac{\nu}{\nu - 2}\lambda$ and $Cov(X) = \Sigma = \frac{\nu}{\nu - 2}P + \frac{2\nu^2}{(\nu - 2)^2(\nu - 4)}\lambda\lambda'$, so $\nu > 4$ to have a defined variance. The bivariate distribution is

$$f_X(x) = c \frac{K_{\frac{\nu+2}{2}}(\sqrt{(\nu+d(x))\lambda'P^{-1}\lambda}) \exp([x-\mu]'P^{-1}\lambda)}{(\sqrt{(\nu+d(x))\lambda'P^{-1}\lambda})^{-\frac{\nu+2}{2}}(1+\frac{d(x)}{\nu})^{\frac{\nu+2}{2}}},$$

with $c = \frac{2^{-\nu/2}}{\Gamma(\frac{\nu}{2})\pi\nu|P|^{1/2}}$, $d(x) = [x - \mu]'P^{-1}[x - \mu]$, and $K_a(b)$ being the modified Bessel function of the second kind. We use the approximations from Yang and Chu (2017) when b is close to zero and b is large. In particular, $\lim_{b\to 0} K_a(b) = \frac{1}{2}\Gamma(a)\left(\frac{b}{2}\right)^{-a}$ and $\lim_{b\to \infty} K_a(b) = \sqrt{\frac{\pi}{2b}}\exp(-b)\left(1 + \frac{4a^2-1}{8b}\left(1 + \frac{4a^2-9}{16b}\right)\right)$. As shown by Lucas et al. (2014), this approximation allows us to cancel the exponential term multiplying the modified Bessel function, adding numerical stability for the skewness effect in the far tails. Note that Eq. (8) conditioned to a realization of W is normally distributed, i.e.,

$$X|W \sim N \left(\underbrace{\begin{bmatrix} \mu_1 \\ \mu_2 \end{bmatrix}}_{\mu_{X|W}} + W \otimes \begin{bmatrix} \lambda_1 \\ \lambda_2 \end{bmatrix}, W \otimes \begin{bmatrix} 1 & \rho \\ \rho & 1 \end{bmatrix} \right)$$

where \otimes is the Kronecker product. Eq. (3) could be rewritten as

$$f_X(x) = \int_0^\infty \phi_{X|W}(x|W) f_W(w) dw, \tag{9}$$

where $\phi_{X|W}(...)$ is the normal probability distribution function with mean $\mu_{X|W}$ and variance matrix $\Sigma_{X|W}$ and $f_{W}(...)$ is the probability distribution function of the inverse

Gaussian with all parameters equal to $\frac{\nu}{2}$.

Eq. (9) allows us to write the cumulative distribution function of the skewed t distribution as

$$F_X(x) = \int_0^\infty \Phi_{X|W}(x|w) f_W(w) dw, \tag{10}$$

where $\Phi_{X|W}$)(...) is the cumulative normal probability distribution function with mean $\mu_{X|W}$ and variance matrix $\Sigma_{X|W}$.

We obtain the copula from the ratio between the joint density function and the product of the marginal distributions. The univariate density of the skewed t distribution is

$$f_X(x) = c \frac{K_{\frac{\nu+1}{2}}(\sqrt{(\nu+d(x))\frac{\lambda^2}{\sigma^2}}) \exp\left(\frac{(x-\mu)}{\sigma^2}\lambda\right)}{(\sqrt{(\nu+d(x))\frac{\lambda^2}{\sigma^2}})^{-\frac{\nu+1}{2}}(1+\frac{d(x)}{\nu})^{\frac{\nu+1}{2}}},$$
(11)

with $c = \frac{2^{1-\frac{\nu+1}{2}}}{\Gamma(\frac{\nu}{2})(\pi\nu)^{\frac{1}{2}\sigma}}$ and $d(x) = \frac{(x-\mu)^2}{\sigma^2}$, and where σ^2 is given by the diagonal elements of P. The copula density function is defined implicitly via

$$c(u,v) = \frac{f_X(F_{X_1}^{-1}(u), F_{X_2}^{-1}(v))}{f_{X_1}(F_{X_1}^{-1}(u))f_{X_2}(F_{X_2}^{-1}(v))}.$$
(12)

Copula function could be easily obtained from Eq. (10) as $C(u, v) = F(F_1^1(u), F_2^{-1}(v))$, i.e.,

$$C(u,v) = \int_0^\infty \Phi_{X|W}(\Phi_{X_1|W}^{-1}(u), \Phi_{X_2|W}^{-1}(v)|w) f_W(w) dw.$$
 (13)

The conditional copula could be obtained following Eq. (10) as

$$C(u|v) = \int_0^\infty \Phi\left(\frac{F_{X_1}^{-1}(u) - \mu_{X_1|X_2,W}}{\sigma_{X_1|X_2,W}}\right) f_{W|X_2}(w)dw, \tag{14}$$

with $\Phi(...)$ being the standardized normal cumulative distribution function and

$$\mu_{X_1|X_2,W} = \mu_{X_1|W} + \frac{\sigma_{12|W}}{\sigma_{X_2|W}^2} \left(F_{X_2|W}^{-1}(v) - \mu_{X_2|W} \right)$$

, with $\sigma_{12|W}$ being the element in column 1 row 2 from matrix $\Sigma_{X|W}$ and

$$\sigma_{X_1|X_2,W} = \sqrt{(1-\rho^2)W}.$$

Latent factor structure

This section explains in detail how the latent factor model works and introduces its bi-factor extension.

Factor copula. Let us assume that the joint behaviour of a matrix of N variables is explained by distribution function with a correlation matrix P, i.e., f(X; P). This model implies estimating $\frac{N(N-1)}{2}$ parameters for the correlation matrix, i.e.,

$$P = \begin{bmatrix} 1 & \rho_{1,2} & \dots & \rho_{1,N} \\ \rho_{1,2} & 1 & \dots & \rho_{2,N} \\ & & & & \\ \rho_{1,N} & \rho_{2,N} & \dots & 1 \end{bmatrix}.$$

Let us assume that a one-factor model is able to explain the dynamics of the dataset, dividing the stochastic behaviour into a systematic part, driven by the factor, and a idiosyncratic part, e.g.,

$$X_i = \rho_i Z + \epsilon_i$$
.

Consequently, the correlation between variable X_i and X_j becomes $\rho_i \rho_j$, approximating the correlation matrix by

$$\tilde{P}_Z = \begin{bmatrix} 1 & \rho_1 \rho_2 & \dots & \rho_1 \rho_N \\ \rho_1 \rho_2 & 1 & \dots & \rho_2 \rho_N \\ & & & & \\ \vdots & & & & \\ \rho_1 \rho_N & \rho_2 \rho_N & \dots & 1 \end{bmatrix}.$$

Note that to estimate this model, we would maximize the joint distribution conditioned on the factor, i.e., $f(X|Z;P) = \prod_{i=1}^{N} f(X_i|Z;\rho_i)$.

Hence, the estimation of \tilde{P}_Z would depend on the factor Z that is chosen to explain the dynamics of the matrix X. The best factor Z^* to explain the joint behaviour of matrix X would be that one that generates a correlation matrix \tilde{P}^* for which $f(X; \tilde{P}^*) > f(X; \tilde{P}_Z)$ for any factor $Z \neq Z^*$. The key element explaining the joint behavior is \tilde{P}_{Z^*} , so we could try to estimate it directly, without explicitly selecting any particular factor if we make some assumptions about the distribution of the factor and the relationship between

²⁹This idea of comparing a latent factor with an explicit factor could lead to a kind of likelihood ratio test to assess if the latent factor (unrestricted model) generates a significant higher likelihood than the explicit factor model (restricted model). The appendix shows more details on how this test should be computed.

the factor and the matrix X, i.e.,

$$f(X; \tilde{P}^*) = \int_{-\infty}^{\infty} \prod_{i=1}^{N} f(X_i|Z; \rho_i) f(Z) dZ.$$

Krupskii and Joe (2013) proposes this approach to define the factor copula, where under the assumption of a certain copula structure, the dependence structure could be estimated as

$$c(U; \tilde{P}^*) = \int_0^1 \prod_{i=1}^N c(u_i, v; \rho_i) dv,$$
(15)

where c(...) is the density copula, U is the matrix of integral distribution functions for matrix X, i.e., $U = F_X^{-1}(X)$, and v is the latent factor driving the dependency between the variables in the dataset.

Similarly, we could obtain the copula as

$$C(U; \tilde{P}^*) = \int_0^1 \prod_{i=1}^N C(u_i|v; \rho_i) dv,$$
(16)

where $C(\ldots | \ldots)$ is the conditional copula.

Latent bi-factor structure The structured factor copula is introduced by Krupskii and Joe (2015), where the dependence between variables is explained by a common or global factor and a group-specific factor. Krupskii and Joe (2015) suggests two ways to generate dependence in non-homogeneous groups. The first approach would be assuming that the common factor and the group-specific factor are independents, which in the case of modeling dependence between financial firms might be difficult to hold. The second

approach assumes that the group-specific factors are correlated via the global factor.³⁰

Estimation approach and computational details

I estimate the parameters of the model following a two-step approach (Joe and Xu 1996). First, parameters of the marginal distribution are estimated by maximum likelihood, and, in a second step copula parameters are estimated by maximum likelihood using pseudo-sample observations from the marginals as given by the integral probability transformations of standardized returns. In other words, the parameters of uniform margins are estimated at the first step and dependence parameters at the second step with parameters of the univariate margins fixed at the estimates obtained from the first step. The two-step estimation approach, also known as inference function for margins (IFM) significantly reduces the computation time, simplifying the estimation process.

The integral from Eq. (15) and the double integral from Eq. (5) could be easily approximated using a Gauss-Legendre quadrature (Stroud et al. 1966) with a good precision using between 25 to 30 quadrature points. The Gauss-Legendre quadrature approximates the integral as a weighted combination of integrands evaluated at quadrature points, e.g., we could write Eq. (15) as

$$c(U; \tilde{P}^*) \approx \sum_{k=1}^{n_q} w_k \prod_{i=1}^N c(u_i, x_k; \rho_i),$$

³⁰The definition of global and regional factors would set the main difference between both approaches. If we define a regional factor as "the co-movement that is not common across regions," we are choosing the former approach, while defining the global factor as the commonality between the regional factors is closer to the latter approach. This definition has implications not only in terms of how to understand the latent factors but also in terms of number of parameters to be estimated. If we have N financial institutions and G regional factors, we have to estimate 2N parameters in the first case and N+G in the second case to get the full dependence structure. For large N and small G, the second approach becomes computationally easier.

where x_k are the nodes, w_k are the quadrature weights, and n_q is the number of quadrature points. Eq. (5) could be approximated as

$$c(U) = \sum_{k_1=1}^{n_q} w_{k_1} \prod_{q=1}^{G} \sum_{k_2=1}^{n_q} w_{k_2} c_V(x_{k_2}, x_{k_1}) \prod_{i=1}^{N_g} c(u_i, x_{k_2}).$$

An attractive property of Gauss–Legendre quadrature is that the same nodes and weights are used for different functions to compute the integral quickly and with a high precision. The same nodes also help in smooth numerical derivatives for numerical optimization.

I also follow a step-optimization approach where the dependence parameters of the copula model are estimated in steps. For the nested copula model, shown in Figure 5, parameters for the group-specific copulas are estimated using data from the corresponding region, as shown in the row T_1 from Figure 5. Within each group, the data is modeled via a latent one-factor model so the estimation is fast and stable, as shown by Krupskii and Joe (2015). Once we have got the estimates for the group-specific copulas, we estimate the parameters of the global copula, stage T_2 in Figure 5, with the other parameters set equal to their estimates. This step-wise approach allows us to get the estimates in a quick way; however, we would need to rely on resampling methods to obtain the standard errors of the model, as this method would give us the standard errors conditional on the previous step. The resampling method would also allow us to get the multivariate distribution of the parameters, which would give us the chance to generate in-sample and out-of-sample forecast bands for the time-varying parameters using the methods shown by Blasques et al. (2016).

Some additional restrictions are made for the estimation of the Skewed Student-t

copula at each stage of the process. First, I assume the same parameters $\lambda_1,\,\lambda_2,\,$ and ν for all the variables modeled within the same factor. This simplification would speed up the estimation because I would need to simulate realization of the Skewed-t distribution, as there is not a closed formula for the inverse cumulative function of the univariate Skewed Student-t distribution. Also, for each copula the number of parameters to estimate would be N+3, where N are the number of variables modeled within the same factor. A second restriction is the use of a "variance targeting" approach to alleviate the complexity of the estimation process (Oh and Patton 2023). In particular, this approach implies using a two-step procedure where the estimates of the constant copula are obtained first and, following some stationarity assumptions, we estimate the GAS dynamics. The constant copula gives us the estimation of the skewness parameters λ , the number of degrees of freedom ν , and a vector of estimates ρ that defines the long-term relationship between the variables and the latent factor. Similar to the variance targeting in the GARCH literature, where the constant term ω is estimated based on the long-run variance, in the GAS approach the unconditional expectation of the loadings in Eq. (6) is $\bar{f}_i = \frac{\omega_i}{1-\beta_i}$ as the expectation of the score is zero (Blasques et al. 2022). The parameters α_i and β_i are assumed to be equal for all the variables linked with the same factor, to further simplify the estimation process.

For the numerical optimization of the constant copula, I used a modified Newton-Raphson algorithm, for which the first and second partial derivatives of the copula density with respect of the parameter vector are needed. This method allows us to get good estimates for a large number of variables and parameters if we are starting from a sensible starting point. Using the differentiation under the integral sign, we can build the first and second derivatives with respect to the parameter vector. The appendix provides the

analytical expressions of the gradient for the Skewed Student-t copula and some details on how these derivatives would match in a factor copula framework, showing how we only need to obtain 4 derivatives and 10 second derivatives to get the gradient and hessian of a latent factor of any number of variables, as all the elements in the gradient and hessian could be obtained from a combination of those outcomes.

The bifactor latent model.

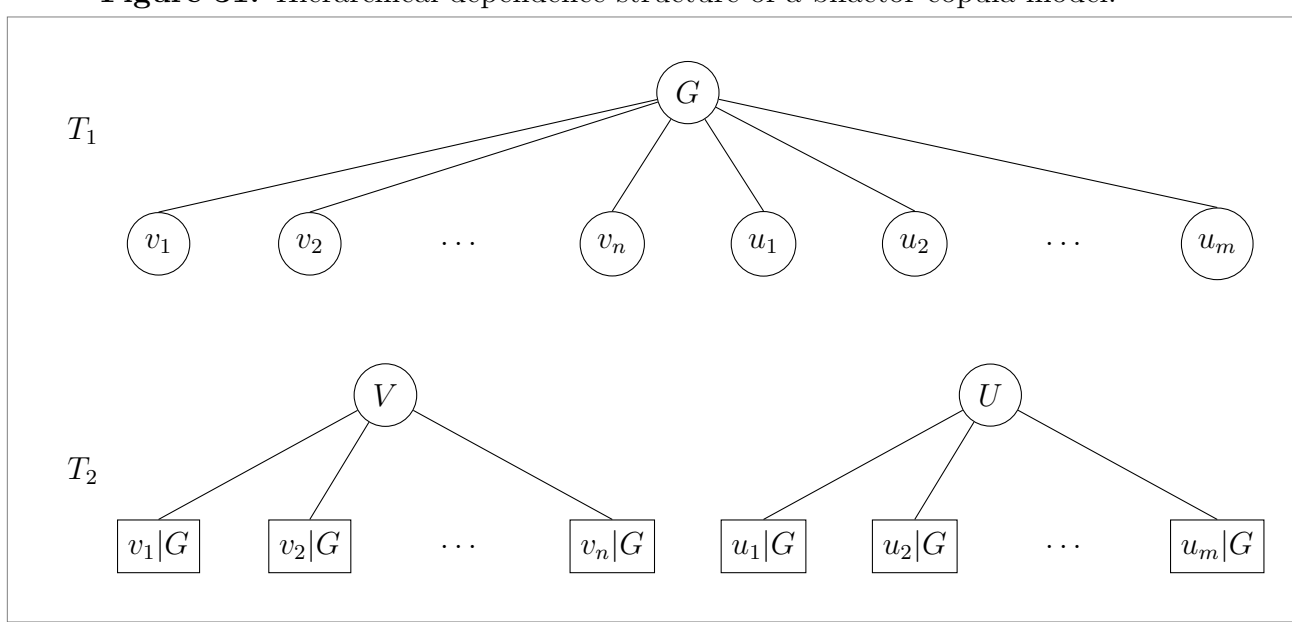


Figure 31: Hierarchical dependence structure of a bifactor copula model.

This figure shows the structure of hierarchical dependence for a bifactor copula.

Starting from the top (T_1) there is one global latent factor that explains the dependence between variables in the dataset. Once that the common dependence is captured by the global factor, the additional dependence between subgroups is captured by the regional factor (T_2) , where depending on the subgroup, the latent regional factor V or U would describe the stronger dependence between variables within the same subgroup than between variables from different subgroups

$$c(v_1, v_2, \dots, v_n, u_1, u_2, \dots, u_m) = \int_0^1 \int_0^1 \prod_{i=1}^n c(C(v_i|G), V) dV \int_0^1 \prod_{k=1}^m c(C(u_k|G), U) dU$$
$$\prod_{i=1}^n c(v_i, G) \prod_{k=1}^m c(u_k, G) dG$$

Row	Bifactor	Nested
Number of parameters (k)	314	166
AIC	-35647.94	-52378.85
BIC	-33087.36	-49875.77

Akaike Information Criterion: $AIC = 2k - 2\log(l)$

Bayesian Information Criterion: BIC = T * log(k) - 2 log(L)

Likelihood ratio test on the factor structure.

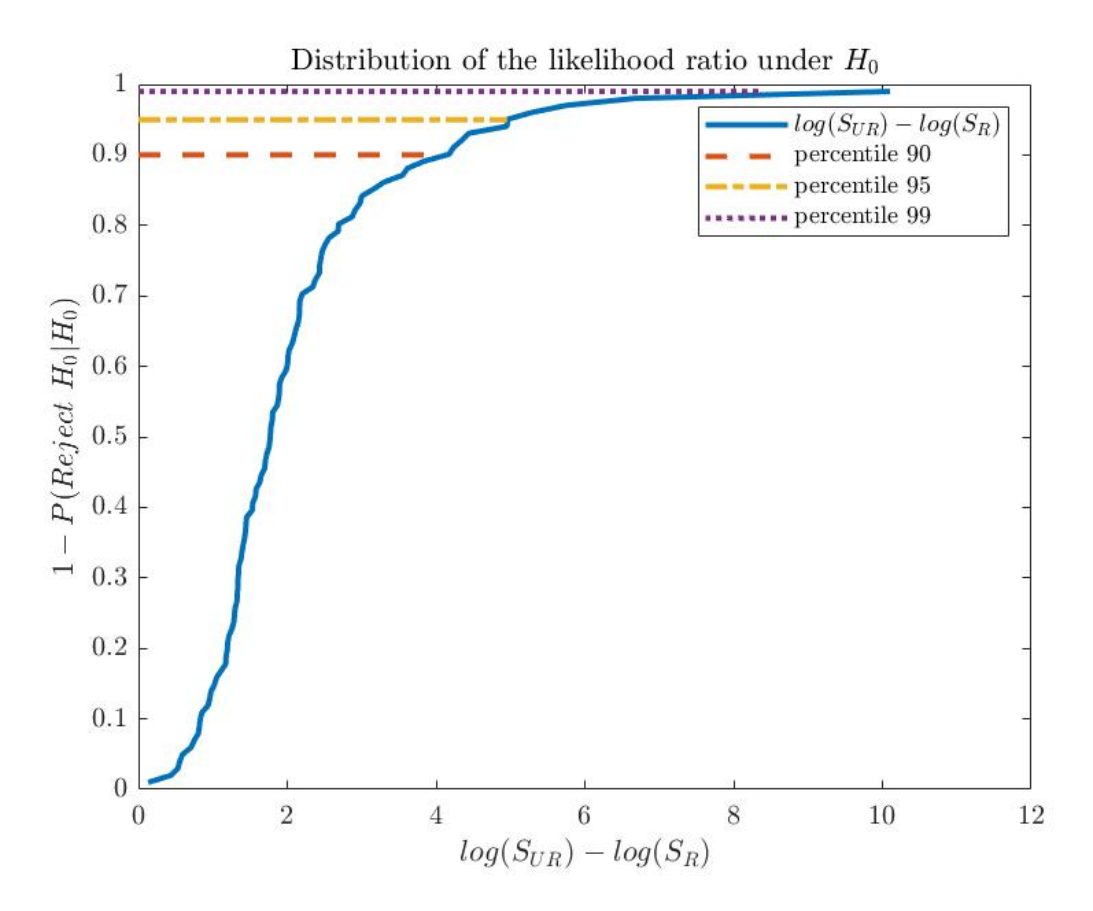
The presentation of the correlation matrix as a result of a factor model makes it possible to distinguish a restricted model, where the factor is known, e.g., a financial index, and an unrestricted model, where the factor is unknown or latent. This distinction between restricted and unrestricted models reminds us about a likelihood ratio test. Actually, we could see the restricted model as a realization of the factor. The issue with this test is similar to what Cai (1994) faced to test a Switching Markov model with a model without structural change, i.e., the distribution function of the factor is not identified under the null hypothesis, which makes the distribution of the likelihood ratio unknown under the null hypothesis. Cai (1994) uses Monte Carlo techniques to get this distribution. I apply the same idea to get the distribution under the null hypothesis that there is no significant increase in the goodness of fit of the latent factor, or in other words, the explicit factor is a realization of a stochastic variable with distribution f(Z).

The MonteCarlo exercise relies on the following steps:

- 1. Using the explicit factor and the estimated correlation matrix, simulate w realizations of the matrix X, i.e., \tilde{X} .
- 2. Estimate the correlation matrix for each of the w simulations of X by using the latent factor as shown in Eq. (16). The likelihood of this model would be S_{UR}^{w} for each simulation w.

- 3. Estimate the correlation matrix for each of the w simulations of X by using the explicit factor. The likelihood of this model would be S_R^w for each simulation w.
- 4. Compute the log difference $log(S_{UR}) log(S_R)$ for all the simulations, which would give us a distribution of the likelihood ratio test under the null hypothesis (see Figure 32).
- 5. Look at the corresponding value for a certain percentile of the distribution and compare it with the likelihood-ratio statistic from the real data. If the likelihood statistic is higher than the corresponding value for the selected percentile, we would reject the null hypothesis with a probability given by that percentile.

Figure 32: Likelihood ratio statistics distribution under the null hypothesis



This chart shows the distribution of the likelihood ratio under the null hypothesis that the dependence structure estimated from an explicit one-factor model is a realization of the dependence structure from the latent factor. The chart is based on a simulation of 100 realizations for a dataset of length T=1000 and N=24 institution.

Measures and indicators in terms of copulas

I present the formulas for the indicators in terms of nested factor copulas, omitting the time subscript to simplify the notation. To obtain the RiS measure, I start an iterative algorithm that initiates with the univariate scenario with highest impact on the domestic financial system; adding institutions up to the measure with N+1 conditioning institutions generates a lower loss than the outcome with N institutions. This means that the stress added by one extra institution is lower than the overall stress distributed

across a smaller set of institutions, which allows us to reach more extreme quantiles in individual institutions.

5.0.1 Return-in-Stress.

The probability of the conditioning subset A in Eq. (1) is defined as

$$P(A) = \int_0^1 \int_0^1 \prod_{i \in A_1} C(q_i^*|v_{a_1}) c(v_{a_1}, v_G) dv_{a_1} \cdots \int_0^1 \prod_{j \in A_M} C(q_j^*|v_{a_M}) c(v_{a_M}, v_G) dv_{a_M} dv_G(17)$$

where the set of institutions are in different M regional latent factors and $q_k^* \in (\alpha, 1)$ for k = i, ..., j is the quantile of the conditioning institution i. The probability of the conditioning scenario, as we are maximizing losses in the case of RiS, would be equal to α , as the lower is the probability of the conditioning scenario and the highest would be the potential impact.

The formula for the RiS in terms of copulas would be

$$RiS = \sum_{j \in B} \omega_{j} E(r_{j}|A)$$

$$= \frac{1}{\alpha} \sum_{j \in B} \omega_{j} \int_{0}^{1} \left[F_{j}^{-1}(u_{j}) \sigma_{j,t} + \mu_{j,t} \right] \int_{0}^{1} \int_{0}^{1} c(u_{j}, v_{b}) c(v_{b}, v_{G}) dv_{b}$$

$$\int_{0}^{1} \prod_{i \in A} C(q_{i}^{*}|v_{a}) c(v_{a}, v_{G}) dv_{a} dv_{G} du_{j}, \qquad (18)$$

where ω_j is the weight of institution j in the conditioned set B.

5.0.2 Expected Shortfall Allocation

The Expected Shortfall decomposition in Eq. (2) implies the definition of domestic (r_d) and foreign (r_f) financial sectors. We present the definition under: (i) the latent nested structure, and (ii) a definition based on n institutions being at the tail, similar to Gravelle and Li (2013). Both definitions lead to similar outcomes if the number of institutions is large enough.³¹

Region tail stress using latent factors. The idiosyncratic section, i.e., $E(r_{i,t}|r_{i,t} \leq VaR_{i,t}(\alpha), r_{d,t} > VaR_{d,t}(\alpha), r_{f,t} > VaR_{f,t}(\alpha))P(r_{d,t} > VaR_{d,t}(\alpha), r_{f,t} > VaR_{f,t}(\alpha)|r_i \leq VaR_{i}(\alpha))$, is defined as

$$\frac{1}{\alpha} \int_0^{\alpha} \left[F_i^{-1}(u_i) \sigma_{i,t} + \mu_{i,t} \right] \int_0^1 \int_{\alpha}^1 c_{d,i}(v_d, u_i) c_{G,d}(w_G, v_d) dv_d \int_{\alpha}^1 c_{G,f}(w_G, v_f) dv_f dw_G du_i, (19)$$

where u_i is the integral probability transformation for institution i, v_d and v_f refer to the domestic and foreign latent factors, and w_G indicates the global latent factor.

The domestic section, i.e., $E(r_{i,t}|r_{i,t} \leq VaR_{i,t}(\alpha), r_{d,t} \leq VaR_{d,t}(\alpha), r_{f,t} > VaR_{f,t}(\alpha))P(r_{d,t} \leq VaR_{d,t}(\alpha), r_{f,t} > VaR_{f,t}(\alpha)|r_i \leq VaR_{i}(\alpha))$ is defined as

$$\frac{1}{\alpha} \int_0^{\alpha} \left[F_i^{-1}(u_i) \sigma_{i,t} + \mu_{i,t} \right] \int_0^1 \int_0^{\alpha} c_{d,i}(v_d, u_i) c_{G,d}(w_G, v_d) dv_d \int_{\alpha}^1 c_{G,f}(w_G, v_f) dv_f dw_G du_i. (20)$$

Note that this formulation when we have M foreign financial systems would be similar, changing $\int_{\alpha}^{1} c_{G,f}(w_{G}, v_{f}) dv_{f}$ by $\prod_{k=1}^{M} \int_{\alpha}^{1} c_{G,f_{k}}(w_{G}, v_{f_{k}}) dv_{f_{k}}$. The definition for the foreign section is more difficult when there is more than one foreign sector, as foreign would be if

³¹In our empirical exercise, a similar idiosyncratic share is found if four institutions are in the tail to define the stress scenario.

any foreign sector is in their tail. To simplify the computation, we just keep in mind that the probability of the foreign section is the probability of not being domestically stressed minus the probability of the idiosyncratic section. In other words, if we define the foreign (domestic) tail stress as B(A) and not being in the tail as $B^c(A^c)$, the probability of the foreign stress is $P(B \cap A^c) = P(A^c) - P(A^c \cap B^c)$, i.e., the foreign section is

$$\frac{1}{\alpha} \int_{0}^{\alpha} \left[F_{i}^{-1}(u_{i}) \sigma_{i,t} + \mu_{i,t} \right] \left(\int_{0}^{1} \int_{\alpha}^{1} c_{d,i}(v_{d}, u_{i}) c_{G,d}(w_{G}, v_{d}) dv_{d} dw_{G} - \right. \\
\left. \int_{0}^{1} \int_{\alpha}^{1} c_{d,i}(v_{d}, u_{i}) c_{G,d}(w_{G}, v_{d}) dv_{d} \int_{\alpha}^{1} c_{G,f}(w_{G}, v_{f}) dv_{f} dw_{G} \right) du_{i}.$$
(21)

In a similar way, knowing that $P(A \cap B) = P(A) - P(A \cap B^c)$, we can define the global section as

$$\frac{1}{\alpha} \int_{0}^{\alpha} \left[F_{i}^{-1}(u_{i}) \sigma_{i,t} + \mu_{i,t} \right] \left(\int_{0}^{1} \int_{0}^{\alpha} c_{d,i}(v_{d}, u_{i}) c_{G,d}(w_{G}, v_{d}) dv_{d} dw_{G} - \right.$$

$$\int_{0}^{1} \int_{0}^{\alpha} c_{d,i}(v_{d}, u_{i}) c_{G,d}(w_{G}, v_{d}) dv_{d} \int_{\alpha}^{1} c_{G,f}(w_{G}, v_{f}) dv_{f} dw_{G} \right) du_{i}.$$
(22)

Region tail stress where at least N institutions are in distress. The computation in case we defined the tail event as at least N domestic/foreign institutions in their tails would be computed as using the complementary probabilities, as the number of institutions must be equal to or higher than N. For instance, in the case of N = 1, this is the complementary probability of no institution at its tail, i.e., the idiosyncratic section

would be

$$\frac{1}{\alpha} \int_{0}^{\alpha} \left[F_{i}^{-1}(u_{i}) \sigma_{i,t} + \mu_{i,t} \right] \int_{0}^{1} \int_{0}^{1} c_{d,i}(v_{d}, u_{i}) \prod_{j=1}^{M_{d}-1} \left(1 - C_{j|d}(\alpha|v_{d}) \right) c_{G,d}(w_{G}, v_{d}) dv_{d}
\int_{0}^{1} c_{G,f}(w_{G}, v_{f}) \prod_{j=1}^{M_{f}} \left(1 - C_{j|f}(\alpha|v_{f}) \right) dv_{f} dw_{G} du_{i},$$
(23)

where M_d is the number of institutions in the domestic financial system and M_f is the number of institutions in the foreign financial system.³² Note that $C_{j|d}(\alpha|v_d)$ capture the probability of institution j being at its tail given a realization of the latent domestic factor (v_d) , so $1 - C_{j|d}(\alpha|v_d)$ is the probability of institution j not being at its tail given the realization of v_d . The product $\prod_{j=1}^{M_d-1} \left(1 - C_{j|d}(\alpha|v_d)\right)$ is the joint probability of no domestic institution being at its tail given the realization of factor v_d . We are able to show this probability as a product because the factor structure implies that institutions are conditionally independent. To build the domestic section, we use the formula $P(A \cap B^c) = P(B^c) - P(A^c \cap B^c)$, i.e.,

$$\frac{1}{\alpha} \int_{0}^{\alpha} \left[F_{i}^{-1}(u_{i}) \sigma_{i,t} + \mu_{i,t} \right] \left(\int_{0}^{1} \int_{0}^{1} c_{d,i}(v_{d}, u_{i}) c_{G,d}(w_{G}, v_{d}) dv_{d} \int_{0}^{1} c_{G,f}(w_{G}, v_{f}) \prod_{j=1}^{M_{f}} \left(1 - C_{j|f}(\alpha|v_{f}) \right) dv_{f} dw_{G} - \int_{0}^{1} \int_{0}^{1} c_{d,i}(v_{d}, u_{i}) \prod_{j=1}^{M_{d}-1} \left(1 - C_{j|d}(\alpha|v_{d}) \right) c_{G,d}(w_{G}, v_{d}) dv_{d} \int_{0}^{1} c_{G,f}(w_{G}, v_{f}) \prod_{j=1}^{M_{f}} \left(1 - C_{j|f}(\alpha|v_{f}) \right) dv_{f} dw_{G} \right) du_{i}. (24)$$

In a similar fashion, we would get the sections of the foreign and global section, just as we already showed. For N=2, the complementary section to the stress event becomes larger, as if none or just one institution under stress would not be enough to trigger the regional stress, e.g.,

$$P(A^c) = \int_0^1 \prod_{j=1}^{M_d-1} \left(1 - C_{j|d}(\alpha|v_d)\right) c_{G,d}(w_G, v_d) dv_d dw_G + \sum_{j=1}^{M_g-1} C_{j|d}(\alpha|v_d) \prod_{k \neq j}^{M_g-2} \left(1 - C_{k|d}(\alpha|v_d)\right) c_{G,d}(w_G, v_d) dv_d dw_G,$$

while for N = 1 we just consider the first addend.

³²We write $M_g - 1$ as institution i is within the M_g financial firms.

Derivatives of the factor copula model

The minus log-likelihood function is defined as

$$S = -\sum_{t=1}^{T} \log(c(u_t, v_t; \Theta)),$$

where Θ is the set of copula parameters. The gradient with respect to the parameters Θ would be

$$\frac{\partial S}{\partial \Theta} = -\sum_{t=1}^{T} \frac{\partial \log(c(u_t, v_t; \Theta))}{\partial \Theta}.$$

Note that using the chain rule we can find the following relationship:

$$\frac{\partial \log(c(u_t, v_t; \Theta))}{\partial \Theta} = \frac{1}{c(u_t, v_t; \Theta)} \frac{\partial c(u_t, v_t; \Theta)}{\partial \Theta}.$$
 (25)

The one-factor copula is defined

$$c(u, v; \Theta) = \int_0^1 c_{u,z}(u, z; \theta_{u,z}) c_{v,z}(v, z; \theta_{v,z}) dz,$$

where $\Theta = [\theta'_{u,z}, \theta'_{v,z}]'$. In the skewed t framework we would have six parameters, i.e., $\Theta = [\rho_{u,z}, \lambda_u, \rho_{v,z}, \lambda_v, \lambda_z, \nu]$. Obviously, the factor model would provide a good alternative for the estimation when the number of variables N is large (N >> 2). Following Leibniz's

integral rule, we can apply the differentiation under the integral sign, e.g.,

$$\frac{\partial c(u, v; \Theta)}{\partial \rho_{u,z}} = \int_{0}^{1} \frac{\partial c_{u,z}(u, z; \theta_{u,z})}{\partial \rho_{u,z}} c_{v,z}(v, z; \theta_{v,z}) dz$$

$$\frac{\partial c(u, v; \Theta)}{\partial \lambda_{u}} = \int_{0}^{1} \frac{\partial c_{u,z}(u, z; \theta_{u,z})}{\partial \lambda_{u}} c_{v,z}(v, z; \theta_{v,z}) dz$$

$$\frac{\partial c(u, v; \Theta)}{\partial \rho_{v,z}} = \int_{0}^{1} c_{u,z}(u, z; \theta_{u,z}) \frac{\partial c_{v,z}(v, z; \theta_{v,z})}{\partial \rho_{v,z}} dz$$

$$\frac{\partial c(u, v; \Theta)}{\partial \lambda_{v}} = \int_{0}^{1} c_{u,z}(u, z; \theta_{u,z}) \frac{\partial c_{v,z}(v, z; \theta_{v,z})}{\partial \lambda_{v}} dz$$

$$\frac{\partial c(u, v; \Theta)}{\partial \lambda_{z}} = \int_{0}^{1} \left(\frac{\partial c_{u,z}(u, z; \theta_{u,z})}{\partial \lambda_{z}} c_{v,z}(v, z; \theta_{v,z}) + c_{u,z}(u, z; \theta_{u,z}) \frac{\partial c_{v,z}(v, z; \nu)}{\partial \lambda_{z}} \right) dz$$

$$\frac{\partial c(u, v; \Theta)}{\partial \nu} = \int_{0}^{1} \left(\frac{\partial c_{u,z}(u, z; \theta_{u,z})}{\partial \nu} c_{v,z}(v, z; \theta_{v,z}) + c_{u,z}(u, z; \theta_{u,z}) \frac{\partial c_{v,z}(v, z; \nu)}{\partial \nu} \right) dz$$

For the derivatives under the integral sign we follow Eq. (25) to get the derivative of the copula as the product between the derivative of the log-copula multiplied by the copula density, e.g., $\frac{\partial c_{u,z}(u,z;\theta_{u,z})}{\partial \rho_{u,z}} = \frac{\partial \log(c_{u,z}(u,z;\theta_{u,z}))}{\partial \rho_{u,z}} c_{u,z}(u,z;\theta_{u,z})$. Once we get the derivative of the factor copula with respect to the parameter, we apply again Eq. (25) to get the derivative of the log-copula with respect to the parameter, e.g., $\frac{\partial \log(c(u_t,v_t;\Theta))}{\partial \rho_{u,z}} = \frac{1}{c(u_t,v_t;\Theta)} \frac{\partial c(u,v;\Theta)}{\partial \rho_{u,z}}$.

The computation of the derivative of the log-copula hugely simplifies the analytical assessment of the gradient vector. The next subsection presents the analytical derivatives with respect to the parameters of the static copula model, as they are needed to compute the static factor copula for a large dimensional dataset. We use a modified Newton-Rapshon method to estimate the constant factor copula, as suggested by Krupskii and Joe (2015), to be used as "variance targeting" to anchor the long-term dependence like Oh and Patton (2023) and Lucas et al. (2014).

Derivative of the GHST log-copula

The log-likelihood copula is defined as

$$\log\left(c(u_t, v_t; \Theta)\right) = \log\left(f(F_{X_1}^{-1}(u), F_{X_2}^{-1}(v); \Theta)\right) - \log\left(f(F_{X_1}^{-1}(u); \Theta)\right) - \log\left(f(F_{X_2}^{-1}(v); \Theta)\right),$$

with its derivative being

$$\frac{\partial \log \left(c(u_t, v_t; \Theta)\right)}{\partial \Theta} = \frac{\partial \log \left(f(F_{X_1}^{-1}(u), F_{X_2}^{-1}(v); \Theta)\right)}{\partial \Theta} - \frac{\partial \log \left(f_{X_1}(F_{X_1}^{-1}(u); \Theta)\right)}{\partial \Theta} - \frac{\partial \log \left(f_{X_2}(F_{X_2}^{-1}(v); \Theta)\right)}{\partial \Theta}, \tag{26}$$

with $f(\ldots, \ldots; \Theta)$ and f_{\ldots} provided by Eq. (3) with N=2 and N=1 respectively.

We provide the derivative of the log-likelihood with respect of each parameter for the marginal and the joint distribution.

Derivative of the joint distribution with respect to the GHST parameters.

$$\log (f(x_1, x_2; \Theta)) = \frac{2 - (\nu + N)}{2} \log(2) - \log(\Gamma(\frac{\nu}{2})) - \frac{N}{2} \log(\pi \nu) - \log(\sqrt{1 - \rho^2})$$

$$+ \log \left(K_{\frac{\nu+2}{2}} \left(((\nu + A)B)^{1/2} \right) \right) + \mathcal{L} + \frac{\nu + 2}{2} \log \left(((\nu + A)B)^{1/2} \right)$$

$$- \frac{(\nu + 2)}{2} \log \left(1 + \frac{A}{\nu} \right)$$

with
$$x_1 = F_{X_1}^{-1}(u)$$
, $x_2 = F_{X_2}^{-1}(v)$, $A = a_1 + a_2 + a_3$ with $a_1 = \frac{(x_1 - \mu_1)^2}{1 - \rho^2}$, $a_2 = \frac{(x_2 - \mu_2)^2}{1 - \rho^2}$
and $a_3 = 2(x_1 - \mu_1)(x_2 - \mu_2)\frac{-\rho}{1 - \rho^2}$. $\mu_1 = 0$, $\mu_2 = 0$, $B = b_1 + b_2 + b_3$ with $b_1 = \frac{\lambda_1^2}{1 - \rho^2}$, $b_2 = \frac{\lambda_2^2}{1 - \rho^2}$ and $b_3 = 2\lambda_1\lambda_2\frac{-\rho}{1 - \rho^2}$. $\mathcal{L} = \ell_1 + \ell_2 + \ell_3$ with $\ell_1 = \frac{(x_1 - \mu_1)\lambda_1}{1 - \rho^2}$, $\ell_2 = \frac{(x_2 - \mu_2)\lambda_2}{1 - \rho^2}$ and

$$\ell_3 = ((x_1 - \mu_1)\lambda_2 + (x_2 - \mu_2)\lambda_1) \frac{-\rho}{1-\rho^2}.$$

Derivative of the joint distribution with respect to the correlation parameter.

eter.
$$\frac{\partial a_1}{\partial \rho} = 2\rho \frac{(x_1 - \mu_1)^2}{(1 - \rho^2)^2} \quad \frac{\partial b_3}{\partial \rho} = 2\lambda_1 \lambda_2 \left(\frac{-1}{1 - \rho^2} + \frac{-2\rho^2}{(1 - \rho^2)^2}\right)$$

$$\frac{\partial a_2}{\partial \rho} = 2\rho \frac{(x_2 - \mu_2)^2}{(1 - \rho^2)^2} \quad \frac{\partial B}{\partial \rho} = 2\rho \frac{\partial b_1}{\partial \rho} + \frac{\partial b_2}{\partial \rho} + \frac{\partial b_3}{\partial \rho}$$

$$\frac{\partial a_3}{\partial \rho} = 2(x_1 - \mu_1)(x_2 - \mu_2) \left(\frac{-1}{1 - \rho^2} + \frac{-2\rho^2}{(1 - \rho^2)^2}\right) \quad \frac{\partial \ell_1}{\partial \rho} = 2\rho \frac{\lambda_1(x_1 - \mu_1)}{(1 - \rho^2)^2}$$

$$\frac{\partial A}{\partial \rho} = \frac{\partial a_1}{\partial \rho} + \frac{\partial a_2}{\partial \rho} + \frac{\partial a_3}{\partial \rho} \quad \frac{\partial \ell_2}{\partial \rho} = 2\rho \frac{\lambda_2(x_2 - \mu_2)}{(1 - \rho^2)^2}$$

$$\frac{\partial b_1}{\partial \rho} = 2\rho \frac{\lambda_1^2}{(1 - \rho^2)^2} \quad \frac{\partial \ell_3}{\partial \rho} = (\lambda_1(x_2 - \mu_2) + \lambda_2(x_1 - \mu_1)) \left(\frac{-1}{1 - \rho^2} + \frac{-2\rho^2}{(1 - \rho^2)^2}\right)$$

$$\frac{\partial b_2}{\partial \rho} = 2\rho \frac{\lambda_2^2}{(1 - \rho^2)^2} \quad \frac{\partial \mathcal{L}}{\partial \rho} = 2\rho \frac{\partial \mathcal{L}}{\partial \rho} = 2\rho \frac{\partial \ell_1}{\partial \rho} + \frac{\partial \ell_2}{\partial \rho} + \frac{\partial \ell_3}{\partial \rho}$$

$$\frac{\partial \log \left(f(x_1, x_2; \Theta)\right)}{\partial \rho} = \frac{\rho}{1 - \rho^2} + \left(\frac{1}{K_{\frac{\nu+2}{2}}\left(\left((\nu + A)B\right)^{1/2}\right)} k_{\frac{\nu+2}{2}}\left(\left((\nu + A)B\right)^{1/2}\right) + \frac{(\nu + 2)/2}{\left((\nu + A)B\right)^{1/2}}\right) \\
- \frac{1}{2}\left((\nu + A)B\right)^{-1/2}\left((\nu + A)\frac{\partial B}{\partial \rho} + B\frac{\partial A}{\partial \rho}\right) + \frac{\partial \mathcal{L}}{\partial \rho} + \frac{(\nu + 2)/2}{\left(1 + \frac{A}{\nu}\right)} \frac{\partial A}{\partial \rho},$$

where
$$k_a\left(b\right) = \frac{\partial K_a\left(b\right)}{\partial b} = -0.5\left(K_{a+1}(b) + K_{a-1}(b)\right)$$

Derivative of the joint distribution with respect to the asymmetric parameter of the first variable. The derivatives $\frac{\partial x_1}{\partial \lambda_1} = \frac{\partial F_{X_1}^{-1}(u;\lambda_1,\nu)}{\partial \lambda_1}$ is computed numerically.

$$\frac{\partial a_1}{\partial \lambda_1} = \frac{2(x_1 - \mu_1)\frac{\partial x_1}{\partial \lambda_1}}{1 - \rho^2} \qquad \frac{\partial b_3}{\partial \lambda_1} = \frac{2\lambda_2 \frac{-\rho}{1 - \rho^2}}{1 - \rho^2}$$

$$\frac{\partial a_2}{\partial \lambda_1} = 0 \qquad \frac{\partial B}{\partial \lambda_1} = \frac{\partial b_1}{\partial \lambda_1} + \frac{\partial b_2}{\partial \lambda_1} + \frac{\partial b_3}{\partial \lambda_1}$$

$$\frac{\partial a_3}{\partial \lambda_1} = 2\frac{\partial x_1}{\partial \lambda_1}(x_2 - \mu_2)\frac{-\rho}{1 - \rho^2} \qquad \frac{\partial \ell_1}{\partial \lambda_1} = \frac{\left(\frac{\partial x_1}{\partial \lambda_1}\lambda_1 + (x_1 - \mu_1)\right)}{1 - \rho^2}$$

$$\frac{\partial A}{\partial \lambda_1} = \frac{\partial a_1}{\partial \lambda_1} + \frac{\partial a_2}{\partial \lambda_1} + \frac{\partial a_3}{\partial \lambda_1} \qquad \frac{\partial \ell_2}{\partial \lambda_1} = 0$$

$$\frac{\partial b_1}{\partial \lambda_1} = \frac{2\lambda_1}{1 - \rho^2} \qquad \frac{\partial \ell_3}{\partial \lambda_1} = \left(\frac{\partial x_1}{\partial \lambda_1}\lambda_2 + (x_2 - \mu_2)\right)\frac{-\rho}{1 - \rho^2}$$

$$\frac{\partial b_2}{\partial \lambda_1} = 0 \qquad \frac{\partial \ell_2}{\partial \lambda_1} = \frac{\partial \ell_1}{\partial \lambda_1} + \frac{\partial \ell_2}{\partial \lambda_1} + \frac{\partial \ell_3}{\partial \lambda_1}$$

$$\frac{\partial \log \left(f(x_1, x_2; \Theta) \right)}{\partial \lambda_1} = \\ + \left(\frac{k_{\frac{\nu+2}{2}} \left(((\nu + A)B)^{1/2} \right)}{K_{\frac{\nu+2}{2}} \left(((\nu + A)B)^{1/2} \right)} + \frac{(\nu + 2)/2}{((\nu + A)B)^{1/2}} \right) \frac{1}{2} \left((\nu + A)B)^{-1/2} \left((\nu + A)\frac{\partial B}{\partial \lambda_1} + B\frac{\partial A}{\partial \lambda_1} \right) + \frac{\partial \mathcal{L}}{\partial \lambda_1} - \frac{(\nu + 2)/2}{\left(1 + \frac{A}{\nu} \right)} \frac{1}{\nu} \frac{\partial A}{\partial \lambda_1},$$

Derivative of the joint distribution with respect to the asymmetric parameter of the second variable. The derivative $\frac{\partial x_2}{\partial \lambda_2} = \frac{\partial F_{X_2}^{-1}(u;\lambda_2,\nu)}{\partial \lambda_2}$ is computed numerically.

$$\frac{\partial a_1}{\partial \lambda_2} = 0 \qquad \frac{\partial b_3}{\partial \lambda_2} = 2\lambda_1 \frac{-\rho}{1-\rho^2}$$

$$\frac{\partial a_2}{\partial \lambda_2} = \frac{2(x_2 - \mu_2)\frac{\partial x_2}{\partial \lambda_2}}{1-\rho^2} \qquad \frac{\partial B}{\partial \lambda_2} = \frac{\partial b_1}{\partial \lambda_2} + \frac{\partial b_2}{\partial \lambda_2} + \frac{\partial b_3}{\partial \lambda_2}$$

$$\frac{\partial a_3}{\partial \lambda_2} = 2\frac{\partial x_2}{\partial \lambda_2}(x_1 - \mu_1)\frac{-\rho}{1-\rho^2} \qquad \frac{\partial \ell_1}{\partial \lambda_2} = 0$$

$$\frac{\partial A}{\partial \lambda_2} = \frac{\partial a_1}{\partial \lambda_2} + \frac{\partial a_2}{\partial \lambda_2} + \frac{\partial a_3}{\partial \lambda_2} \qquad \frac{\partial \ell_2}{\partial \lambda_1} = \frac{\left(\frac{\partial x_2}{\partial \lambda_2}\lambda_2 + (x_2 - \mu_2)\right)}{1-\rho^2}$$

$$\frac{\partial b_1}{\partial \lambda_2} = 0 \qquad \frac{\partial \ell_3}{\partial \lambda_2} = \left(\frac{\partial x_2}{\partial \lambda_2}\lambda_1 + (x_1 - \mu_1)\right)\frac{-\rho}{1-\rho^2}$$

$$\frac{\partial b_2}{\partial \lambda_2} = \frac{2\lambda_2}{1-\rho^2} \qquad \frac{\partial \mathcal{L}}{\partial \lambda_2} = \frac{\partial \ell_1}{\partial \lambda_2} + \frac{\partial \ell_2}{\partial \lambda_2} + \frac{\partial \ell_3}{\partial \lambda_2}$$

Derivative of the joint distribution with respect to the number of degrees of freedom. González-Santander (2023) shows that the n-th derivative of the modified Bessel function of the second kind is

$$\frac{\partial^n}{\partial \nu^n} K_{\nu}(t) = \frac{1}{2} \int_{-\infty}^{\infty} x^n \exp(\nu x - t \cosh x) dx,$$

where cosh is the hyperbolic cosine. For n=1, we can find a closed-form solution for non-integral ν (see Brychkov 2016, González-Santander 2018) defined as

$$\begin{split} \frac{\partial K_{\nu}(t)}{\partial \nu} & = & \frac{\pi}{2} \csc(\pi \nu) \left\{ \pi \cot(\pi \nu) I_{\nu}(z) - [I_{\nu}(z) + I_{-\nu}(z)] \left(\frac{z^2}{4(1 - \nu^2)} \,_{3}\mathbf{F}_{4} \left(\begin{bmatrix} 1, 1, \frac{3}{2} \\ 2, 2, 2, -\nu, 2 + \nu \end{bmatrix} | z^2 \right) + \log(\frac{z}{2}) - \psi(\nu) - \frac{1}{2\nu} \right) \right\} \\ & + \frac{1}{4} \left\{ I_{-\nu}(z) \Gamma^2(-\nu) \left(\frac{z}{2} \right)^{2\nu} \,_{2}\mathbf{F}_{3} \left(\begin{bmatrix} \nu, \frac{1}{2} + \nu \\ 1 + \nu, 1 + \nu, 1 + 2\nu \end{bmatrix} | z^2 \right) - I_{\nu}(z) \Gamma^2(\nu) \left(\frac{z}{2} \right)^{-2\nu} \,_{2}\mathbf{F}_{3} \left(\begin{bmatrix} -\nu, \frac{1}{2} - \nu \\ 1 - \nu, 1 - \nu, 1 - 2\nu \end{bmatrix} | z^2 \right) \right\}, \end{split}$$

where ${}_{p}\mathbf{F}_{q}$ is the generalized hypergeometric function and $\psi(\dots)$ is the digamma function. The derivatives $\frac{\partial x_{1}}{\partial \lambda_{1}} = \frac{\partial F_{X_{1}}^{-1}(u;\lambda_{1},\nu)}{\partial \nu}$ and $\frac{\partial x_{2}}{\partial \nu} = \frac{\partial F_{X_{2}}^{-1}(u;\lambda_{2},\nu)}{\partial \nu}$ are computed numerically.

$$\frac{\partial a_1}{\partial \nu} = \frac{2(x_1 - \mu_1)\frac{\partial x_1}{\partial \nu}}{1 - \rho^2} \qquad \frac{\partial b_3}{\partial \nu} = 0$$

$$\frac{\partial a_2}{\partial \nu} = \frac{2(x_2 - \mu_2)\frac{\partial x_2}{\partial \nu}}{1 - \rho^2} \qquad \frac{\partial B}{\partial \nu} = \frac{\partial b_1}{\partial \nu} + \frac{\partial b_2}{\partial \nu} + \frac{\partial b_3}{\partial \nu}$$

$$\frac{\partial a_3}{\partial \nu} = 2\left((x_2 - \mu_2)\frac{\partial x_1}{\partial \nu} + (x_1 - \mu_1)\frac{\partial x_2}{\partial \nu}\right)\frac{-\rho}{1 - \rho^2} \qquad \frac{\partial \ell_1}{\partial \nu} = \frac{\left(\frac{\partial x_1}{\partial \nu}\lambda_2\right)}{1 - \rho^2}$$

$$\frac{\partial A}{\partial \nu} = \frac{\partial a_1}{\partial \nu} + \frac{\partial a_2}{\partial \nu} + \frac{\partial a_3}{\partial \nu} \qquad \frac{\partial \ell_2}{\partial \nu} = \frac{\left(\frac{\partial x_2}{\partial \nu}\lambda_2\right)}{1 - \rho^2}$$

$$\frac{\partial b_1}{\partial \nu} = 0 \qquad \frac{\partial \ell_3}{\partial \nu} = \left(\frac{\partial x_2}{\partial \nu}\lambda_1 + \frac{\partial x_1}{\partial \nu}\lambda_2\right)\frac{-\rho}{1 - \rho^2}$$

$$\frac{\partial b_2}{\partial \nu} = 0 \qquad \frac{\partial \ell_2}{\partial \nu} = \frac{\partial \ell_1}{\partial \nu} + \frac{\partial \ell_2}{\partial \nu} + \frac{\partial \ell_3}{\partial \nu}$$

$$\frac{\partial \log \left(f(x_1, x_2; \Theta) \right)}{\partial \nu} = \frac{1}{2} \log(2) + \psi(\frac{\nu}{2})/2 - \frac{1}{\nu}$$

$$\frac{\frac{\partial K_{\frac{\nu+2}{2}} \left(((\nu+A)B)^{\frac{1}{2}} \right)}{\partial \nu} \frac{1}{2} + \frac{1}{2} k_{\frac{\nu+2}{2}} \left(((\nu+A)B)^{\frac{1}{2}} \right) ((\nu+A)B)^{\frac{-1}{2}} \left[(\nu+A)\frac{\partial B}{\partial \nu} + (1+\frac{\partial A}{\partial \nu})B \right]}{K_{\frac{\nu+2}{2}} \left(((\nu+A)B)^{\frac{1}{2}} \right)} + \frac{\log \left(\left[(\nu+A)B \right]^{\frac{1}{2}} \right)}{2} + (\nu+2) \frac{\left[(\nu+A)B \right]^{\frac{-1}{2}} \left\{ (\nu+A)\frac{\partial B}{\partial \nu} + (1+\frac{\partial A}{\partial \nu})B \right\}}{\left[(\nu+A)B \right]^{\frac{1}{2}}}$$

$$- \frac{\log \left(1 + \frac{A}{\nu} \right)}{2} - \frac{(\nu+2)/2}{\left(1 + \frac{A}{\nu} \right)} \left[\frac{\partial A}{\partial \nu} \frac{1}{\nu} - \frac{A}{\nu^2} \right]$$

Hessian of the factor copula model

We could apply the rule of chain on Eq. (25) to get the second derivative

$$\frac{\partial^2 \log(c(u_t, v_t; \Theta))}{\partial \theta_1 \partial \theta_2} = \frac{-1}{c(u_t, v_t; \Theta)^2} \frac{\partial c(u_t, v_t; \Theta)}{\partial \theta_1} \frac{\partial c(u_t, v_t; \Theta)}{\partial \theta_2} + \frac{1}{c(u_t, v_t; \Theta)} \frac{\partial^2 c(u_t, v_t; \Theta)}{\partial \theta_1 \partial \theta_2}.$$

We apply again the differentiation under the integral sign as we did for the gradient to obtain the second derivative with respect to the parameters of the Skewed t distribution.

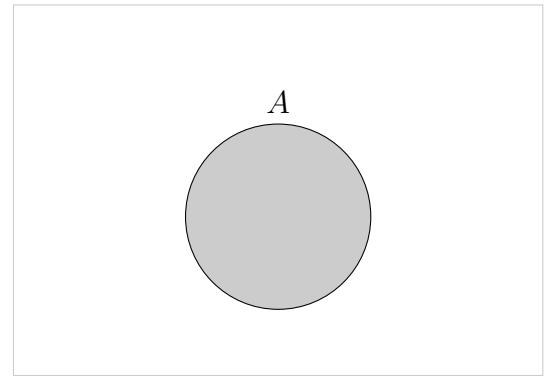
For numerical minimization in a high dimensional dataset, we need the gradient and hessian to use a modified Newton-Raphson algorithm, where the gradient indicates the direction to follow to minimize the minus log-likelihood and the hessian indicates the size of the step in that direction.

Venn diagrams

Venn diagrams are visual representations of sets that help us draw probabilities of multivariate scenarios. To show how it works, let us imagine the set A includes all the possible scenarios where financial firm i is in its left tail, i.e., firm i is under stress. The area of the circle below indicates the probability of that event. The area outside the circle indicates the probability of financial firm i not being under stress.

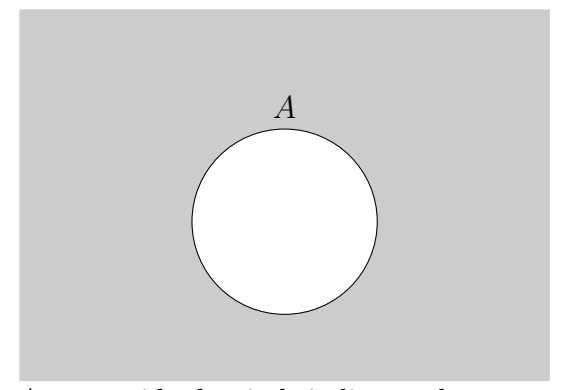
Figure 33: Venn diagram – 1 set

(a) Probability of A



Area within the circle indicates the probability of set A, that gathers all the scenarios where financial institution i is under stress, i.e., the performance of firm i is below the threshold marked by its α percentile.

(b) Probability of not A

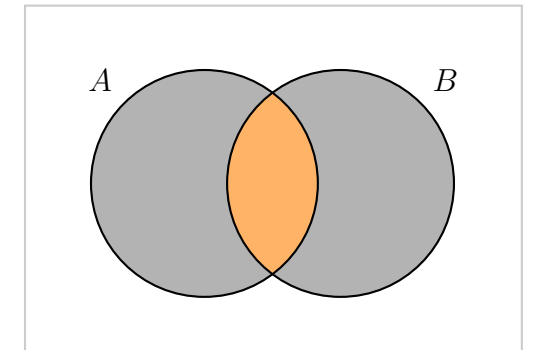


Area outside the circle indicates the complementary probability of set A, that gathers all the scenarios where financial institution i is not under stress, i.e., the performance of firm i is above the threshold marked by its α percentile.

The use of Venn diagrams helps compute the analytical expression of the tail decomposition up to the fifth term. Let us imagine we have a second institution j, and the set B gathers all the potential events where institution j is below its percentile α . The probability of both institutions i and j being below their percentiles α is $P(A \cap B)$, which in terms of copulas is $C_{i,j}(\alpha,\alpha)$. The orange area in the left two-set Venn graph below indicates that probability. The probability of institution i being under stress and institution j not under stress is measured by $P(A) - P(A \cap B)$, which in terms of copulas would be $\alpha - C_{i,j}(\alpha,\alpha)$. This probability is captured by the Venn diagram in the orange area in the below right graph.

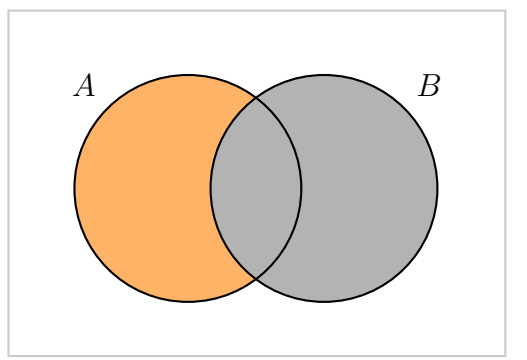
Figure 34: Venn diagram – 2 sets

(a) Probability of A and B



Area in orange indicates the probability of set A and B, i.e., both financial institutions i and j under stress (below the threshold marked by its α percentile).

(b) Probability of A and not B

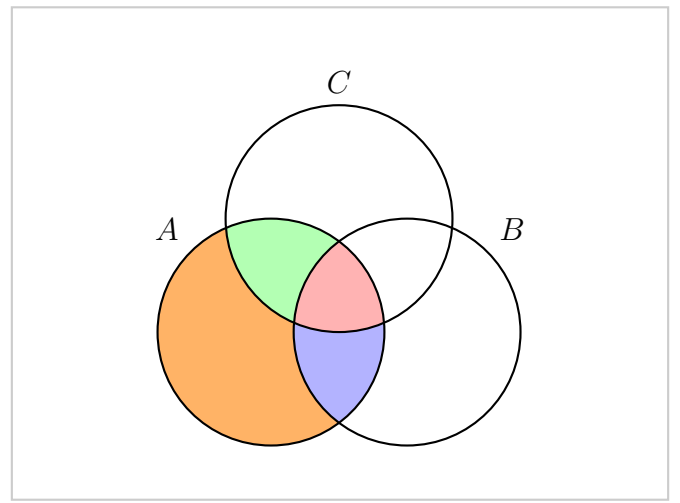


Area in orange indicates the probability of set A and not B, i.e., financial institutions i is under stress (below percentile α) but institution j is not.

Let us imagine we have a third financial institution k and set C indicates the scenarios where returns of firm k are under percentile α . The Venn diagram with three sets becomes more interesting, as we could see that some common areas need to be accounting when building the probabilities. For instance, the probability of set A and C^C and B^C , i.e., only firm i is below its percentile α , could be built as $P(A)-P(A\cap C)-P(A\cap B)+P(A\cap B\cap C)$. $P(A\cap C)$ is the green and red areas, while $P(A\cap B)$ is the blue and red areas. When we are subtracting those areas, we are counting twice the red area, so we need to sum it

back to get the right amount. The red area is $P(A \cap B \cap C)$. In terms of copulas, we could write this probability as $\alpha - C_{i,j}(\alpha, \alpha) - C_{i,k}(\alpha, \alpha) + C_{i,j,k}(\alpha, \alpha, \alpha)$.

Figure 35: Venn diagram – 3 sets

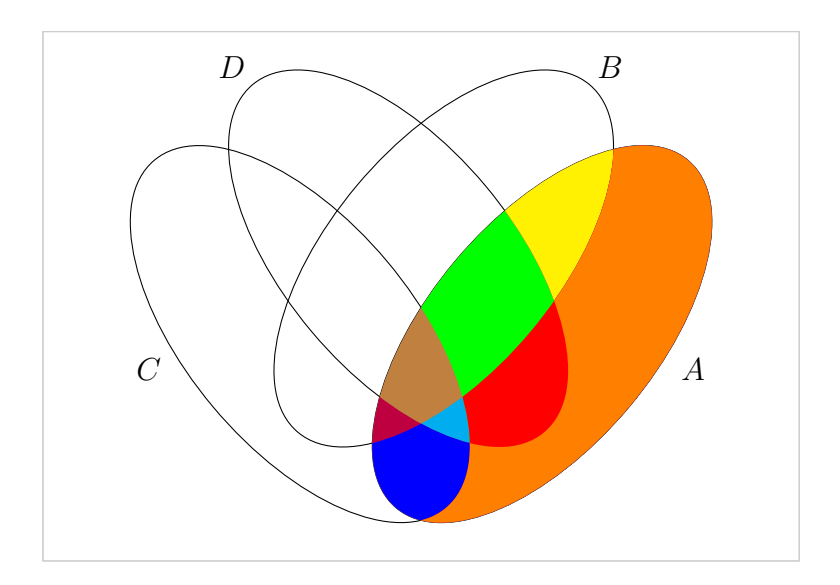


Area in orange indicates the probability of set A and not B and not C. Note that, to get this area, we could subtract from A the common area with C and the common area with B. Because when subtracting those areas you are counting twice the red area (that is common with B and C), you have to sum it back to compensate and get the right area.

The introduction of a fourth institution l, and the set of scenarios D associated with stress tail events for institution l, generates a decomposition of 8 possible areas of A, as shown by the hereinbelow figure. $P(A \cap B) = C_{i,j}(\alpha,\alpha)$ includes the yellow, green, brown, and red wine areas. $P(A \cap C) = C_{i,k}(\alpha,\alpha)$ includes the blue, cyan, red wine, and brown areas. $P(A \cap D) = C_{i,l}(\alpha,\alpha)$ includes the brown, cyan, red, and green areas. $P(A \cap B \cap C) = C_{i,j,k}(\alpha,\alpha,\alpha)$ includes brown and red wine areas, $P(A \cap B \cap D) = C_{i,j,l}(\alpha,\alpha,\alpha)$ covers the green and brown areas, and $P(A \cap C \cap D) = C_{i,k,l}(\alpha,\alpha,\alpha)$ covers the brown and cyan areas. $P(A \cap B \cap C \cap D) = C_{i,j,k,l}(\alpha,\alpha,\alpha,\alpha)$ encompasses the brown area. To get the probability of only institution i getting its returns under its threshold, i.e., the orange area, implies a set of corrections for the areas that are double or triple counted. $P(A \cap (B \cup C \cup D)^c) = P(A) - P(A \cap B) - P(A \cap C) - P(A \cap D) + 2P(A \cap B \cap C)$

 $C \cap D$) + $P(A \cap B \cap D)$ + $P(A \cap B \cap C)$ + $P(A \cap C \cap D)$, which in terms of copulas would be rewritten as $\alpha - C_{i,j}(\alpha, \alpha) - C_{i,k}(\alpha, \alpha) - C_{i,l}(\alpha, \alpha) + 2C_{i,j,k,l}(\alpha, \alpha, \alpha, \alpha) + C_{i,j,l}(\alpha, \alpha, \alpha) + C_{i,j,l}(\alpha, \alpha, \alpha)$.

Figure 36: Venn diagram - 4 sets



The colors of this Venn diagram show different decompositions of set A depending on which other areas are held in common. Getting the orange area, the unique area of A, implies a set of adjustments from the combination of common areas.

The latent factor structure simplifies heavily the calculations, as we can work with the conditional distribution integration over the factor. Let us imagine that those four institutions depend on a factor X that fully explains the dependence structure. Then $P(A \cap B^c) = P(A) - P(A \cap B)$ could be rewritten as $\sum_i P(A|X = x_i) - P(A|X = x_i)P(B|X = x_i)$, where x_i is a realization of the factor and we are summing all across the potential realizations of the factor. Note that the joint probability can be expressed as a product because the dependence between the variables is fully captured by the

factor. Conditional on the factor, the variables are independent. Note that $P(A) - P(A \cap B) = P(A)(1 - P(B|A))$, just by taking P(A) as common multiplier and knowing that $P(B|A) = \frac{P(A \cap B)}{P(A)}$. When we have a factor structure, this implies $P(A \cap B^c) = \sum_i P(A|X=x_i)(1-P(B|X=x_i))$. The probability $P(A \cap (B \cup C)^c) = P(A) - P(A \cap C) - P(A \cap B) + P(A \cap B \cap C)$ could be written as $P(A)[1-P(C|A)-P(B|A)+P(B \cap C|A)]$, which under the factor structure would be $\sum_i P(A|X=x_i)[1-P(C|X=x_i)-P(B|X=x_i)+P(B|X=x_i)P(C|X=x_i)] = \sum_i P(A|X=x_i)[1-P(B|X=x_i)-P(C|X=x_i)]$. In the four institution example, $P(A \cap (B \cup C \cup D)^c) = P(A \cap B^c \cap C^c \cap D^c) = \sum_i P(A|X=x_i)(1-P(B|X=x_i))(1-P(B|X=x_i))(1-P(C|X=x_i))$, which greatly removes the complexity of the calculations.